ALKALI-FUSION PROCESSES FOR THE RECOVERY OF ZIRCONIA AND ZIRCONIUM CHEMICALS FROM ZIRCON SAND

Zola Kwela

ALKALI-FUSION PROCESSES FOR THE RECOVERY OF ZIRCONIA AND ZIRCONIUM CHEMICALS FROM ZIRCON SAND

A dissertation submitted by
Zola Nigel Kwela
In partial fulfilment of the requirements of the degree of

Masters of Science
In the
Faculty of Engineering, Built Environment and Information Technology
University of Pretoria
Pretoria, 000 2

30 /11/ 2 000 at 16h00

E-mail: zolakaso@hotmail.com

ABSTRACT

There are two industrial sources of zirconia: zircon and baddeleyite [1-5]. The baddeleyite reserves in Phalaborwa (the world's major baddeleyite source) are expected to be depleted by the year 2 005 [1-3]. This leaves the Russian Baddeleyite (Kola Peninsula) and zircon as the only industrial sources of zirconia.

The major drawback to zircon use is the large amounts of impurities it is found concentrated with, especially radioactive impurities (Uranium and Thorium) [2-3]. Acid leaching of zircon does not remove these impurities [4-5]. The impurities are usually included in the zircon lattice. The tetragonal structure of zircon with the high coordinated bisdisphenoids ZrO_8 and low coordinated tetrahedra SiO_4 create a safe (inaccessible and stable) habitat for these impurities [7].

Processes for the recovery of zirconia and zirconium chemicals rely heavily on precipitation or crystallisation techniques for purification [8-16]. Precipitation techniques need to be repeated to obtain the required purity. The purity of products from such methods is still suspect, as there still remains a high radioactivity content after purification [2]. The long process time is another disadvantage of these precipitation processes. These factors together are the reason for the high cost of zirconia and zirconium chemicals.

Zirconium and its compounds are regarded to be of low toxicity [1-6]. This implies that they have a great potential of replacing numerous high toxic chemicals. Prominent examples are seen in leather tanning and paints. In leather tanning chromium chemicals can be replaced. In paints lead driers and chromium chemicals for corrosion resistance can be replaced.

The objective of this study was to characterise and optimise the De Wet's zirconium extraction processes for the beneficiation of zircon sand into high purity zirconia and zirconium chemicals. However, at each process step some factors were varied e.g. fusion temperature, reactant mole ratios and composition of leach solutions. Attention was also paid to reducing the total number of process steps. The products produced at each step were analysed. Particular attention was given to the fate of the radioactive impurities.

Characterisation of the decomposition step, showed that within the zircon tetragonal structure, the SiO_4 tetrahedra linkages are less stable than the ZrO_8 bisdisphenoids linkages. This was shown by the preference of sodium for the SiO_4 tetrahedra.

Fusion for 336 hours with periodic intermediate milling proved the preference of sodium for attacking the SiO_4 tetrahedra linkages. This selectivity was clearly demonstrated when decomposing zircon in sodium poor (< 4 moles NaOH per mol of zircon) and low temperature (e.g. 650°C) reaction conditions. The advantage of fusing at 650°C with a mole (or even two moles) of sodium hydroxide is that it leads to minimal (< 5% m/m Na_2O) sodium in the insoluble solids after the removal of soluble silicates. This is a solution to alkali fusion processes, as high amounts of water are usually required to wash out the neutralised sodium salt e.g. 50g of NaCl usually requires a litre of distilled water to reach levels below 600 ppm Na_2O. This reaction condition can be employed when synthesising products where low amounts of sodium are required in the final products e.g. when synthesising zirconia for the ceramic industry.

When fusing for two hours without the intermediate milling step the following results were observed. The reaction at 850°C when fusing a mole of zircon with two moles of sodium hydroxide, was the most efficient in consuming sodium hydroxide. Near complete zircon decomposition was at 850°C when fusing a mole of zircon with six moles of sodium hydroxide. Characterisation with XRD, Raman and IR spectroscopy was misleading as complex spectra were measured, indicating many different phases present. The inconsistency was partly attributed to non-homogeneity in the samples due to NaOH migration.

When fusing for 336 hours with the intermediate milling step the following results were observed. The reaction at 850°C when fusing a mole of zircon with a mole of sodium hydroxide was the most efficient in consuming sodium hydroxide. This reaction condition was able to liberate 0.58 moles of zirconia per mole of sodium hydroxide. The highly improved efficiency was attributed to the formation of phases Na_2ZrSiO_5, $Na_4Zr_2Si_3O_{12}$ and ZrO_2. The process is pseudo-catalytic as it liberates zirconium while showing minimal sodium consumption. Decomposition at 650°C also showed improved efficiency but not as efficient as the 850°C sub-stoichiometric fusion. The improved decomposition was attributed to the polymerisation of the orthosilicate monomers Na_4SiO_4 to the metasilicate chains Na_2SiO_3.

Complete decomposition of zircon was observed at 850°C when fusing a mole of zircon with four moles of sodium hydroxide. The improved efficiency of this reaction condition was attributed to the formation of the phases Na_2ZrSiO_5, Na_2ZrO_3 and Na_2SiO_3. The phase Na_2ZrSiO_5 minimises sodium consumption.

The intermediate milling step was not introduced in these processes. It was moved from milling after to milling during fusion. Besides the improved zircon decomposition, there is no need for further milling after fusion as the powder has a small particle size ready for water dissolution.

Washing in-situ ZBS (ZBS that was prepared from in-situ hydrous zirconia with stoichiometric amounts of sulphuric acid) once with 0.5M HCl was necessary to remove radioactive impurities to levels below parts per million.

Washing Ref. ZBS (ZBS that was prepared by precipitation from a zirconyl chloride solution with stoichiometric amounts of sulphuric acid) leads to negligible zirconia losses (< 2% m/m ZrO_2 when digesting with 1M HCl). This method offers a solution to the zirconia losses associated with washing in-situ ZBS with mineral acids. The zirconia and zirconium chemicals synthesised here are the purest obtained to date, when compared to other zirconium recovery processes. The processes used are far too rapid (in terms of time and number of steps) when compared to precipitation, crystallisation or ion-exchange techniques. The purity is attributed to the digestion of impurities in a mineral acid (e.g. HCl or HNO_3) environment. In this environment the ZBS remains insoluble.

The high amounts of silica concentrated in the unreacted zircon can be separated by physical means from the undecomposed zircon due to the large density difference between the two. This allows re-circulation of unreacted zircon.

The alkali silicate by-product contains radioactive impurities below parts per million. This is an indication that the radioactivity impurities remained insoluble during water leaching. The radioactive impurities can be collected by precipitation or crystallisation and disposed of safely.

KEYWORDS: Baddeleyite, Characterisation, Design, Efficiency, in-situ ZBS, Optimise, Process, Ref. ZBS, Sub-stoichiometric, Zircon, Zirconia and Zirconium chemicals

REFERENCES

1. Hedrik, J. B. (1997) Zirconium, U.S. Geological Survey-Minerals Information.
2. Skidmore, Charles (1998) Zr oxides and chemicals, Sources, markets and Outlook, Industrial Minerals.
3. Reeves, R. G. (2 000) Zircon out West, Progress on the escalante Utah zircon trend, Industrial Minerals.
4. Blumenthal, W.B. (1958) The Chemical Behaviour of Zirconium, Van Nostrand, N.J., U.S.A. New York.
5. Anil K. Mukherji, (1970) Analytical Chemistry of Zirconium and Hafnium, Pergamon press.
6. Ralph Nielsen, Teledyne Wah Chang, (1996) Ullman's Encyclopaedia of Industrial Chemistry, A (28) 543-567.
7. Hyde, B. G. Andersson, S. (1989) Inorganic crystal structures, A Wiley-Interscience publication, New York.
8. Jenkins, D. H. (1986) Process for the production of high purity zirconia powder. International patent WO 86/04614. World intellectual property organisation.
9. Hancock, J.D. (1977) A review of conventional and novel processes for the extraction of zirconia from zircon. Mineral Science and Engineering, 1 (9) 25-31.
10. Olby, J. K. (1963) Manufacture of zirconium oxide from zircon, U.S. Patent 3,109,704.
11. Recasens, J. Urffer, D. Ferlanda, P. (1992) Reactive zirconium oxide and its preparation, U.S. Patent 5149510.
12. Farnoworth, F. Jones, S. L. and McAlpine, I. (1980) The Production, Properties and uses of zirconium chemicals, Magnesium Elektron Ltd. Twickenham, U. K.
13. Houchin, M. R. Jenkins, B.E. Sinha, (1990) H.N Production of high quality zirconia for ceramics, Mineral, Materials and Industry 14th congress of the council of mining and metallurgy Institute.
14. Schoenlaub, R. A. (1955) Production of calcium zirconate, U. S. Patent 2,721,117

15. Schoenlaub, R. A. (1974) Method of Manufacturing zirconium oxide and salts, U. S. Patent 3,832,441.
16. Herzfield, H. (1914) German patent 290, 878 followed by (1916) J. Soc. Chem. Ind., (35) 634.

In memory of my late mother Nobahle Tissang

And learned friend Dr Willem de Wet.

Sidudla mgane wam ndiyakuthanda.

Kutheni izolo ubungekho?

Ndiyakutshela udlala ngam!

ACKNOWLEDGEMENTS

"This thesis symbolises a reunion of friends with some of the finest talents in zirconium process chemistry, engineering and molecular spectroscopy. I hope the joy and tears that I shared with the people involved along with the integrity, energy and love that each and everyone brought to this work, is as much a part of your learning experience as it was and still is for me."

Zola Kwela

Special Thanks

Dr. W. de Wet you were a very diligent old man. Thanks for the many stories you told me. I was very privileged to have worked with you. You taught me so much in such a brief period.

Prof. Walter Focke thanks for the never-ending energy, the constructive criticism, for being so approachable and for being a friend. Walter I cannot compare you to anyone, but the great man that you are.

Prof. D de Waal, for your contributions in my research and criticism, Danita thank you. For making me meet Bouchaib, I owe you.

Dr. B. Manoun thanks for working with me, although you never took me to the Mosque! I won't forget the jokes from Morocco. Now I know why Morocco won't host the soccer world cup.

Dr J. Nel your contribution came at a very critical time and made things very easy for me.

Thanks to Sabina Verryn and Maggi Loubser, for the exhaustive XRD and XRF.

Thanks to Morgan Govender who helped me a great deal when work seemed to overwhelm me.

My fellow students, together we employed guerrilla tactics to get through a bush full of booby traps.

TABLE OF CONTENTS

TABLE OF CONTENTS CONTINUED… PAGE

TABLE OF CONTENTS CONTINUED… PAGE

TABLE OF CONTENTS CONTINUED… PAGE

TABLE OF CONTENTS CONTINUED… **PAGE**

TABLE OF CONTENTS CONTINUED… PAGE

ABBREVIATION LIST

AFDZ	Alkali fused decomposed zircon
AZST	Acid zirconium sulphate trihydrate
BZC	Basic zirconium carbonate
BZS	Basic zirconium sulphate
Ca-PSZ	Calcia partially stabilised zirconia
Ca-CSZ	Calcia cubic-stabilised zirconia
Ce-TZP	Ceria tetragonal zirconia polycrystal
CSZ	Cubic stabilised zirconia
c-ZrO_2	Cubic zirconia
DZ	Dissociated zircon
DP	Decomposed product
Mg-CSZ	Magnesia cubic-stabilised zirconia
Mg-PSZ	Magnesia partially stabilised zirconia
m-ZrO_2	Monoclinic zirconia
PSZ	Partially stabilised zirconia
R-AZST	Radioactive zirconium sulphate
Ref. ZBS	Reference zirconium basic sulphate
SEM	Scanning electron microscope
TZP	Tetragonal Zirconia polycrystal
t-ZrO_2	Tetragonal zirconia
XRD	X-ray diffraction
XRF	X-ray fluorescence
ZBC	Zirconium basic carbonate
ZBS	Zirconium basic sulphate
ZOC	Zirconyl chloride
ZST	Zirconium sulphate tetrahydrate

Chapter 1

INTRODUCTION

There are two industrial sources of zirconia- zircon and baddeleyite [1-5]. South Africa has the largest reserves of zircon sand [1-3], with the completion of phase two in Namakwa, the production of zircon is to be increased by about 133 000 tons per annum [2]. This is sure to put South Africa as the leading producer of this mineral in the near coming future. The baddeleyite reserves in Phalaborwa are expected to be depleted by the year 2 005 [1-3]. This leaves the Russian baddeleyite (mined in the Kola Peninsula) and zircon as the only industrial sources of zirconia.

The major drawback to zircon use is the large amounts of impurities it is usually found concentrated with, especially radioactive impurities (Uranium and Thorium) [2-3]. Acid leaching of zircon does not remove impurities to acceptable levels [4-5, 18]. The impurities are usually included in the zircon lattice. The tetragonal structure of zircon with the high coordinated bisdisphenoids ZrO_8 and low coordinated tetrahedra SiO_4 create a safe (inaccessible and safe) habitat for these impurities [7, 18].

The production of high purity zirconia and zirconium chemicals from zircon sand by current means also does not remove these impurities to acceptable low levels [4-6, 8-15, 18]. The radioactivity level is still suspect. This can simply be blamed on the purification methods: magnetic separation, mechanical separation and predominantly precipitation. A disadvantage of the precipitation method is the slow nature requiring long process times. Precipitation is a process that needs to be repeated to achieve the required levels.

In 1914, Herzfield [16] patented the process of crystallising zirconyl chloride from saturated solutions of hydrochloric acid. Another purification process that has been exploited throughout the years is the formation of sulphate compounds. Zirconium sulphate tetrahydrate can be crystallised from saturated solutions. Zirconium basic sulphate can be precipitated from a zirconyl chloride solution with stoichiometric amounts of sulphuric acid [4-6]. Most processes proposed throughout the years have been exploiting this basic purification method [8-15]. The methods have been exploiting, repeated crystallisation or even combinations of both chlorine and sulphate systems [8]. These methods are time consuming and have effluents (chlorine or sulphate) associated with them. Solvent extraction and ion exchange methods have also been investigated [17-18]. The purity of the products is still suspect.

Recently, De Wet [19] patented a process were he prepared in-situ ZBS and digested the impurities with a mineral acid (e.g. HCl, HNO_3 or HCl/HNO_3). The method is very rapid because it does not precipitate the ZBS but prepares it from a hydrated zirconia source e.g. $ZrO_2.nH_2O$. ZBS is stable to mineral acid washes, even digestion with 1.0 M HCl at 90°C leads to negligible zirconia losses (~10 % m/m). De Wet exploits the ZBS stability to synthesise the purest zirconium compounds to date rapidly.

The objective of this study was to characterise and optimise the De Wet's alkali fusion processes for the beneficiation of zircon sand into high purity zirconia and zirconium chemicals. However, at each process step some factors were varied e.g. fusion temperature, reactant ratios and composition of leach solutions. Reducing the number of process steps was also explored. The products produced at each step were analysed. Particular attention was given to the fate of the radioactive impurities.

REFERENCES

1. Hedrik, J. B. (1997) Zirconium, U.S. Geological Survey-Minerals Information.
2. Skidmore, C. (1998) Zr oxides and chemicals, Sources, markets and Outlook, Industrial Minerals.
3. Reeves, R. G. (2 000) Zircon out West, Progress on the escalante Utah zircon trend, Industrial Minerals.
4. Blumenthal, W.B. (1958) The Chemical Behaviour of Zirconium, Van Nostrand, N.J., U.S.A. New York.
5. Anil K. Mukherji, (1970) Analytical Chemistry of Zirconium and Hafnium, Pergamon press.
6. Ralph Nielsen, Teledyne Wah Chang, (1996) Ullman's Encyclopaedia of Industrial Chemistry, A (28), 543-567.
7. Hyde, B. G. Andersson, S. (1989) inorganic crystal structures, A Wiley-Interscience publication, New York.
8. Jenkins, D. H. (1986) Process for the production of high purity zirconia powder. International patent WO 86/04614. World intellectual property organisation.
9. Hancock, J.D. (1977) A review of conventional and novel processes for the extraction of zirconia from zircon. Mineral Science and Engineering, 1 (9) 25-31.
10. Olby, J. K. (1963) Manufacture of zirconium oxide from zircon, U.S. Patent 3,109,704.
11. Recasens, J. Urffer, D. Ferlanda, P. (1992) Reactive zirconium oxide and its preparation, U.S. Patent 5149510.
12. Farnoworth, F. Jones, S. L. and McAlpine, I. (1980) The Production, Properties and uses of zirconium chemicals, Magnesium Elektron Ltd. Twickenham, U. K.
13. Houchin, M. R. Jenkins, B.E. Sinha, (1990) H.N Production of high quality zirconia for ceramics, Mineral, Materials and Industry 14th congress of the council of mining and metallurgy Institute.
14. Schoenlaub, R. A. (1955) Production of calcium zirconate, U. S. Patent 2,721,117
15. Schoenlaub, R. A. (1974) Method of Manufacturing zirconium oxide and salts, U. S. Patent 3,832,441.
16. Herzfield, H. (1914) German patent 290, 878 followed by (1916) J. Soc. Chem. Ind., (35) 634.
17. Murty, B. N. Yadav, R. B. and Syamsundar, S. (1994) Preparation of high-purity zirconia from zircon: an anion-exchange purification process (29) 249.

18. Molapisi, J. J. (1998) The removal of radioactive compounds from fluorozirconic acid solutions, MSc Thesis, University of Pretoria, Pretoria, South Africa.
19. De Wet, W. J. (1999) Method for treating zircon sand, S. A. patent 2000/2797.

Chapter 2

ZIRCONIUM MINERAL SOURCES

2.1 ZIRCONIUM

Zirconium, chemical symbol Zr and electron configuration [Kr]$4d^2 5s^2$, is a ductile, lustrous, heavy metallic element with a high melting point of approximately 1 852°C. Like titanium, zirconium metal is hard and corrosion resistant, resembling stainless steel in appearance [1-3]. Zirconium belongs to the titanium subgroup IVB of the periodic table with a normal valency of four, whilst its coordination number can reach eight [2-3]. Its atomic number is 40 and that of Hafnium is 72. It mainly forms colourless compounds, which are regarded to be of low toxicity [3].

TABLE 2.1: MINERALS CONTAINING ZIRCONIUM [4] (Concentration in mass percent)

NAME	OBSERVED ZrO_2 CONTENT
Industrially important	
Baddeleyite	Up to ~97.4 – 97.5% ZrO_2
Zircon	$ZrSiO_4$ with up to 66% ZrO_2
Metal zirconium silicates	
Anderbergite	A complex vanadium-zirconium silicate
Catapleiite	$Na_2ZrSi_6O_{15}.3H_2O$ with up to ~40% ZrO_2
Dalyite	$K_2ZrSi_6O_{15}$
Elpidite	$Na_2ZrSi_6O_{15}.3H_2O$ with up to 20% ZrO_2
Minerals containing Zirconium as Impurities	
Chalcolamprite	A zirconium niobate-silicate, ~5.7% ZrO_2
Aahrenite	Usually about 3-4% ZrO_2
Arfvedsonite	Up to ~7% ZrO_2
Astrophyllite	$(K, Na)(Fe,Mn,Al)_4(Zr, Ti, Si)_{14}(OH, F)_2$
Aurlite	Up to ~3% ZrO_2
Beckelite	Up to ~2.5% ZrO_2
Cerite	Up to ~8% ZrO_2
Columbite	Up to ~11% ZrO_2
Endeolite	Up to ~3.8% ZrO_2
Eucolite and Eudialite	$Na_{13}(Ca,Fe)_6Cl(Si, Zr)_{20}O_{52}$ with up to 17% ZrO_2
Fergusonite	Up to ~2% ZrO_2
Guarinite and Hiortdahlite	$Na_2Ca_4F_2(Si, Zr)_5O_{14}$ with up to 22% ZrO_2
Loranskite	Up to 20% ZrO_2
Lorenzenite (Ramsayite)	Up to ~11.9% ZrO_2
Polymignite	Up to ~29% ZrO_2
Uhligite	$Ca(Ti, Zr)O_5.Al_2TiO_5$, up to 33% ZrO_2
Zirkelite	$(Ca, Fe)_{0.2}(Zr, Ti, Th)O_2$ with up to 53% ZrO_2

Zirconium does not occur in nature freely as the element, but as zirconium silicates in zircon and its metamic forms, zirconium dioxide in baddeleyite, zirconium silicates with sodium, calcium, etc., zirconium carbonates with sodium, calcium etc., and others (Table 2.1) [4].

In addition zirconium is found as an impurity in many minerals such as titanates, niobanates, tantaloniobates, rare-earth silicates, etc... [4].

The number of known minerals containing zirconium exceeds thirty, but only baddeleyite and zircon are currently of industrial importance [3].

Zirconium is the eighteenth most abundant element and the ninth most abundant metal in the Earth's crust. It has an average element abundance of 160-165 parts per million (Table 2. 2) [4-5].

TABLE 2.2: ABUNDANCE OF THE ELEMENTS OF THE TITANIUM GROUP IN THE EARTH'S CRUST [8]

ELEMENT	CONCENTRATION (ppm)	RANKING
Titanium	6 320	9
Zirconium	160-165	18
Hafnium	2.8	45

Hafnium, chemical symbol Hf and electron configuration $[Xe]4f^{14}5d^{2}6s^{2}$, is an element of the zirconium subgroup that always accompanies zirconium and does not form its own minerals[1]. Usually the hafnium to zirconium ratio in different ores varies from approximately 0.01 to 0.02. This also reflects their abundance ratio in the earth's crust.

It is possible to find ores (Hafnon, hafnium orthosilicate) with a hafnium content larger than 95% (m/m) as was the case with a tantalum ore found in Mozambique [6]. Usually ores with a high hafnium content contain more radioactive elements [6].

Hafnium, like zirconium, is also highly resistant to corrosion and exhibits similar chemical properties. Zirconium is practically unaffected by water, hydrochloric, nitric, dilute sulphuric acid, alkali solutions, even on heating. Dissolution of both metals is observed in HF and mixtures of HCl with HNO_3 [1]. Upon heating, both metals readily react with oxygen or nitrogen to form metal oxides or nitrides.

FIGURE 2.1 A picture of Zircon Sand [Picture by: www. zrchem.com]

2.2 ZIRCON

Zircon, the natural form of zirconium silicate $ZrSiO_4$, is the most abundant and widely distributed zirconium commercial mineral [3]. It is found as an accessory mineral in silica rich igneous rocks such as granite, pegmatite, and nepheline syenite [3, 6]. Sedimentary and metamorphic rocks also contain zircon but in small amounts [6]. Because of its high specific gravity of 4.6-4.8, zircon is found concentrated with other heavy minerals such as rutile, ilmenite, monazite, leucoxene and garnet in river and beach sands with titanium and iron as the main constituents [6, 10].

Zircon is usually produced as a by-product in the mining and processing of heavy-mineral sands for the recovery of the titanium minerals, rutile and ilmenite; consequently there are no mines totally devoted to zircon [6]. Typical zircon chemical and physical analysis are provided in Table 2.3 and 2.4 below.

TABLE 2.3: TYPICAL ZIRCON CHEMICAL ANALYSIS (Concentration in mass percent)

COMPOSITION	RICHARD'S BAY	NAMAKWA ZIRCON	SARM13	UTAH ZIRCON
$ZrO_2 + HfO_2$	66.2	66.2	63.31	68.45
SiO_2 (total)	32.6	32.46	32.56	
Fe_2O_3	0.05	0.05	0.187	< 0.1
TiO_2	0.11	0.11	0.295	0.03
Al_2O_3	1.2	0.24	0.61	0.07
Na_2O				
Cr_2O_3	< 0.01	< 0.01		< 0.01
CaO	< 0.05	0.05	0.14	0.02
P_2O_5	0.11	0.11		
V_2O_5	0.01	0.01		
Y_2O_3				
MgO			440 ppm	< 0.01
U		235 ppm	328 ppm	
Th		165 ppm	300 ppm	
U + Th		400 ppm	628 ppm	< 150 ppm

The grades called Superfine and microfine are prepared from the mineral zircon mined at Richard's bay in South Africa. The concentration of the radioactive compounds was not supplied, but by looking at SARM 13, the XRF standard (SABS approved, originally in 1981 and revision date not given) of zircon sand from the same place, a broad-spectrum analysis is given. The zircon grade from Utah has been found to contain the least amount of radioactivity when compared with other zircon grades [12].

The physical properties of some of the above mentioned zircon grades are given below.

TABLE 2.4: TYPICAL ZIRCON PHYSICAL ANALYSIS (COMMERCIAL GRADES)

Parameter	Superfine (5μm)	Microfine (6μm)
Mean particle size d_{50}	1.55μm	1.7μm
Melting point	2 200°C	2 200°C
Specific gravity	4.6-4.8	4.6-4.8
pH	7.1-8.8	7.1-8.8
Loss on ignition	0.15-0.35%	0.15-0.35%

TABLE 2.5: ZIRCONIUM MINERAL PRODUCTION BY COUNTRY 1/ 2/

(Production in metric tons)

COUNTRY	1993	1994	1995	1996	1997 e/
Australia	414 000	511 000 r/	518 000 r/	502 000 r/	424 000 3/
South Africa e/ 6/	243 000	226 000	250 000	300 000	360 000
Brazil 4/	13 252	17 064	16 343	17 000 r/	17 000
China e/	15 000	15 000	15 000	15 000	15 000
India e/	17 000	18 000	18 000	19 000	19 000
Indonesia e/	2 500	2 500	2 000	2 000	2 000
Malaysia	2 184	1 656	3 790	4 511 r/	2 500
Russia e/ 5/	2 500	3 000 r/	4 000 r/	4 500 r/	5 000
Sierra Leone e/	1 200	1 300	---	---	---
Sri Lanka	14 401	22 310	21 971 r/	15 863	16 000
Thailand	707	326	---	---	---
Ukraine	70 000	65 000	60 000	55 000	65 000
United States	W	W	W	W	W

KEY: e/ Estimated. r/ Revised. W/ Withheld to avoid disclosing company confidential data. 1/ World data and estimated data are rounded of to three significant figures 2/ includes data available through June 18, 1998. 3/ Reported figures. 4/ Includes production of baddeleyite-caldasite. 5/ Includes baddeleyite production. 6/ Includes production of by-product zircon from titanium sands mining and 10 000-15 000 tons per year baddeleyite from Phalaborwa Mining Co. Ltd. [5].

The world production of zirconium mineral concentrates in 1997 was estimated to be 926 000 metric tons (Table 2.5). This was a decrease of approximately 1% compared to 1996, excluding the production from the United States (U.S). Australia and South Africa supplied about 85% of all production outside the U.S. Australia is still the largest producer at approximately 400 000 metric tons per annum. South Africa produces around 300 000 metric tons mostly from Richards Bay. Namakwa sands is also expected to increase production soon with the completion of the construction of another zircon plant, Phase 2 in the year 2 000. This is expected to contribute about 133 000 metric tons per annum [12].

2.3 BADDELEYITE AND ZIRCONIA

Baddeleyite is the naturally occurring monoclinic form of zirconia. It always contains a small amount of hafnium oxide together with other impurities [3, 11]. Baddeleyite is the second most important zirconium mineral after zircon, when compared in terms of availability and price [3].

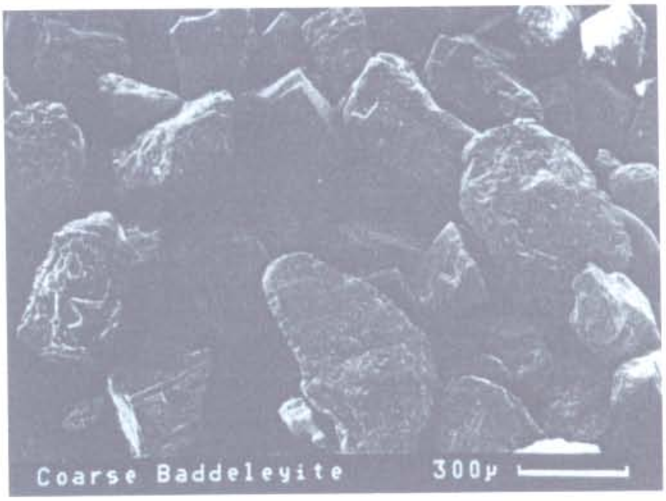

FIGURE 2.2 SEM micrograph of coarse South African Baddeleyite [9]

PMC recovers baddeleyite as a by-product of one of the world's largest open-cast copper mines, whilst Foskor recovers the mineral from phosphate deposits [11]. Beneficiation of the mineral at PMC is by gravity separation of heavy minerals, followed by acid leaching or magnet separation to produce commercial Grades **1**, **2** and **3** as shown in Table 2.6 below. The baddeleyite grades produced by Foskor, labelled **99E** in the same Table 2.6. The Baddeleyite grade, labelled Grade **R**, has the lowest radioactivity level. Kovdor Mining and Dressing Mills produce it as a by-product from iron ore mining in the Kola Peninsula.

TABLE 2.6: CHEMICAL COMPOSITION OF BADDELEYITE [11]

(Concentration in mass percent)

COMPOSITION	GRADE **1**	GRADE **2**	GRADE **3**	GRADE **99E**	GRADE **R**
$ZrO_2 + HfO_2$	99.0 min	99.0 min	99.0 min	> 98	97.5-98.4
SiO_2 (total)	0.25-0.5	0.25-0.4	0.25-0.35	< 1.0	0.5-0.8
TiO_2	0.20-0.30	0.20-0.25	0.20-0.25	≤ 0.3	0.15
ThO_2	0.005-0.025	0.005-0.025	0.005-0.025		
ThO_2/U_3O_8					0.03-0.05
U_3O_8	0.07-0.10	0.07-0.10	0.07-0.10		
CeO_2	0.05-0.1	0.05-0.10	0.05-0.1		
Total activity				< 500Bq/g	
Fe_2O_3	0.10-0.3	0.06-0.20	0.06-0.20	≤ 0.3	0.1-0.15
CuO	0.01-0.1	0.01-0.1	0.01-0.1	≤ 0.05	0.01 max
Al_2O_3	0.03-0.05	0.03-0.05	0.03-0.05		0.01-0.03
CaO	0.05-0.1	0.05-0.1	0.05-0.1		0.30-0.50
P_2O_5	0.10-0.20	0.05-0.10	0.05-0.10	< 0.05	0.15-0.30
SO_3					0.07-0.16

The physical properties of the above mentioned baddeleyite grades are given below in Table 2.7 below.

TABLE 2.7: PHYSICAL PROPERTIES OF BADDELEYITE ORES [11]

Property	Grade **1**, **2** and **3**	Grade **99E**	Grade **R**
Colour	Grey-black sand	Black powder	Red sand-like powder
Bulk density	3.1 g/cm^3	3.05-3.15g/cm^3	
Melting point	2 700°C		
Specific gravity	5.8-6.0	± 5.76	
Crystal structure	Monoclinic	Monoclinic	

2.4 CONCLUSIONS

1. Zirconium and Hafnium are elements of the titanium subgroup (IVB). They have very similar physical and chemical properties.
2. Hafnium is usually contained within the crystal lattice of zirconium minerals.
3. Zirconium usually occurs in nature as zircon or zirconia. It is also an impurity in many compounds such as titanates, niobanates, tantaloniobanates, rare-earthsilicates, etc.
4. Zircon the most important zirconium mineral, is usually found concentrated with other heavy minerals such as rutile, ilmenite, monazite, leucoxene garnet, etc.
5. Zircon has the following physical properties: specific gravity of 4.6, melting point is approximately 2 200°C and Hardness in Mohs approximately 7.5.
6. The main producers of zirconium minerals in the world are Australia and South Africa. Together they supplied approximately 85% of a total of 926 000 metric tons in the year 1997. South Africa is expected to increase production by about 133 000 metric tons in the year 2 000 due to the completion of Phase 2 in Namakwa.
7. Baddeleyite is the naturally occurring monoclinic form of zirconia. South Africa produces baddeleyite that is virtually silica free. They are also the main producers of this mineral.
8. Grade R from Russia has the lowest radioactivity content than any other grades produced commercially.

2.5 REFERENCES

1. Elinson, S. V. and Petrov, K. I. (1969) Analytical chemistry of zirconium and hafnium, translated by N. Kaner, Ann Arbor, London.
2. MacDermott, T. E. (1973) The structural chemistry of zirconium compounds, Coordination Chemistry Reviews, (11) 1-20.
3. Farnworth, E. Jones, S. L. and McAlpine, I. (1980) The Production, Properties and uses of zirconium chemicals, Magnesium Elektron Ltd. Twickenham, U.K.
4. Blumental, W. B. (1958) The chemical behaviour of zirconium, Nostrand Company, inc., New York.
5. Hedrik, J. B. (1997) Zirconium, U.S. Geological Survey-Minerals Information.

6. Nielsen, R. and Chang, T. W. (1996) Ullman's Encyclopaedia of Industrial Chemistry, A (28) 543-567.

7. McColm, I. J. (1994) Dictionary of Ceramic Science and Engineering, second edition, Plenum press, New York.

8. Lee, J. D. (1991) Concise inorganic chemistry, John Wiley, New York.

9. Stevens, R. (1986) Zirconia and Zirconia ceramics, Magnesium Elektron Ltd., Twickenham, U.K.

10. Burt, R. (1999) The role of gravity concentration in modern processing plants, Minerals Engineering 11 (12) 1291-1300.

11. Skidmore, C. (1998) Zr oxides and chemicals, Sources, markets and Outlook, Industrial Minerals.

12. Reeves, R. G. (2 000) Zircon out West, Progress on the escalante Utah zircon trend, Industrial Minerals.

CHAPTER 3

ZIRCONIUM APPLICATIONS

[Picture by: www.zrchem.com]

3.1 INTRODUCTION

Zirconium chemicals are used in diverse applications. Of all the zirconium consumed, about 95% is in the form of zircon, zirconia and zirconium chemicals; the remainder is consumed as the metal and its alloys [1]. The major consumer of zirconia is the refractory industry with approximately 15 000 metric tons per annum, for the year 1998 [1, 13-14]. It is estimated that the consumption of zircon for zirconia in the year 2 000 could be around 37-40 000 tons [13-14]. This chapter highlights only but a few of the uses of zircon, zirconia and zirconium chemicals, with emphasis on the most popular applications.

3.2 ZIRCON

Zircon is the mineral in which zirconium silicate $ZrSiO_4$ occurs in nature [2, 6]. Zirconium silicate exhibits some resistance towards acids and cold alkali solutions, but it is readily attacked by sodium hydroxide NaOH, at approximately 600°C and even more vigorously by sodium oxide Na_2O [2, 3]. Table 3.1 below supplies the physical properties of zircon necessary for its industrial applications.

TABLE 3.1: SELECTED PROPERTIES OF ZIRCON [18-19]

Property	Value
Range of found densities, g/cm^3	3.9-4.8
Melting point, °C	2250
Coefficient of linear expansion α, between 1250-1550°C	$35\text{-}42 \times 10^{-7}$
Thermal conductivity, W/mK	4.0-5.86
Hardness, Mohs	7.5
Refractive index (n_D^{20})	1.85
Decomposition temperature, °C	1676

3.3 ZIRCONIA

Zirconia is the oxide ZrO_2 that occurs in nature as the mineral baddeleyite. Zirconia usually exhibits three phases at different temperatures: monoclinic [m-ZrO_2; C_{2h}^5 ($P2_1/c$); Z=4] below 1 000°C, tetragonal [t-ZrO_2; D_{4h}^{15} ($P4_2/nmc$); Z=2] above 1 170°C and cubic [c-ZrO_2; O_h^5 (Fm3m); Z=4] above 2 370°C until its melting point at 2 700°C [2, 5, 17]. A fourth phase orthorhombic zirconia o-ZrO_2 has also been found, but is metastable under atmospheric pressure and transforms to into m-ZrO_2 [18]. It is this polymorphism that limits the use of zirconia, because transformation from the tetragonal to the monoclinic phase is usually accompanied by a volume shrinkage of about 3-5%, enough to cause fracture [5]. The high temperature cubic phase can be stabilised by the addition of cubic oxides such as yttria Y_2O_3, magnesia MgO, calcia CaO, even rare earth oxides [2, 5].

Partially stabilised zirconia (PSZ) can be thermally cycled to produce metastable tetragonal zirconia within the grains of cubic zirconia. The PSZ materials exhibit higher toughness than fully stabilised zirconia materials due to the stress induced martensitic transformation of the tetragonal metastable grains to the monoclinic form in the stress field of a propagating crack [2, 4].

Zirconia is fairly unreactive to many fluxes, melts, molten glass, phosphates, borate, alkalis and acids but is attached by hot concentrated sulphuric acid and hydrofluoric acid.

TABLE 3.2: ESTIMATED WORLD ZIRCONIA CONSUMPTION BY DIFFERENT MARKETS [13-14]

Zirconia use	ZrO_2 derived From zircon	Baddeleyite	Total in Metric Tonnes
Refractories	5 000	10 000	15 000–15 500
Ceramic Pigment, Glazes and Opacifiers	3 000	3 000	6 000
Abrasives	1 500	2 000	3 500
Electronics	1 400-2 000		1 400 – 2 000
Oxygen Sensors	600-850		600 – 850
Glass/Gemstones	350-750		350 – 750
Advanced Ceramics/ Catalysis	2 000		2 000
Onward processing for above markets	1 900	4 000	5 900
Total	17 000	19 000	36 000

3.4 ZIRCONIUM CHEMICALS

This group of chemicals encompasses all the other zirconium chemicals except zirconia and zircon. Table 3.4 shows the diverse applications of zirconium chemicals. Surprisingly only a small amount approximately 10% (about 50-60Kt/a) of the world's produced zircon (about 900Kt/a) is used for the production of zirconium chemicals (Table 3.3) [11]. The use of these chemicals results primarily from their ability to complex with carboxyl groups to form an insoluble organic compound [18].

Zirconium basic sulphate (ZBS) can be used for the production of zirconium basic carbonate (BZC), $Zr_2O_3(OH)_2CO_2.nH_2O$ [11-12]. BZC and ZBS play central roles in the production of many zirconium chemicals. F. Farnworth et. al. (1980) [12] provides more information on the synthesis and applications of these chemicals.

TABLE 3.3: THE WORLD CONSUMPTION OF ZIRCONIUM CHEMICALS (in metric tons) [13]

Product	World Production Capacity
Zirconium Oxychloride ZOC	25 000
Basic Zirconium Carbonate BZC/ZBC	15-18 000
Zirconium sulphates	5–6 000
Basic Zirconium Sulphate	5–6 000
Ammonium Zirconium Carbonate	4-6 000
Zirconium acetate	1 000
Potassium Hexafluorozirconate	1 000
Total	56 000 – 63 000

Zirconium Oxychloride (ZOC) is the largest produced zirconium chemical. ZOC can be regarded as the zirconium chemical with the most possible growth. Many other chemicals can be made from ZOC and with the effects of global warming the use in antiperspirants should increase [13].

3.5 APPLICATIONS

3.5.1 FOUNDRY

Zircon is used as foundry material. This use can be attributed to zircon's low thermal conductivity, high melting point, and chemical stability [3]. Zircon is wetted less easily by molten metal or alloy, thus it produces smooth surfaces on metal or alloy. This is one of the largest consumer of the mineral [18].

3.5.2 REFRACTORY

Zircon is used as a refractory material. This can be attributed to its high melting point of approximately 2 250°C, chemical stability and mechanical strength (hardness in Mohs, approximately 7.5). The use of zircon as a refractory has decreased significantly due to the zircon shortages in the late 1980s being substituted by less expensive refractories such as alumina spinels [2]. The glass and steel industries usually use zircon as a refractory. Fused zircon and alumina zirconia silica (AZS) refractories have a high resistance to molten glass, for this property they are used in the glass industries. The steel industries use zircon in ladles and continuous casting nozzles [2].

Since the early 1980s this has been an area of major growth for baddeleyite. As seen in Table 3.2 this is the major market for zirconia consumption of about 15 000 tons per annum. This area is expected to grow due to the continuous casting of steel in its production that requires high corrosion resistant refractory nozzles, sliding gates and entry tubes with high melting points [13].

3.5.3 ABRASIVES

This was one of the first major applications of zirconia. Zirconia is fused together with alumina to form alumina zirconia abrasives. The zirconia content is approximately 25–40% [2]. The zirconia consumption for this market was about 3 500 tons per annum, but this is expected to decrease due to the growing trend of near net casting which requires little use of machinery with high quality alumina zirconia abrasive grinding wheels [14-15].

3.5.4 OPACIFIER

Another major use for zircon is as an opacifier for tile glazes and porcelain enamels. This use can be attributed to zircon's high refractive index, which gives the glaze a white, opaque appearance [3]. Certain grades of paints use zirconia to coat the surfaces of Titania pigment particles. The zirconia coating acts as an ultra violet stabiliser by minimising the excitation of Titania preventing the ultra violet degradation of the paint molecules [2]. Zirconia has also been used instead of Titania as the pigment in white camouflage paints because it more closely simulates snow in the infrared and microwave spectral region [2].

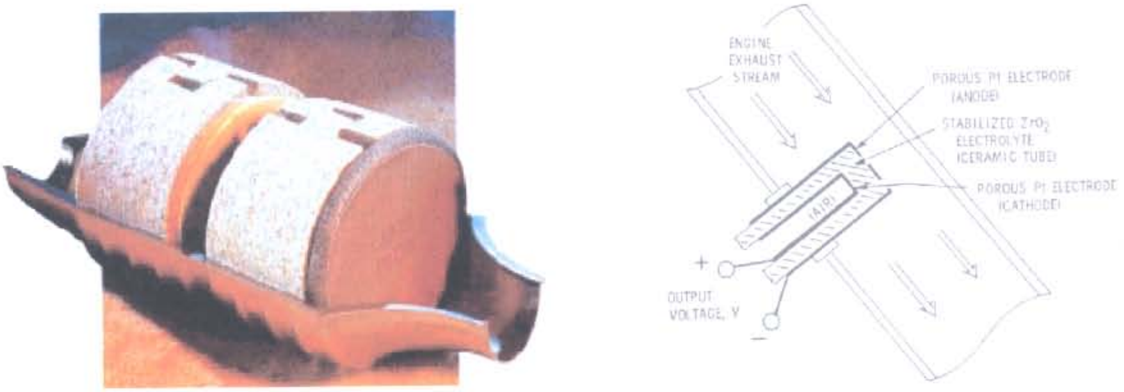

(a) (b)

FIGURE 3.1: (a) A picture of a zirconia-supported palladium and zirconium couple in vehicle exhaust emission control [7]. (b) A Schematic illustration of a zirconia exhaust sensor (cross sectional view) [16].

3.5.5 OXYGEN SENSORS

Zirconia is used as oxygen sensors. This market consumes about 600-850 tons of zirconia per annum [13-14]. One example of the oxygen sensor is the exhaust gas sensor [Figure 3.1 (b)], which usually consists of a zirconia tube with porous platinum electrodes formed on both its inner and outer surfaces. The function of the sensor is to regulate the air-fuel mixture entering the engine by closed-loop process control utilising the zirconia tube as an electrochemical sensor [16].

3.5.6 CATALYSIS

Zirconia is used in catalysis. As seen in Table 3.2 this market consumes approximately 2 000 tons of zirconia per annum. There has been a significant amount of work done in this area and possibly an area of huge industrial growth. Zirconia is used in automobile exhaust systems as catalytic converters, were zirconia forms part of a *wash-coat* in converting poisonous gases into environmentally safe gases [Figure 3.1 (a)] [7]. Zirconia is capable of catalysing a number of reactions, typical examples are as follow: hydrogenation, oxidation, electro-catalysis, esterification, polymerisation and etc. [7]. Zirconium chemicals e.g. Ammonium basic zirconium carbonate (BZC-NH_4) is also used as a reagent to produce catalysts [12].

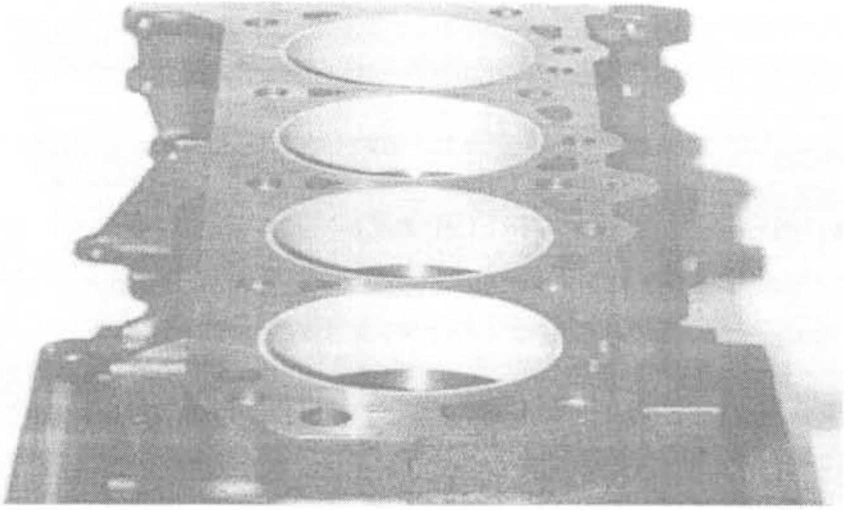

FIGURE 3.2: A picture of partially stabilised zirconia cylinder liners [10]

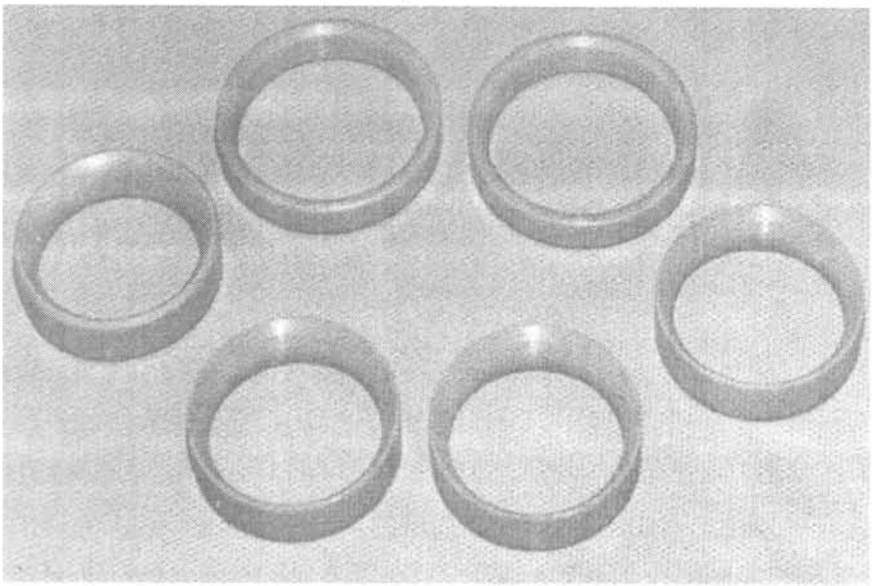

FIGURE 3.3: A picture of a partially stabilised zirconia valve seats [10]

3.5.7 ADVANCED CERAMICS

Partially stabilised zirconia ceramics, PSZ-ceramics, have been commercialised since 1970 [10]. PSZ-ceramics with varying amounts of stabilising cubic oxides show different properties in response to stress at different loading conditions [5, 8, 10]. Dworak et. al. (1983) [10] shows how PSZ-ceramics can be applied to wire drawing technology, thermal shock conditions, combustion engines (cylinder liners, valve seats, bypass valve guides), etc. (Figures 3.2-3.3). PSZ-ceramics can be applied for insulation to these adverse reaction conditions due to their low thermal conductivity, high fracture toughness and high strength.

FIGURE 3.4: A picture of water based paints containing zirconium chemicals [7]

.

3.5.8 PAINT DRYERS

Zirconium chemicals e.g. BZC, ZBS, ZOC and BZC-NH_4, are used in solvent-based alkyds paints as dryers in place of toxic lead dryers and in water-based paints as thixotropes [7]. Zirconium compounds are also used in metal treatment where zirconium fluorides improve the adhesion of coatings on aluminium metals.

3.5.9 PIGMENTS

Zirconia is used in the formation of ceramic pigments. As seen in Table 3.2 approximately 6 000 tonnes of zirconia is consumed by this market. Zirconia can be used together with silica SiO_2 to form zircon based pigments, where the colour is due to the lattice distortion caused by a dopant, like vanadium [9].

TABLE 3.4: Applications of Zirconium Chemicals, Industry and Function [11-12, 13, 18]

Zr Compound	Application	Industry	Note
$BZC\text{-}NH_4$ or ZrA	Waterproofing	Paper & Textiles	Replaces volatile formaldehyde resins
ZrA	Bacteriostatic &antifungicidal	Textiles	Improves wash fastness and Cu salts
$BZC\text{-}NH_4$	Reagent	Catalysis	Production of catalysts
K_2ZrF_6	Suppressant	Paint	Lowers organic solvent emissions
	Flame resistance	Wool	Improves wash fastness and replaces Ti and Cu salts
H_2ZrF_6 or ZrA	Grain refiner	Alloys	Grain refiner (Mg/Al alloys)
ZOC	Corrosion resistance	Paint	Replaces Cr chemicals.
ZOC	Coupling agent	Paint	Replaces silanes
ZOC, AZST	Bacteria oxidation	Antiperspirants	Captures oxygen to oxidise dead bacteria
	Tanning	Leather	Polypeptide cross-linking, (Replaces Cr chemicals)
$\propto\text{-}Zr(HPO_4)_2.H_2O$	Ion exchange	Medical	Kidney dialysis
AZST	U.V stability, abrasion resistance	TiO_2 Pigments	Coating of titanium pigments
ZBS	U.V stability and Starting material	TiO_2 pigment, Processing	Coating of titanium pigments, and Production of zirconium chemicals
ZBC	Starting material	Processing	Production of zirconium chemicals
BZC, ZBS, ZrO	Drier	Paint	Replaces Pb dryers and improves gloss
BZC	Rheology and Thixotropy	Cement and Paint	Replaces organic chemicals and provides a clear finish

KEY: ZrA is an abbreviation for zirconium acetate $H_2ZrO_2(C_2H_3O_2)_2$. BZC or ZBC is basic zirconium carbonate $Zr_2O_3(OH)_2CO_2.nH_2O$. ZOC is zirconium oxychloride $[Zr_4(OH)_8(H_2O)_{16}]C_{18}$ AZST is zirconium sulphate $Zr(SO_4)_{2\cdot4}H_2O$. $BZC\text{-}NH_4$ is ammonium zirconium carbonate $(NH_4)_3ZrOH(CO_3)_3.2H_2O$. ZrO is Zirconium Octoate.

3.6 CONCLUSIONS

1. Zircon is used in plasma spraying, as a refractory, as an opacifier and as foundry. This can be attributed to the chemical and physical properties of zircon.
2. Zirconia, its use is restricted by polymorphism. Partial or full stabilisation with cubic oxides of the cubic phase of zirconia is possible.
3. Zirconia is consumed mainly by the refractory industry. Other uses include ceramic pigments, glazes, opacifiers, electronics, Oxygen sensors, glass, gemstones, advanced ceramics and catalysis.
4. ZBC or ZBS play a central role in the production of zirconium chemicals. Approximately 10% of the produced world zircon is used in the synthesis of zirconium chemicals.

3.7 REFERENCES

1. Hedrick, J. B. (1997) Zirconium, U. S. Geological Survey-Minerals information.
2. Stevens, R. (1986) Zirconia and Zirconia ceramics, Magnesium Elektron Ltd., Twickenham, UK.
3. Nielsen, R. Chang, T. W. (1996) Ullman's Encyclopaedia of Industrial Chemistry, A (28) 543-567.
4. McColm, I. J. (1994) Dictionary of Ceramic Science, second edition, Plenum press, New York.
5. Green, D. J. Hannik, R. and Swain, M.V. (1989) Transformation toughening of ceramics, CRC Press, Florida.
6. Elinson, S. V. and Petrov, K. I. (1969) Analytical chemistry of zirconium and hafnium, Ann Arbor-Humphrey, London.
7. Moles, P. (1998) Zirconium Compounds in Catalysis, http:// www.zrchem.com/
8. Vegter, R. H. (1999) Diffusion bonding of Zirconia, PhD. Thesis, Delft University of Technology, Delft, The Netherlands.

9. Batchelor, R. W. (1974) British Ceramic Society (73) 297.

10. Dworak, U. Olapinski, H. Fingerle, D. and Krohn, U. (1983) ZrO_2 Ceramics for Internal Combustion Engines, Advances in ceramics, Science and Technology of zirconia II (12) 480-487.

11. Zeiss, A. L. and Gieskke, W. E. (1997) Potential for industrial applications of locally produced zirconium chemicals, S. A. J. Chem., (3) 50.

12. Farnworth, E. Jones, S. L. McAlpine, I. (1980) The Production, Properties and uses of zirconium chemicals, Magnesium Elektron Ltd. Twickenham, U. K.

13. Skidmore, C. (1998) Zirconium Oxides/Chemicals: A Review of Raw Materials, Markets and Future Prospects, Industrial Minerals.

14. Mitchell, V. (1995) Zirconia Overview: 1 980–2 000, A paper presented to the industrial minerals information Ltd., Munich, Germany.

15. Pond, J.B. and Depalma, T. (1973) Automot. Ind. (149) 29.

16. Ali, A. A. M. Zaki, M. I (1999) Thermal and Spectroscopic studies of polymorphic transitions of zirconia during calcination of sulphated and phosphated $Zr(OH)_4$ precursors of solid acid catalysts, Thermochimica Acta; (336) 17-25

17. Sumaya, R. Ashida, T. Kume, S. (1986) J. Am. Ceram. Soc., (68) 314.

18. Goodwin, F. E. (1994) Zirconium and Zirconium compounds, Kirk-Othmer encyclopaedia of chemical technology, (25) 852-889.

19. Eppler, R. A. (1996) Ceramic colorants, Ullman's Encyclopaedia of Industrial Chemistry, A (5) 545-555.

CHAPTER 4

THE CHEMISTRY OF ZIRCONIUM

[Picture by: www.zrchem.com]

4.1 INTRODUCTION

The chemistry of zirconium and hafnium is very similar than for any two known congeneric elements [1-4]. This can be attributed to the lanthanide contraction effect that causes both the atomic and ionic radii (14.5 and 8.6nm for Zr and Zr^{4+} and 14.4 and 8.5nm for Hf and Hf^{4+} respectively) to be almost identical [1-5].

The chemistry of zirconium has been pursued only along two lines, the aqueous chemistry and the non-aqueous chemistry. Both methods have their problems. In aqueous solution, zirconium compounds are hydrolysed to hydroxy species then to polymeric species [1- 5]. For the non-aqueous chemistry, solubility of reagents and the use of anhydrous reagents posses a problem of maintaining the anhydrous reaction conditions.

4.2 THE AQUEOUS CHEMISTRY

4.2.1 THE ZIRCONYL GROUP $[Zr=O]^{2+}$

Does the zirconyl group exist, or not? Solovkin and Tsvetkova concluded that this species rarely exists. They based their conclusion on stoichiometric evidence and infra red spectra being vague and bond separation being inconsistent with that expected.

Confusion about the existence of the zirconyl group came from the assumption that zirconium existed in solution as the $[Zr=O]^{2+}$ ions. Thus formulae of chlorides, sulphates, nitrates, and other salts were written as $ZrO(SO_4)$ or $ZrOCl_2.8H_2O$. Well this is not always the case, as it has it been established [11] that zirconium exists in solution predominantly as the tetramer $[Zr_4(OH)_8.16H_2O]^{8+}$.

In contrast, the zirconyl group was observed with the aid of infrared spectroscopy in thiocyanate compounds and with the aid of thermogravimetric analysis the formula $Me[ZrO(SCN)_3H_2O].H_2O$ where Me is NH_4, Rb, K or Cs containing two hydroxyl groups was suggested. Clearfield (1964) [11], opposed this deduction by saying that the sharp absorption band at 913 and 927cm^{-1}could have been due to the δ (SCN) harmonics.

4.3 TETRAMERS

Zielen and Connick. (1956) [9] studied the polymeric nature of the aqueous zirconium species at metal concentration greater than 10^{-3}M and hydrogen ion concentration less than 1M, using spectrophotometric indication reactions. Johnson et al. (1956) [10] also studied this system but used ultracentrifugation. Both confirmed the existence of tetramers, $[Zr_4(OH)_8.16H_2O]^{8+}$, and trimers, $Zr_3(OH)_4^{8+}$, in solution.

Light scattering studies of zirconyl chloride in 2.80M hydrochloric and metal ion concentration of 0.02-0.04M lead to the conclusion that at this concentration range the predominant species is the trimer with a total charge of three. While at lower acid concentrations, such as 0.75M H^+, the polymer appears to be a metal hexamer with a charge less than unity.

Clearfield et al. (1956) [11] provided direct evidence for the existence of polymeric species by X-ray data on zirconyl halides. The halides react vigorously with water to form salts commonly referred to as zirconyl halides. These easily crystallised halides have a general molecular formula $ZrOX_2.8H_2O$ ($X \equiv Cl^-, Br^-, I^-$) were the zirconyl ion is possibly a tetramer, $[Zr(OH)_2.4H_2O]_4^{8+}$. The halogen ions are not bonded to the zirconium atoms but are held in the crystal by electrostatic forces and hydrogen bonds.

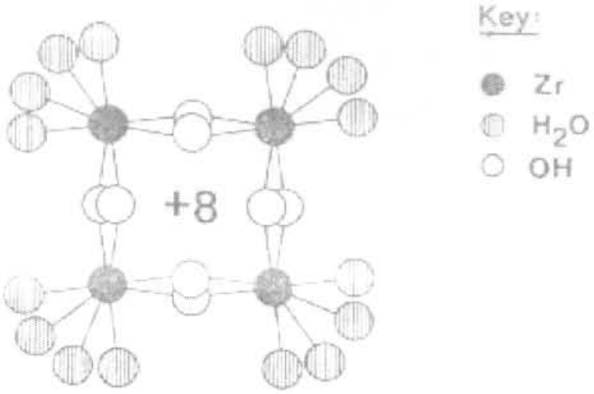

FIGURE 4.1 The structure of the $[Zr_4(OH)_8(H_2O)_{16}]^{8+}$ associated with zirconyl chloride

In the zirconyl ion, four zirconium atoms are located at the corners of a slightly distorted square and are joined by double hydroxyl bridges above and below the plane of the square.

These four oxygen atoms and four more from water molecules are situated about the zirconium at the vertices of an Archimedian antiprism [11].

Hydrolytic polymerisation of these tetramers can be readily achieved by simply ageing, heating or by reduction in acidity [1-5].

4.4 ZIRCONIUM HYDROXIDE CHLORIDES

The compound $ZrOCl_2.8H_2O$ commonly called zirconyl chloride, zirconium oxychloride, and zirconium oxide dichloride are all common names given to zirconium hydroxide dichloride. The real structure is, $[Zr_4(OH)_8.16H_2O]Cl_8.12H_2O$ [1-4, 13]. The hydroxide dichloride is prepared by dissolving hydrous zirconium oxide or zirconium carbonate in hot hydrochloric acid or by hydrolysis of zirconium tetrachloride in water [1-4, 19].

Zirconium hydroxide monochloride, $[Zr_4(OH)_{12}.16H_2O]Cl_4$ is formed in solution by reacting equimolar amounts of hydrochloric acid with hydrous zirconium oxide or zirconium basic carbonate, or by the action of hydrogen peroxide on zirconium hydroxide dichloride [13].

4.5 HYDROLYSIS AND POLYMERISATION

Zirconium and Hafnium compounds have a tendency to hydrolyse in aqueous solutions; this can be attributed to the high charge and small radius [1-4, 13]. Simple zirconium salts, such as tetrahalides react readily with water to form oxyhalides (of general formula $ZrOX_2.8H_2O$) and strongly reducing the pH. For instance, the halide $ZrCl_4$ dissolves in water to form the oxychloride $ZrOCl_2.8H_2O$ and releasing two H^+(aq) ions for oxygen thus, decreasing the pH [1-4]. At 0.05M of a solution of the respective salt the pH is as low as 1. Solovkin (1957) [4] established the following equilibrium reaction and its constants in aqueous solutions at 25°C:

$$Zr^{4+} + nH_2O \leftrightarrow Zr(OH)_n^{4-n} + nH^+$$

SCHEME 4.1 A diagrammatic representation of the reaction for the formation of the hydroxide. For n = 1, the equilibrium constant $K_1 = 0.6$; n = 2, $K_2 = 0.24$; n = 3, $K_3 = 0.09$ and for n = 4, $K_4 = 0.068$.

From the reaction above it can be seen that at low H^+(aq) ion concentration, the formation of the hydroxide increases. The degree of hydrolysis is dependent on the concentration of the initial solution as was noted with increases in dilute solution [4]. Temperature and time was also observed to have extensive effects on hydrolysis.

Clearfield (1964) [12] refluxed aqueous slurries of gelatinous hydrous zirconia that were precipitated from the zirconium chloride or nitrate solutions. He also observed the large decrease in pH on dissolution of the chloride. During refluxing the anions in the hydrous oxide were displaced by hydroxyl groups. The refluxing was capable of transforming the amorphous gel particles into a crystalline product. The initial mixture contained cubic and monoclinic crystallites. After long periods of continued refluxing, the slurries were converted to colloidal, crystalline, hydrous zirconia sols (Figure 4.2).

X-ray line broadening showed that the crystallites contained 12-24 unit cells or differently 48-96 monomer units. The inter-planar spacing of the sol and gel particles were observed to be identical and very close to those in the calcined oxides. The Zr-Zr distance in the sheets is 35.6nm compared to 35.8nm in cubic zirconia. This lead to the observation that within the crystallites the composition must be close to $[ZrO_2]_n$, but the crystalline hydrous oxide particles still retained coordinated water. The crystallites were also observed to contain hydroxyl groups as indicated by their ion exchange properties [17].

The tetramer was also observed to be very stable and it remained intact under very acidic solutions. Each zirconium atom in the tetramer complex is bonded to two sets of double hydroxyl bridges, lying in planes, which are nearly at right angles to each other. Thus it would be expected that olation between any two adjacent tetramer units would occur in such a way as to place the diol bridges at right angles to those already present. But each tetramer group contains numerous olation sites; thus growth can occur can occur in many directions depending on the rate of crystallisation (Figure 4.3). If the olation process were carried indefinitely it would lead to the formation of sheets of composition $[Zr(OH)_4]_n$. Each zirconium atom, not at the edge of the sheet, is surrounded by eight hydroxyl groups in the form of a distorted cubic arrangement, thus changing the original square antiprism coordination to the coordination present in cubic zirconia.

4.6 CARBONATES

Basic zirconium carbonate (ZBC), of empirical formula $ZrO_2.CO_2.xH_2O$ [1-4]. The ratio of $ZrO_2 : CO_2$ has been observed to vary considerably, from 4 : 1 to 1 : 1 depending on the method of preparation [20]. Adding sodium carbonate solution to a solution of zirconium basic sulphate normally produces ZBC. Adding sodium carbonate to a solution of zirconium sulphate to a pH of approximately 6.75 has been observed to precipitate the carbonate $Zr_2O_3(OH)_2CO_2.nH_2O$ with a $ZrO_2 : CO_2$ ratio of 1 : 0.8 [19].

ZBC reacts with sodium or ammonium carbonate solutions to give water-soluble double carbonates e.g. $NH_4[Zr_2O(OH)_3(CO_3)_3]$. None of these carbonates combined with ammonia, confirming the absence of HCO_3^- [1-4].

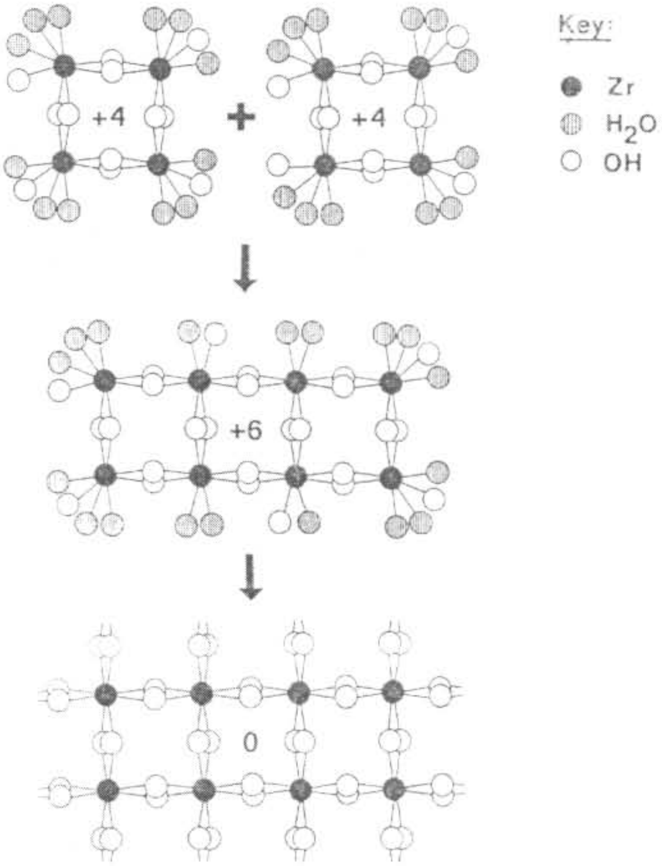

FIGURE 4.2: Schematic representation of the tetramer combination sequence. Polymerisation occurs through olation between the tetramer units. Olation describes the formation of hydro-bridges as a result of hydrolysis.

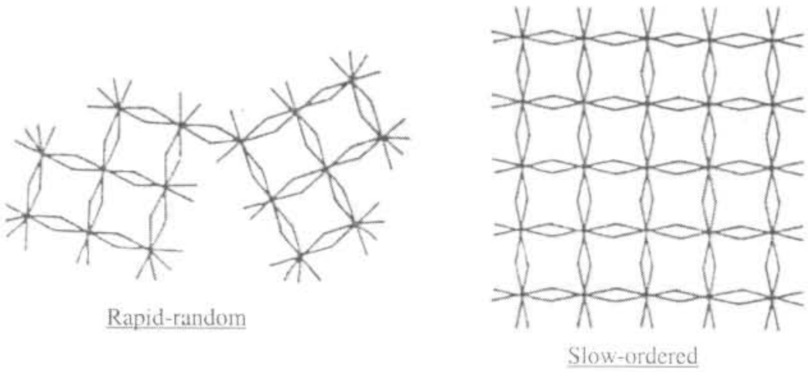
Rapid-random

Slow-ordered

FIGURE 4.3 Schematic representation of the tetramer combination sequence of (a) rapid and (b) slow addition of base upon the structure of gelatinous hydrous zirconia

4.7 ZIRCONIUM SULPHATES

Bear et al. (1971) [15] studied the phase system $Zr(SO_4)_2$-H_2O with respect to its normal salts, where the ratio of Zr/SO_4 in the molecular formula, is one is to two. Thus distinguishing them from the basic and acidic sulphates, where the Zr/SO_4 ratio is greater and less than one is to two, respectively. They were able to establish, with the aid of XRD data, the structure and the conditions under which each sulphate exist.

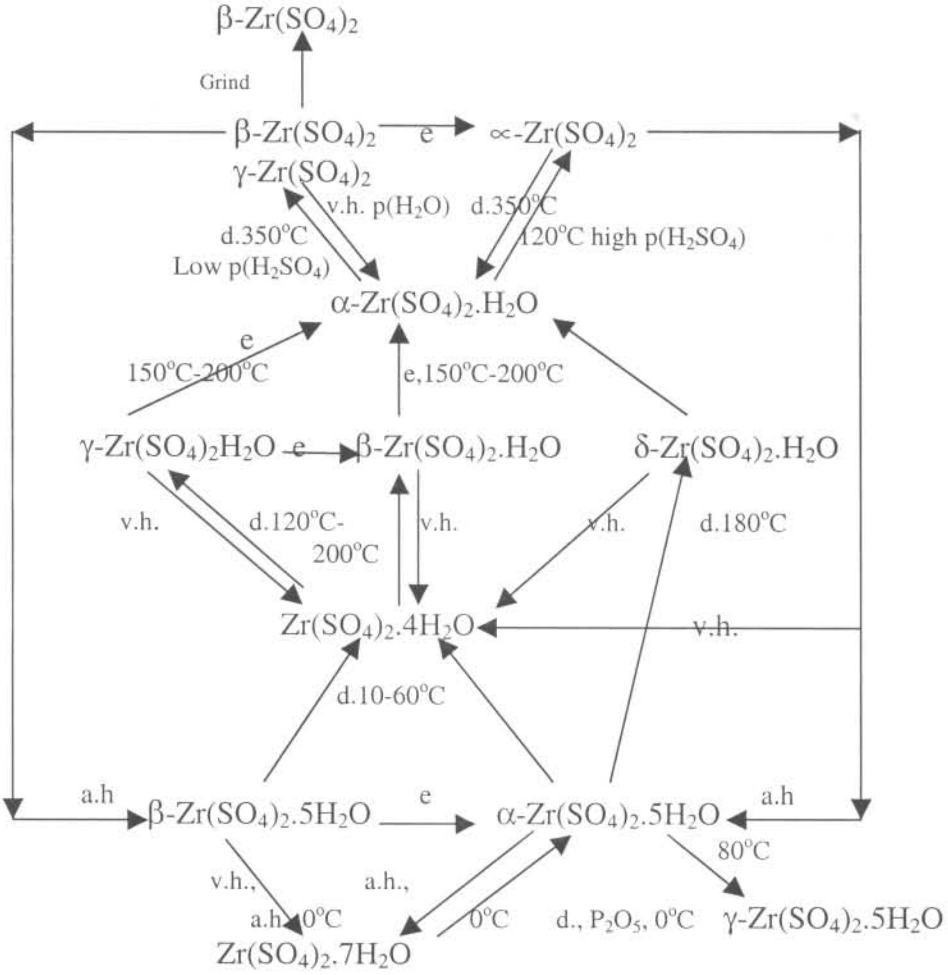

FIGURE 4.4 A diagrammatic representation of the chemical inter-relationships in the $Zr(SO_4)_2$-H_2O system [15]

KEY: a.h., aqueous hydration; v.h., vapour hydration;

e, equilibration; d, decomposition

The sulphate ion strongly complexes the zirconium atom, as is seen in the series [13]:

$$OH^{-} > CO_3^{2-} > PO_4^{3-} \sim C_2O_4^{2-} > SO_4^{2-} > NO_3^{-} > Cl^{-} > ClO_4^{-} > Br^{-} \sim I^{-}$$

SCHEME 4.2 A representation of the zirconium complex series

In comparison to the sulphate, the nitrate, chloride, and perchlorate ions are weak complexing agents and show little tendency to form bridges between zirconium atoms. The sulphate is capable of displacing the hydroxy group from a hydrolysed zirconium species to form sulphate bridges between zirconium atoms.

Further proof of the complexing ability of the sulphate ion is seen in the large number of salts that form between the zirconium ion and the sulphate ion [1]. The well-known stable normal sulphate, zirconium sulphate tetrahydrate, $Zr(SO_4)_2.4H_2O$, often called acid zirconium sulphate trihydrate (AZST), crystallises easily out of relatively strong sulphuric acid solutions [2]. Decreasing the acidity or diluting zirconium sulphate solutions, will result in the precipitation of a variety of zirconium basic sulphates (ZBS) [1-4].

Normal zirconium sulphate crystals consist of infinite sheets of zirconium atoms linked together by sulphate groups [12]. Four different sulphates are bonded to each zirconium atom while each sulphate group is bonded to two zirconium atoms. Sheets rather than chains form because no two sulphates have more than one zirconium atom in common [12]. Four water molecules can coordinate to each zirconium atom thus forming a square antiprism with the four sulphate oxygen atoms [2-3, 12].

Dissolution of zirconium sulphate sheets occurs by scission of the bonds between zirconium atoms and the sulphate groups. This usually occurs by displacement of sulphate by hydroxy groups to anionic species [12].

$$[Zr(SO_4)_2.4H_2O]_n + 2nH_2O \Leftrightarrow n[Zr(OH)_2(SO_4)_2.4H_2O]^{2-} + 2nH^+ \tag{1}$$

$$[Zr(SO_4)_2]_n + 3nH_2O \Leftrightarrow n/2[Zr_2(OH)_3(SO_4)_4]^{3-} + 3nH^+ \tag{2}$$

$$[Zr(SO_4)_2]_n + 4nH_2O \Leftrightarrow n/3[Zr_3(OH)_4(SO_4)_6]^{4-} + 4nH^+ \tag{3}$$

SCHEME 4.3 Reaction (**1**) shows that two sulphate groups are displaced for each zirconium atom. Reaction (**2**) and (**3**) have similar implications but with the omission of coordinated water to the zirconium sulphate.

The anionic species would not be expected to exist for any appreciable length of time because of the unsatisfactory bonding conditions. Rather they would be expected to stabilise by olation or by formation of sulphate bridges. This serves as bases for the formation of zirconium basic sulphates form the anionic species [2, 12].

Consider the basic sulphate with the molecular formula, $ZrO_2.SO_3.H_2O$. This basic sulphate consists of species $[Zr(OH)_2]_n{}^{2+}$, which forms chains in which each zirconium atom is bonded to four hydroxyl groups. A series of olation reactions with displacement of sulphate groups, makes this structure possible [12]. The remaining sulphate groups form bridges between the chains. The general formula for ZBS is, $Zr_5O_{(10-x)}(SO_4)_3$ where $3.5 > x > 1.8$. The most common basic sulphate is $Zr_5O_7(SO_4)_3.nH_2O$ [13]. Basic sulphates of type $Zr_n(OH)_{2n+2}(SO_4)_{n-1}$ have also been proposed [12].

Recently, Squattrito and Clearfield (1987) [16] has provided the crystal structure and synthesis of a new complex basic zirconium sulphate $Zr_{18}O_4(OH)_{38.8}(SO_4)_{12.6}.33H_2O$. This further emphasises the diversity of these basic salts with departure from those previously reported.

4.8 CONCLUSIONS

1. The chemistry of zirconium and hafnium is more similar than any other two congeneric elements. This can be attributed to the near identical atomic and ionic radii.
2. The zirconyl group rarely exists for zirconium aqueous chemistry.
3. At metal concentrations greater than 10^{-3}M and hydrogen ion greater than 1M, tetramers and trimers exists in zirconium solutions.
4. Many different zirconium normal sulphates exist at different reaction conditions
5. The sulphate strongly complexes the zirconium ion.
6. Disulphato-oxy-zirconic acid trihydrate $H_2ZrO(SO_4)_2.3H_2O$, commonly called acid zirconium sulphate trihydrate (AZST) $Zr(SO_4)_2.4H_2O$, is a stable normal sulphate.
7. AZST crystallises easily out of relatively strong sulphuric acid solutions. The crystals consist of infinite sheets of zirconium atoms linked together by sulphate groups. Four different sulphates are bonded to each zirconium atom while each sulphate is bonded to two zirconium atoms.
8. Decreasing the acidity or diluting zirconium sulphate solutions, will result in the precipitation of a variety of zirconium basic sulphates.
9. Simple zirconium salts like $ZrCl_4$ are hydrolysed in water to form zirconium hydroxide chlorides $[Zr_4(OH)_8.16H_2O]Cl_2.8H_2O$.
10. Adding sodium carbonate to a solution of zirconium sulphate to a pH of approximately 6.75 has been observed to precipitate the carbonate $Zr_2O_3(OH)_2CO_2.7H_2O$ with a $ZrO_2 : CO_2$ ratio of 1 : 0.8
11. ZBC reacts with sodium or ammonium carbonate solutions to give water-soluble double carbonates e.g. $NH_4[Zr_2O(OH)_3(CO_3)_3]$.

4.9 REFERENCES

1. Larsen, E.M. (1970) Zirconium and Hafnium chemistry, Advan. Inorg. Chem. Radiochem, (13) 1.
2. Blumenthal, W.B. (1958) The Chemical Behaviour of Zirconium, Van Nostrand, N.J., U.S.A., New York.
3. Mukherji, A. K. (1970) Analytical Chemistry of Zirconium and Hafnium, Pergamon press.
4. Elinson, S.V. and Petrov, K. I. (1969) Analytical Chemistry of the elements, Ann Arbor-Humphrey science publishers.
5. Cotton, F. A. and Wilkinson, G. (1997), Advanced Inorganic Chemistry, John Wiley and Sons, New York.
6. MacDermott, T. E. (1973) The structural chemistry of zirconium compounds, Coordination Chemistry, (11) 1-20.
7. Wells, A. F. (1984) Structural Inorganic Chemistry, Clarendon Press, Oxford.
8. Von Zelewsky, A. Stereochemistry of Coordination Compounds, (1996) by John Wiley, A textbook series.
9. 9. Zielen, A. and Connick, R. J. (1956) J. Am. Chem. Soc. (78) 5785.
10. Johnson, J. and Kraus, K. J. (1956) J. Am. Chem. Soc. (78) 26
11. Clearfield, A. and Vaughan, P. A. (1956) The crystal structure of zirconyl chloride octahydrate and zirconyl bromide, Acta. Cryst.,(9) 555
12. Clearfield, A. (1964) Structural aspects of Zirconium Chemistry. Rev. Pure and Appl. Chem. (14) 91.
13. Nielsen, R. Chang, T. W. (1996) Ullman's Encyclopaedia of Industrial Chemistry, A (28) 543-567.
14. Brunton, G. (1965) J. Inorg. Nucl. Chem., (27) 1173.
15. Bear, I. J. and Mumme, W.G. (1971) Normal Sulphates of Zirconium and Hafnium Rev. Pure and Appl. Chem., (21) 189.
16. Squattrito, P.J. Rudolf, P. R. and Clearfield, A. (1987), Inorg. Chem. (26) 4 240-4 244
17. McDonald, C. B. (1958) J. Inorg. Nucl. Chem., (6) 236.
18. Mamott, G.T. Barnes, P. Tarling, S. E. Jones, S. L. Norman C. J. (1991), Journal of Materials Science (26) 4054-4061.
19. Fenner, J. and Goldschmidt, T. (1981), U. S. Patent, 4, 283, 377.
20. Pospelova, L. A. and Zaitssev, L. M. (1966), Russ. J. Inorg. Chem. (11) 995.

CHAPTER 5

ZIRCONIA EXTRACTION PROCESSES

[Picture by: Chemical & Engineering news, march 13 2000]

5.1 INTRODUCTION

Many processes exist for the extraction of zirconia, especially from zircon. The main differences, besides starting with different reagents, are in the number of extraction steps, the purity and yield of the resultant zirconia. Some processes also put some emphasis on the recovery of by-products and their methods of disposal. The hunt is for processes with the highest yield and purity at minimal costs ideally with a minimal number of process steps. This chapter takes a detailed look at some of the extraction processes of zirconia from zircon, with emphasis given to the alkali fusion method, for it is this method that was investigated.

Zircon is a refractory mineral that exhibits some resistance towards acids and cold alkali solutions, but it is readily attacked by sodium hydroxide NaOH, above 600°C and even more vigorously by sodium oxide, Na_2O [1-2]. The stability of zircon suggests that aggressive reaction conditions and reagents have to be used to decompose the zircon crystal lattice or dissociate the zircon into silica and zirconia. Thermal methods like the Plasma arc furnace are capable of dissociating the zircon and chemical methods like the alkali fusion are capable of decomposing the zircon lattice into reactive species like Na_2ZrO_3, Na_2SiO_3. Dissociation in this case refers to the breaking down of the lattice into the units MO_2 (where M is ideally Zr or Si); and decomposition, the formation of complex metal zirconates and silicates.

Processes for the recovery of zirconium compounds have three fundamental steps in common [3]. Firstly, the decomposition or dissociation of zircon either by chemical or thermal methods. Secondly, the treatment of the decomposition products, usually by making soluble and insoluble compounds. Thirdly, the isolation of zirconium compounds, usually from residual silica, rare earth's and other impurities. For zirconia recovery a fourth step exists, where the zirconium compounds are calcined to produce zirconia.

5.2 THERMAL DISSOCIATION (Figure 5.1)

METHOD 1

This reaction occurs in plasma arc furnace [3-5] or an advanced electric reactor. The zircon sand is heated in the presence of carbon at approximately 2 000°C. The zircon is dissociated to zirconia and silica at temperatures above 1 750°C [3]. The silica is reduced to the volatile monoxide at temperatures higher than 2 400°C, which re-oxidises outside the furnace to silica (fumed silica).

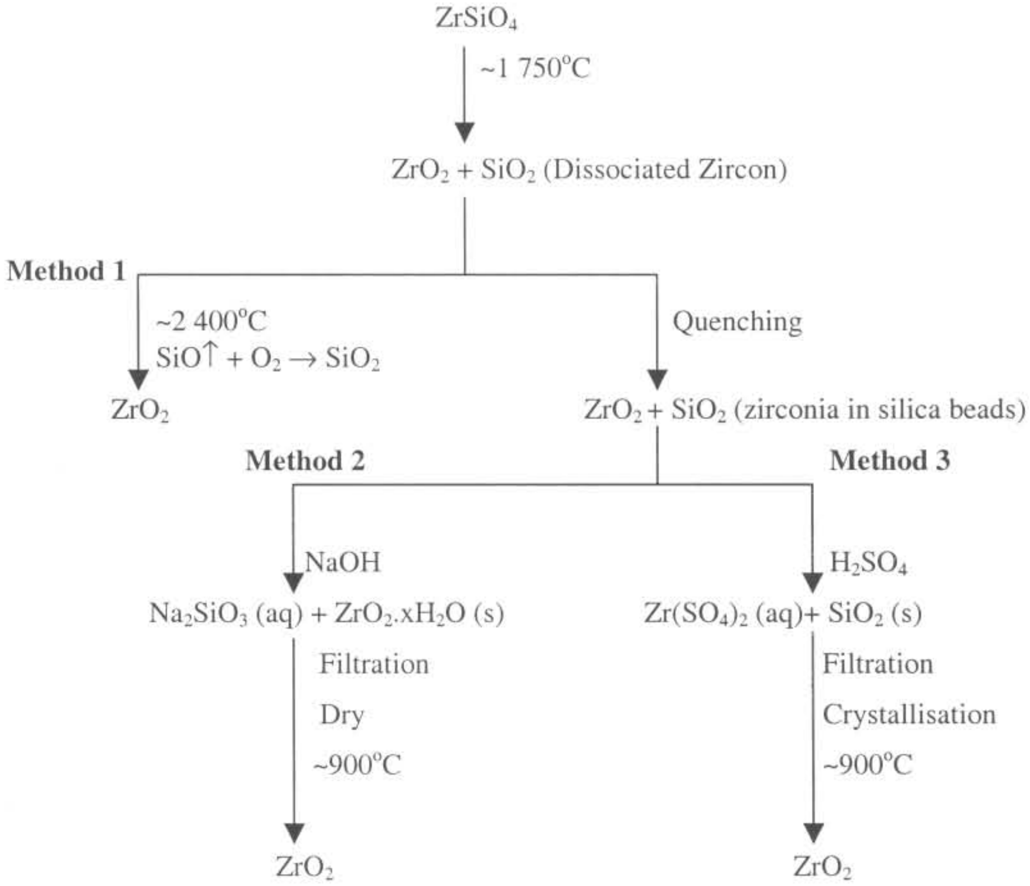

FIGURE 5.1 A Diagrammatic Representation of the Thermal Decomposition of zircon

METHOD 2

The dissociated zircon can be quenched to produce intimately mixed crystals of zirconia in a bead of amorphous silica. The crystallites can be very small, usually less than 0.1μm in diameter. The agglomerates can range in size from 2 to 20 μm depending on how the crystallites are joined [4]. The amorphous silica can be dissolved by a solution of boiling sodium hydroxide NaOH, to yield a soluble sodium silicate and an insoluble zirconium oxide residue [4-5, 13].

METHOD 3

The zirconia can be leached with sulphuric acid to yield a soluble zirconium sulphate, usually AZST and insoluble silica gel [4-5]. Heating the zircon to 2 100-2 300°C can vary the size of the agglomerates, where the silica is liquid and the zirconia is solid. The zirconia is produced as compact clusters of crystallites with a size range of 0.01-0.1μm, sufficient to allow rapid leaching out of zirconia by sulphuric acid [4]. Temperature and acid concentration have also been shown to affect the extraction of zirconia from dissociated zircon [9].

When the particle size is approximately 75 μm (obtained after milling) about 3-4 hours are required to extract approximately 90% of the zirconia. If the dissociated zircon is not ground, then only 64% of zirconia is obtained over the same period. Thus the zirconia has to be ground below 75μm to achieve good results [9].

Separation of products by filtration is followed by the production of AZST crystals by either evaporative crystallisation or salting out. Calcination of the zirconium sulphate between 900°C-1 000°C is usually how the zirconia is produced [3-5].

Evaporative crystallisation refers to water removal usually between 121-123°C. When the desired temperature is reached heating is stopped the solution is then cooled to room temperature. The crystals are filtered and washed with H_2SO_4 [9]. Salting out refers to the exploitation of a minimum in ZrO_2 solubility in the system ZrO_2-SO_3-H_2O between 45-55% (m/m) SO_3 were the zirconium crystallises out as $Zr(SO_4)_2.4H_2O$ [1, 9]. Comparison of the AZST formed from salting out showed a lower impurity level than the evaporative technique, but longer calcination times are required to lower the SO_3 content in the final material zirconia [9].

5.3 CHLORINATION (Figure 5.2)

The milled zircon sand is pelletised with coke to obtain an intimate mixture. It is directly chlorinated with chlorine gas, in a fluidised bed or shaft furnace at 800-1 200°C [3-5], producing zirconium and silicon tetrachloride. Since the reaction is endothermic, supplemental energy is supplied usually by heating the interior graphite walls of the chlorinator.

The zirconium tetrachloride is distilled and collected in a condenser at about 150-180°C [3-4] or 200°C [5] and the silicon tetrachloride at –10°C [3-4] or –20°C [5] in a secondary condenser.

METHOD 1

The zirconium tetrachloride can simply be calcined to zirconia and the silicon tetrachloride to silica [1-2].

METHOD 2

The zirconium tetrachloride can be hydrolysed with water to form zirconium oxychloride [1-2, 8]. Cooling the saturated solution from 65 to 20°C can cause crystallisation of zirconium oxychloride. This step is carried out to separate the major impurities such as titanium, aluminium, iron and silicon chlorides [1-2, 4]. The crystals can then be dried at approximately 85°C and calcined to zirconia [4].

METHOD 3

Adding ammonia solution to a solution of zirconium oxychloride leads to the precipitation of hydrous zirconia [4]. The precipitate can be calcined to produce zirconia powder agglomerates consisting of randomly oriented fine crystallites.

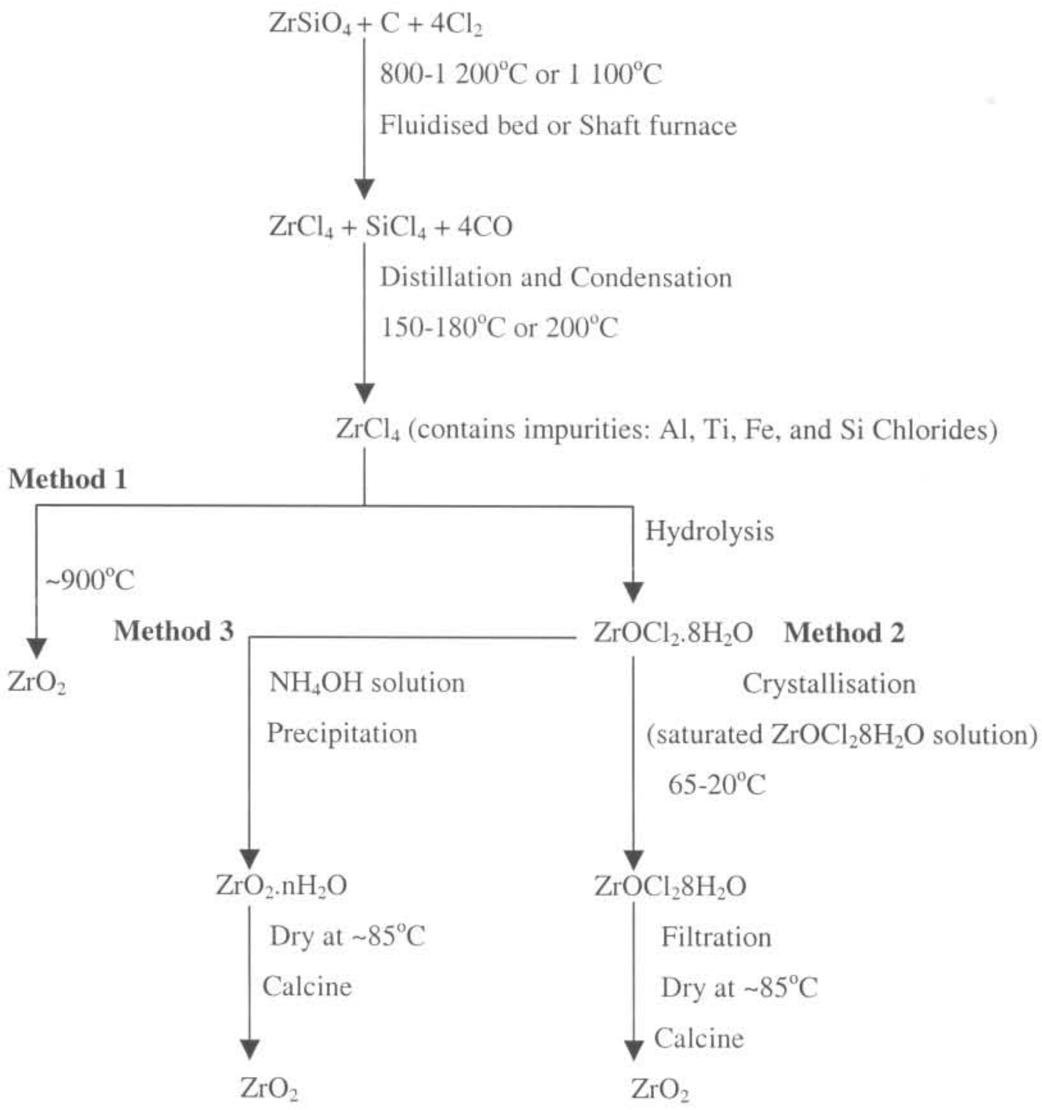

FIGURE 5.2 A Diagrammatic representation of the Different Chlorination processes

5.4 LIME FUSION (Figure 4.3)

Lime or dolomite can be reacted with zircon to produce calcium zirconylsilicate, calcium zirconate and calcium silicate even mixtures of zirconia and calcium or magnesium silicate [1-5, 11-12]. The thermodynamic parameters (at atmospheric pressure) for the existence of these various phases are: temperature, mole ratio of the zircon to the lime.

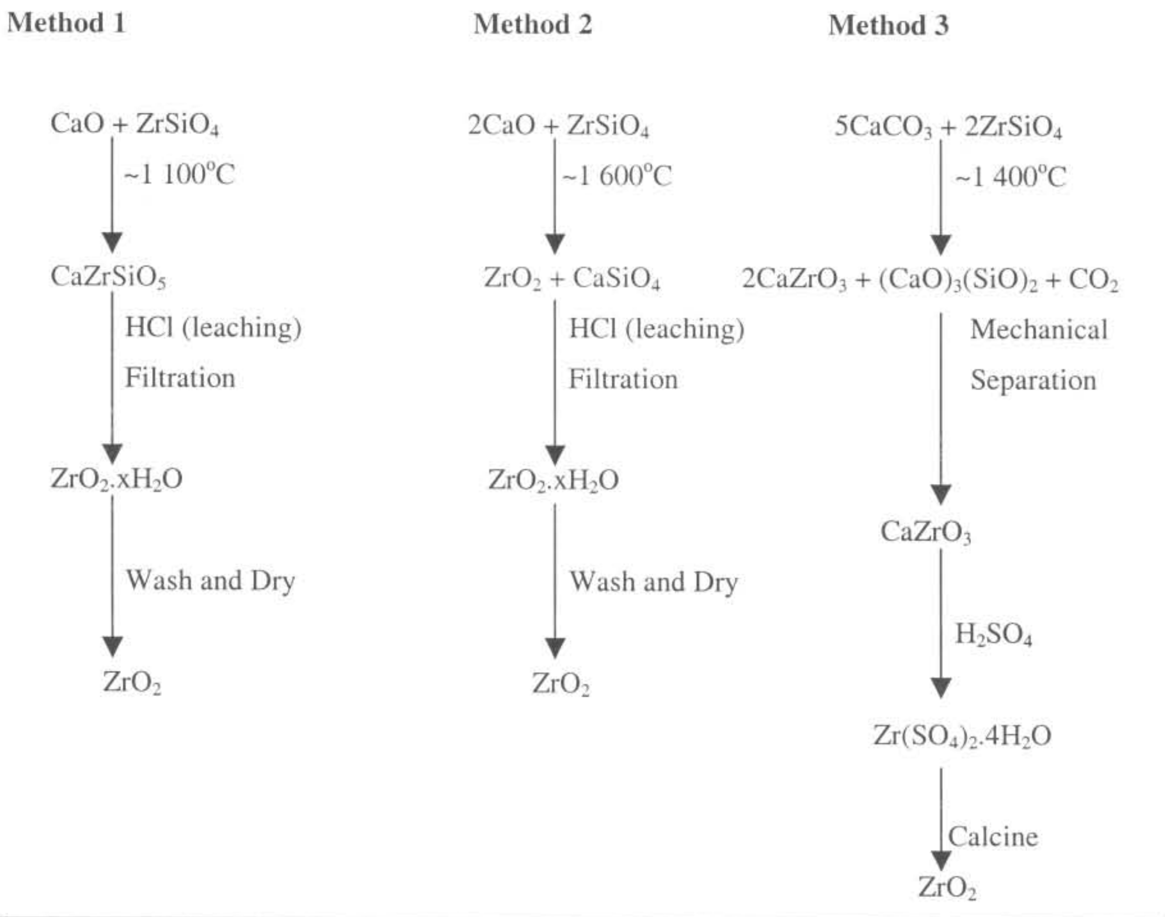

FIGURE 5.3 A diagrammatic representation of the various Lime Fusion processes

METHOD 1AND 2

The calcium and silica can be removed by leaching the fusion product with hydrochloric acid. The remaining hydrous zirconia is then washed and dried [3-4].

METHOD 3

The fused product disintegrates into very fine calcium silicate powder and coarse calcium zirconate crystals. Mechanical means can be employed to recover the calcium zirconate coarse crystals [5, 12]. Calcium zirconate crystals of a large size (30-50μm), for easy separation, are developed at a temperature region of 1 700-2 000°C [12]. The calcium zirconate is acid soluble and can easily be converted into zirconium salts such as AZST or the oxide.

4.5 CARBIDING (Figure 5.4)

The zircon is converted into carbide in an open top electric arc furnace at approximately 2 500°C. An intimate mixture of zircon and coke is continuously fed into the furnace. Insufficient carbon is used so that silicon monoxide is vaporised [5].

When the furnace is full it is cooled and the contents separated, the unreacted surface shell from the reacted. The block is broken and crushed to a diameter size less than 75 mm [5]. The ingot can be chlorinated immediately from the furnace to increase its purity [1-5]. If not, oxidation in a furnace leads to zirconia with approximately 5% of silica [5].

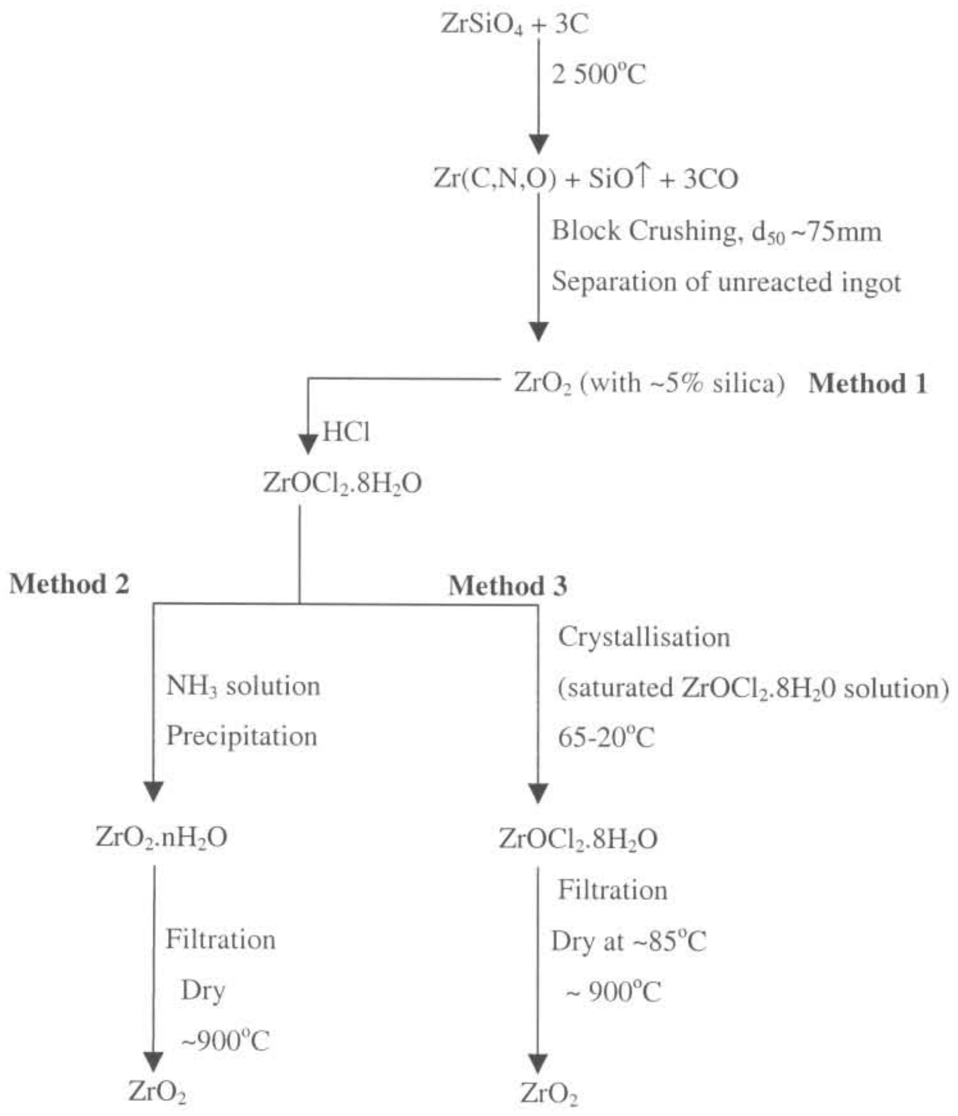

FIGURE 5.4 A diagrammatic representation of the Carbiding Processes

5.6 FLUOROSILICATE FUSION (Figure 5.5)

Zircon can be fused with potassium hexafluorosilicate at approximately 700°C to produce potassium hexafluorozirconate [5]. The fusion reaction can also be carried out in a rotary furnace at temperatures between 650-750°C [10]. The fused product is milled and leached in 1% HCl solution at ~85°C for two hours.

The saturated solution is filtered while it is still hot to remove the insoluble silica and then allowed to cool to crystallise the potassium hexafluozirconate. A zirconium hydroxide is precipitated with ammonium hydroxide from a three percent solution of potassium hexafluozirconate. The hydroxide is then filtered, washed, and then calcined to zirconia.

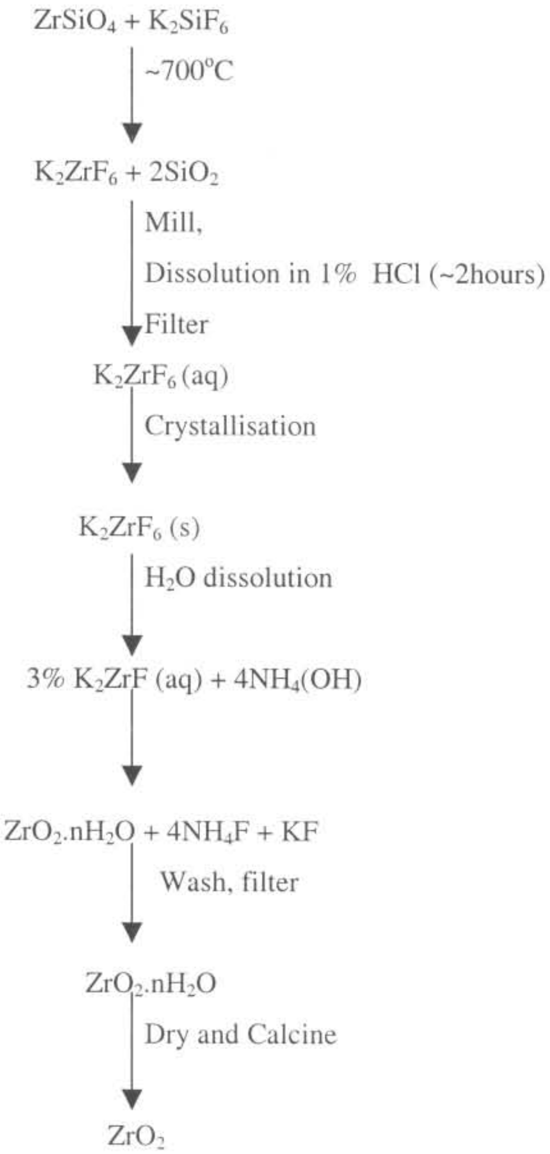

FIGURE 5.5 A diagrammatic representation of the Potassium hexafluozirconate process

5.7 CAUSTIC FUSION

This process involves the decomposition of zircon by fusion with sodium hydroxide or sodium carbonate in different mole ratios to form reactive species.

5.7.1 SUB-STOICHIOMETRIC CAUSTIC FUSION (Figure 5.6.1)

An acid soluble sodium zirconate is produced by reaction of zircon with sodium carbonate at low mole ratios. This reaction usually occurs at approximately 1 000°C as follows [1, 3-5].

$$ZrSiO_4 + Na_2CO_3 \rightarrow Na_2ZrSiO_5 + CO_2\uparrow$$

SCHEME 5.1 Reaction of zircon with sodium carbonate at sub-stoichiometric levels

METHOD 1

The fused product, usually sodiumzirconylosilicate Na_2ZrSiO_5, is milled and added to a concentrated mineral acid (e.g. HCl) to produce zirconium salts and silica gel. The zirconium salts are then separated from the silica [5]. The zirconyl chloride is then crystallised from a saturated solution or precipitated with ammonia [4].

METHOD 2

The milled fused product can be leached with water and the insoluble sodium zirconyl silicate digested with hot hydrochloric acid. The silica precipitate can simply be filtered and the zirconyl chloride treated with sulphuric acid to precipitate a zirconium basic sulphate [10, 14]. The sulphate can simply be calcined directly to zirconia. The sulphate can be converted to the hydroxide with ammonia and calcined to zirconia.

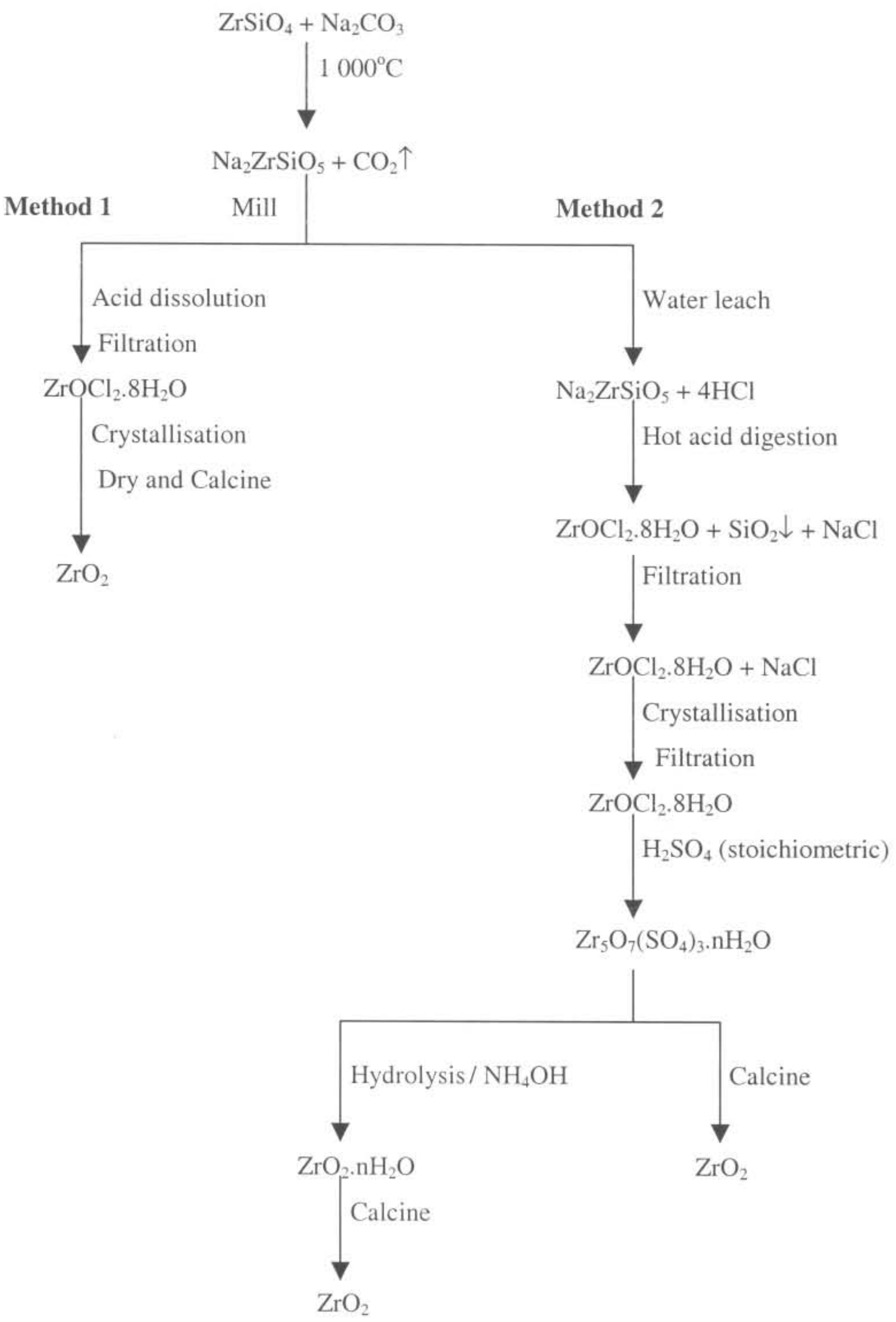

FIGURE 5.6.1 A diagrammatic representation of the Sub-stoichiometric caustic soda fusion

5.7.2 SLIGHT EXCESS CAUSTIC SODA FUSION (Figure 5.6.2)

Zircon is fused with sodium hydroxide in a one is to four mole ratio at approximately 650°C to produce sodium zirconate and sodium silicate [1, 3-5]. This reaction can also occur with sodium carbonate above 1 000°C [3-5].

$$ZrSiO_4 + 4NaOH \rightarrow Na_2ZrO_3 + Na_2SiO_3 + 2H_2O \uparrow$$

SCHEME 5.2 Reaction of zircon with sodium hydroxide in a one is to four mole ratio at 650°C

The fused product is crushed and dissolved in water. The sodium silicate is dissolved by water. The sodium zirconate is hydrolysed by water to soluble sodium hydroxide and insoluble hydrous zirconia [3-5]. The liquid phase is separated from the solids by filtration. Numerous ways exist on how to treat the hydrous zirconia to produce zirconia of different purity.

METHOD 1

The hydrous zirconia can be simply fired to zirconia [1-2, 5, 8].

METHOD 2

Another way could be by using hydrochloric acid, where the hydrous zirconia is treated with hydrochloric acid to produce zirconium oxychloride, $ZrOCl_2.8H_2O$. The separation of insoluble products and the precipitation of zirconium hydroxide with drying and calcination resulting in zirconia follow this step [3-5].

METHOD 3

A method that is capable of producing zirconia of very high purity for alkali fusion is the one that uses hydrochloric acid and sulphuric acid [9]. In this method the hydrous zirconia is initially digested with hydrochloric acid to form zirconyl chloride and soluble chlorides of the radioactive elements. The AZST is crystallised with the addition of sulphuric acid (salting out). The AZST precipitate is then washed to remove the soluble chlorides of the radioactive chlorides. The AZST is then calcined to zirconia.

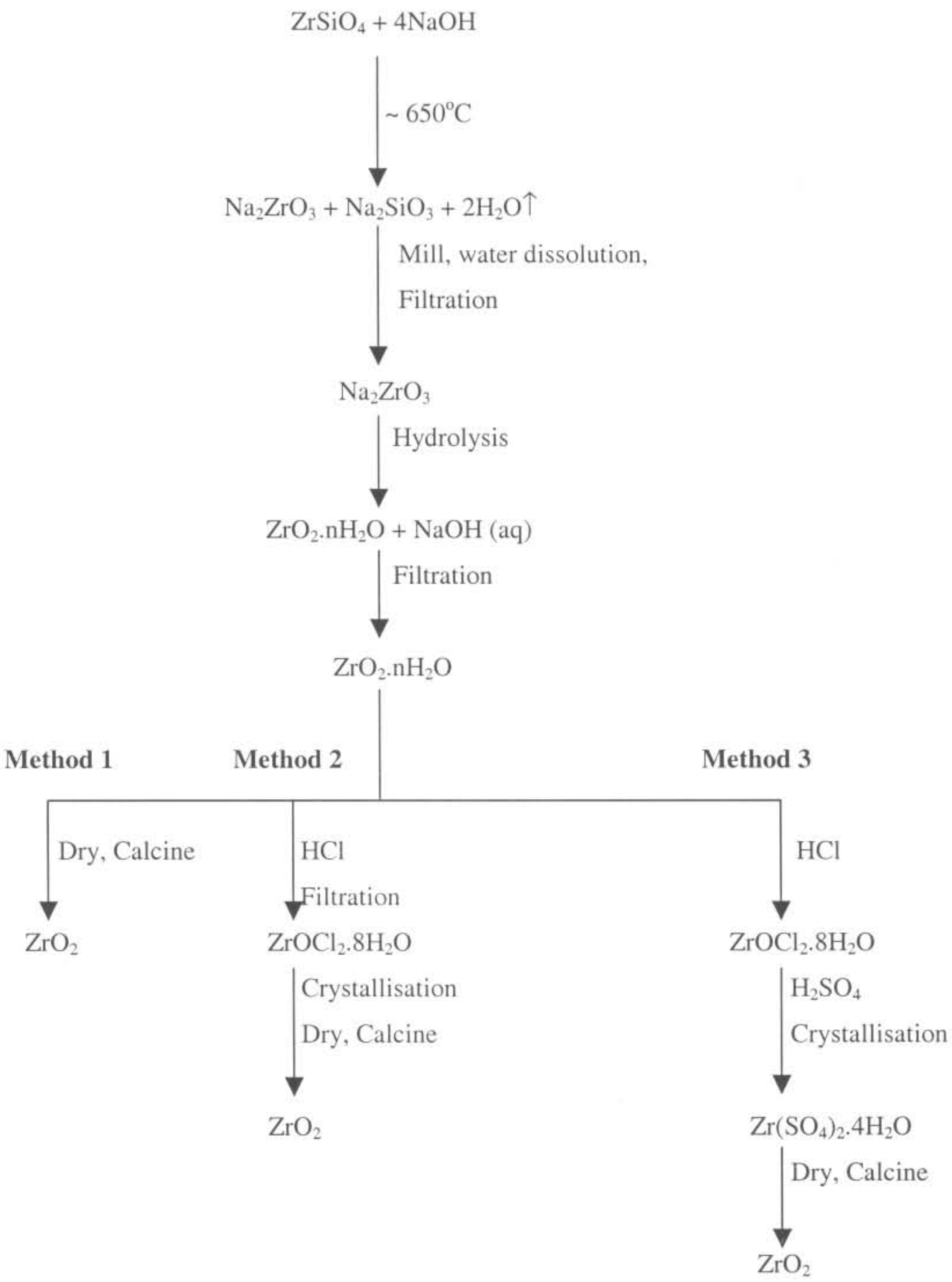

FIGURE 5.6.2 A diagrammatic representation of the various pathways of an Alkali Fusion process.

5.7.3 HIGH-STOICHIOMETRIC CAUSTIC FUSION (Figure 5.6.1-5.6.2)

By adjusting the mole ratio and reaction conditions it is possible to produce almost complete conversion. Consider the reaction at approximately 600°C of the mole ratio [3-4]:

$$ZrSiO_4 + 6NaOH \rightarrow Na_2ZrO_3 + Na_4SiO_4 + 3H_2O\uparrow$$

SCHEME 5.7.3: Reaction of zircon with six moles of caustic soda

In this particular case fusion improves dramatically with almost complete conversion of zircon to sodium zirconium silicate and sodium silicate thus leading to higher zirconia (and silica) yields. This reaction is also possible with sodium carbonate but at higher temperatures above 1 000°C.

The fused product is crushed and slurried in water. The silicate is dissolved in water and separated from the zirconate. The sodium zirconate is hydrolysed by the water to sodium hydroxide and a complex hydrated hydroxide. The sodium hydroxide is separated from the gelatinous complex zirconium hydroxide [3-4]. There are numerous methods of treating the complex hydrated hydroxide similar to those for the sub-stoichiometric and slight excess fusion.

5.8 CONCLUSIONS

1. Zircon is dissociated by thermal methods, for example plasma, at temperatures greater than 1 750°C. At temperatures greater than 2 400°C, the silica is volatilised to the monoxide and re-oxidised to the dioxide outside the oven. The silica volatilisation temperature can be lowered to 2 000°C in the presents of carbon.
2. At temperatures less than 2 400°C, further chemical processing is required, especially to obtain a product of higher purity. This processing is limited by the size of the agglomerates (2-20μm). For sufficient rapid leaching the mean particle size must be between 0.01 and 0.1μm.
3. To obtain highly pure products, precipitation methods are used. For example, the salting out method which refers to the exploitation of a minimum in ZrO_2 solubility in the system ZrO_2-SO_3-H_2O between 45-55% (m/m) SO_3 were the zirconium crystallises out as $Zr(SO_4)_2.4H_2O$.
4. The disadvantage of such methods is the time spent while stirring. For the above example there is also the need for long calcination to lower the SO_3 content. An additional step, for example $ZrO_2.nH_2O$ precipitation and $(NH_4)_2SO_4$ effluent washing can alternatively be employed.
5. Chlorination processes also exploit such precipitation methods, but use zirconyl chloride as the precipitate. The factors time, effluent and number of steps come into play.
6. Alkali fusion methods can decompose zircon into reactive species at lower temperatures when compared to thermal methods. These species can be exploited with the traditional methods of precipitation obtain pure products.
7. Zircon can be fused with potassium hexafluorosilicate at approximately 700°C to produce potassium hexafluorozirconate.
8. Zircon can be decomposed with different moles of caustic soda at approximately 600°C. The presence of the various complex metal zirconium silicates depends heavily on the fusion mole ratio. For example Na_2SiO_3 and Na_2ZrO_3, form in the presents of four moles sodium hydroxide for a mole of zircon.
9. The sodium content in zirconates can be minimised by hydrolysis to the hydroxide $ZrO_2.nH_2O$. The problem is the long process time while heating.
10. Depending on what route is taken, the traditional precipitation and crystallisation routes can be employed to obtain a pure product.

5.9 REFERENCES

1. Blumenthal, W.B. (1958) The Chemical Behaviour of Zirconium, Van Nostrand, N.J., U.S.A. New York.
2. Anil K. Mukherji, (1970) Analytical Chemistry of Zirconium and Hafnium, Pergamon press.
3. Farnoworth, F. Jones, S. L. and McAlpine, I. (1980) The Production, Properties and uses of zirconium chemicals, Magnesium Elektron Ltd. Twickenham, U. K.
4. Stevens, R. (1986) Zirconia and Zirconia ceramics, Magnesium Elektron Ltd., Twickenham, U. K.
5. Ralph Nielsen, Teledyne Wah Chang, (1996) Ullman's Encyclopaedia of Industrial Chemistry, A (28) 543-567.
6. Jenkins, D. H. (1986) Process for the production of high purity zirconia powder. International patent WO 86/04614. World intellectual property organisation.
7. John Kenneth Olby, (1963) Manufacture of zirconium oxide from zircon, U.S. Patent 3,109,704.
8. S.V. Elinson, and K. I. Petrov, (1969) Analytical Chemistry of Zirconium and Hafnium Ann Arbor-Humphrey, London.
9. Houchin, M. R. Jenkins, B.E. Sinha, (1990) H.N Production of high quality zirconia for ceramics., Mineral, Materials and Industry 14th congress of the council of mining and metallurgy Institute.
10. Hancock, J.D. (1977) A review of conventional and novel processes for the extraction of zirconia from zircon. Mineral Science and Engineering, 1 (9) 25-31.
11. Schoenlaub, R. A. (1955) Production of calcium zirconate, U. S. Patent 2,721,117
12. Schoenlaub, R. A. (1974) Method of Manufacturing zirconium oxide and salts, U. S. Patent 3,832,441.
13. 13. Recasens, J. Urffer, D. Ferlanda, P. (1992) Reactive zirconium oxide and its preparation, U.S. Patent 5149510.
14. Deutsche Gold-UND Silber-Scheideanstalt, (1961) Process for the production of Zirconium Compounds, more especially Basic Zirconium Sulphate, German patent, 971, 594.

CHAPTER 6

THE STRUCTURE OF ZIRCON

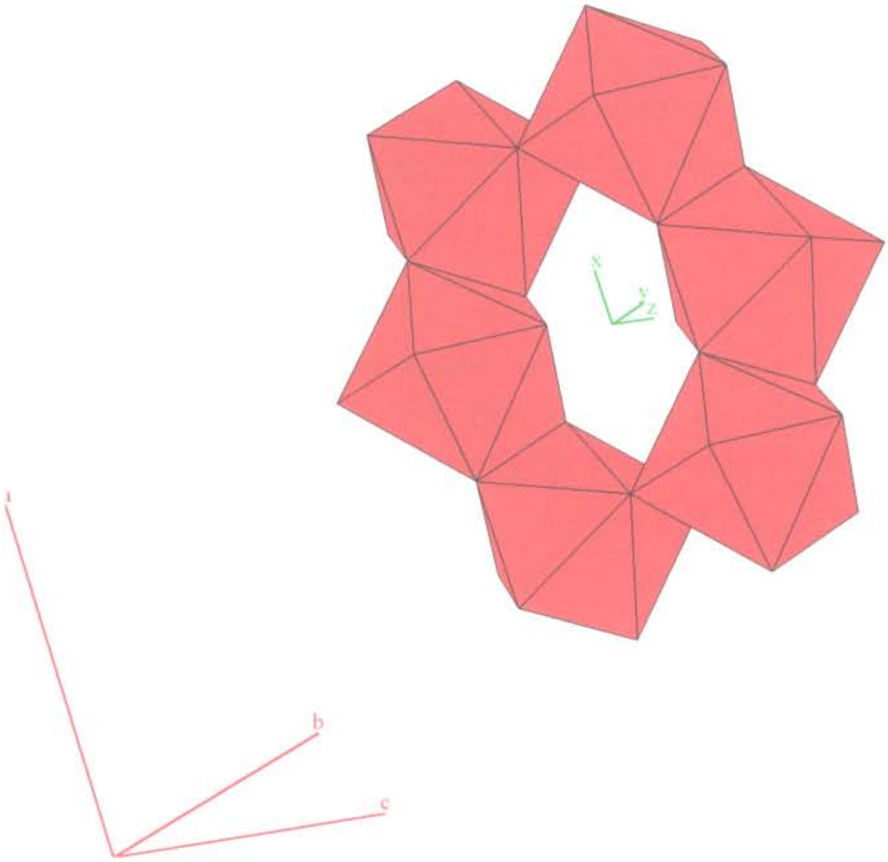

Six ZrO_8 bisdisphenoids edge cell connected Ring.

6.1 INTRODUCTION

This chapter tries to explain the structure of zircon because this could serve as bases to explaining the decomposition of zircon by alkali-metal hydroxides. The structure of zircon was originally reported [1] as having the rutile-type structure, although this was later corrected [2]. Bragg and Claringbull (1965) [3] referred zircon to the rutile group because of similarities in cell dimension, which was later dismissed by X-ray data [4]. Nyman et. al. (1984) [4] showed that zircon actually was related to the rutile-type structure, which it was originally confused with, by simply relating the two structures by replacing the Ti atoms with the Zr and Si atoms in the rutile structure. The structures ABX_4 and MX_2 are actually very similar so it is easy to understand the reason for the confusion.

6.2 ZIRCON STRUCTURE

Clarification on the structure of zircon was suggested by Nyman et. al. (1984) [4] who related a number of structure types, especially those of ABX_4 compounds with a large size difference between A and B atoms. These structures were observed to consist of AX_8 bisdisphenoids or dodecadeltahedron and BX_4 tetrahedra.

The bisdisphenoid can be resolved into two penetrating tetrahedra, one elongated and the other squat with common $\bar{4}$ axis. The bisdisphenoids can also be described as consisting of two interpenetrating, concentric tetrahedra. One tetrahedra being elongated and the other being compressed along the common $\bar{4}$ axis. When the zircon structure is projected on (110), rods of alternating edge-shared tetrahedra and bisdisphenoids in zircon replace the rods of edge-shared octahedra in rutile.

The zircon structure has been related to the rutile structure by Hyde and Andersson (1989) [6], suggesting that the titanium atoms in the chains of edge-sharing rutile octahedra can be replaced by alternating larger Zr and Si atoms. The larger cations have a longer bond length to oxygen thus the higher coordination number in the bisdisphenoid ZrO_8 and lower coordination in the SiO_4 tetrahedra. In zircon the bisdisphenoids share edges in both (100) and (010) layers thus all shifts are parallel throughout the tetragonal structure.

The zircon structure can be shown as two bounded projections (Figure 6.1). Structures with AX_8 and BX_4 coordination, like zircon, are very closely related to structures MX_2, with MX_6 octahedra. In zircon the corresponding octahedral structure is that of rutile, derived by substituting alternately large Zr and small Si atoms for Ti atoms in the chains of edge sharing TiO_6 octahedra in the rutile type.

ZIRCON DATA TABLE 6.1 [6]

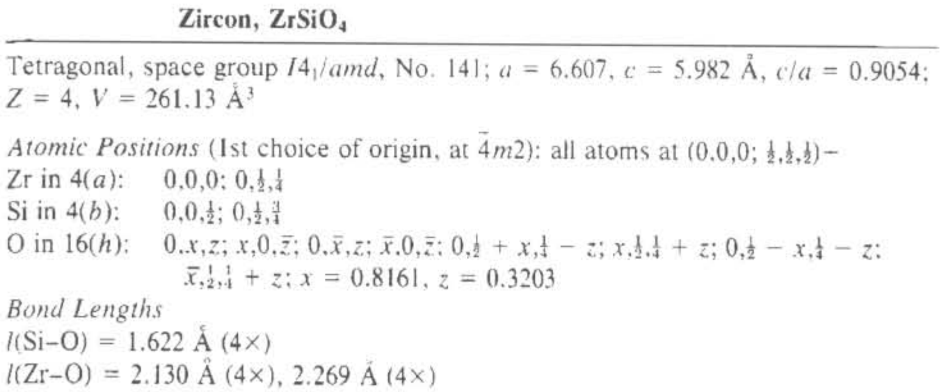

Zircon, $ZrSiO_4$

Tetragonal, space group $I4_1/amd$, No. 141; $a = 6.607$, $c = 5.982$ Å, $c/a = 0.9054$; $Z = 4$, $V = 261.13$ Å^3

Atomic Positions (1st choice of origin, at $\bar{4}m2$): all atoms at $(0,0,0; \frac{1}{2},\frac{1}{2},\frac{1}{2})-$
Zr in 4(*a*): $0,0,0; 0,\frac{1}{2},\frac{1}{4}$
Si in 4(*b*): $0,0,\frac{1}{2}; 0,\frac{1}{2},\frac{3}{4}$
O in 16(*h*): $0,x,z; x,0,\bar{z}; 0,\bar{x},z; \bar{x},0,\bar{z}; 0,\frac{1}{2}+x,\frac{1}{4}-z; x,\frac{1}{2},\frac{1}{4}+z; 0,\frac{1}{2}-x,\frac{1}{4}-z;$
$\bar{x},\frac{1}{2},\frac{1}{4}+z; x = 0.8161, z = 0.3203$

Bond Lengths
l(Si–O) = 1.622 Å (4×)
l(Zr–O) = 2.130 Å (4×), 2.269 Å (4×)

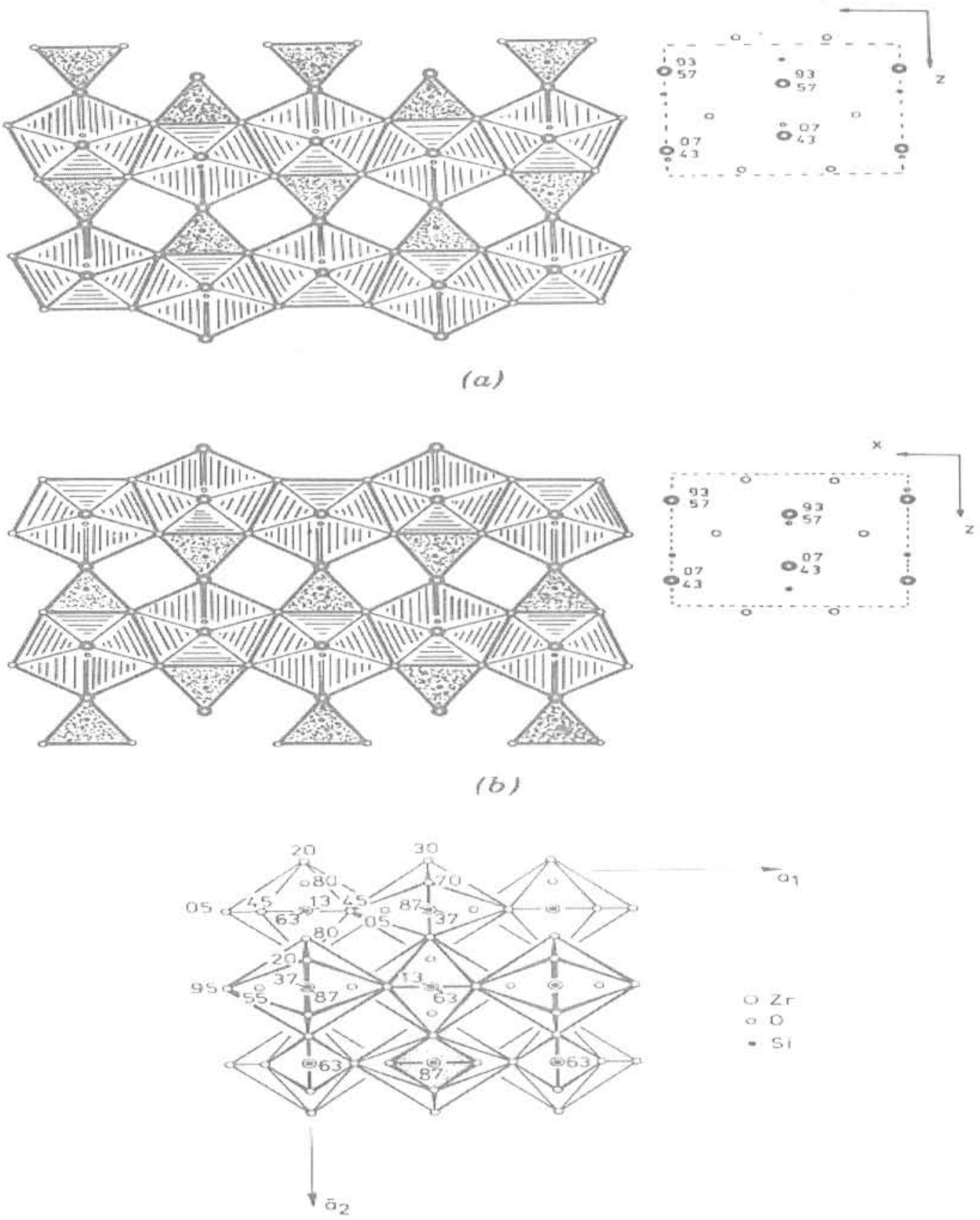

FIGURE 6.1 Bounded projections of the $ZrSiO_4$ structure projected on the (010) [≡ (100)]. [6] *(a)* $0.43 \leq y / b \leq 1.07$; (b) $0.93 \leq y/ b \leq 1.57$; Cations are at heights ¾ and 1¼ respectively. The bisdisphenoids share edges in both the x and y directions. Parallel to z are infinite rods of alternating ZrO_8 bisdisphenoids and SiO_4 tetrahedra that also share the edges. (c) Is the (001) projection.

With the aid of a crystallographic programme, CaRIne crystallographie 3.0, it was also possible to construct a three dimensional projection of the zircon structure by substituting the crystallographic data in Table 6.1 in the parameters stipulated by the programme.

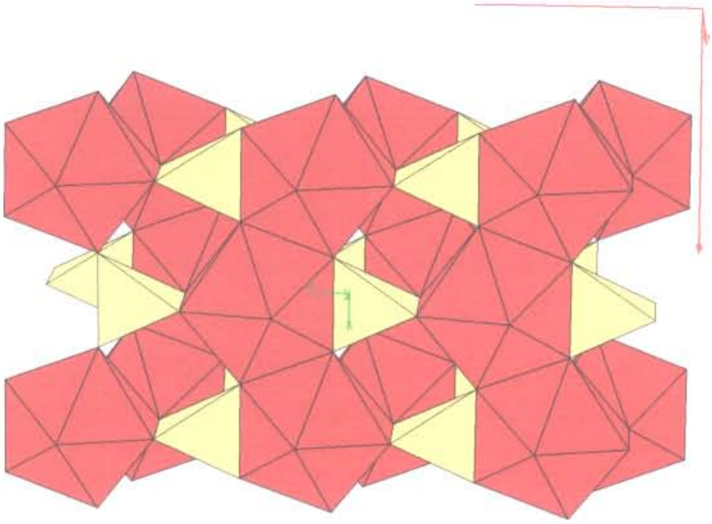

FIGURE 6.2 A three dimensional projection of the structure of zircon. The yellow regions represent the SiO_4 tetrahedra, the red ones are the ZrO_8 bisdisphenoids. The edge cell connection between the SiO_4 tetrahedra and the ZrO_8 bisdisphenoids can be seen. The SiO_4 tetrahedra are further linked to the adjacent ZrO_8 bisdisphenoids by corners.

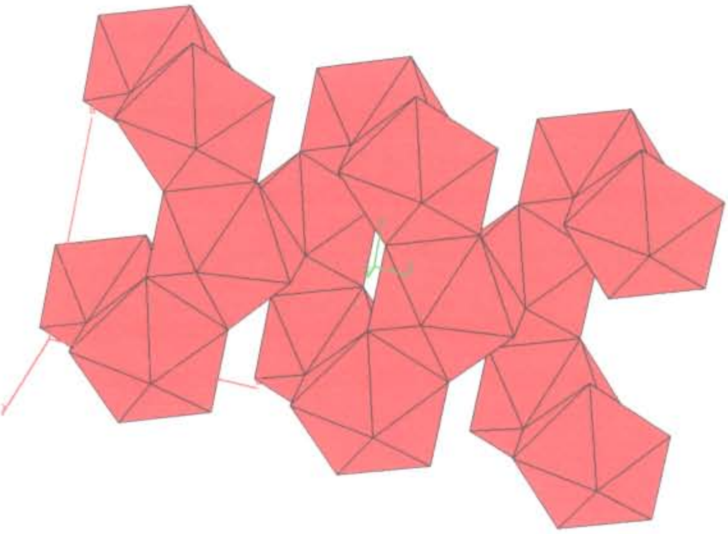

FIGURE 6.3 The edge cell connection of the bisdisphenoids results in the formation of ZrO_8 rings. A further edge cell connection joins the adjacent ZrO_8 rings. This continuous connection of the ZrO_8 explains zircon's stability and the habitat of various impurities.

6.3 CONCLUSIONS

1. Zircon is of structure type ABX_4, with a large size difference between A and B, consists of AX_8 bisdisphenoids and BX_4 tetrahedra.
2. The bisdisphenoids ZrO_8 consist of two interpenetrating concentric tetrahedra. One being elongated and the other being compressed along the common $\bar{4}$ axis.
3. The smaller silicon cation is of lower coordination in the tetrahedra SiO_4.
4. The bisdisphenoids share edges in both (100) and (010) layers thus all shifts are parallel throughout the tetragonal structure.
5. The zircon tetragonal structure is of two bounded projections, with ZrO_8 and SiO_4 coordination.
6. In zircon the corresponding octahedral structure is that of rutile, derived by substituting alternately large Zr and small Si atoms in the chains of edge sharing TiO_6 octahedra in the rutile type.

6.4 REFERENCES

1. Vegard, L. (1916) Phil. Mag. Ser. 6 (32) 65
2. Vegard, L. (1926) Phil. Mag. Ser 7 (1) 1151
3. Bragg, W. L. and Claringbull G. F. (1965) Crystal structures of minerals. Bell, London.
4. Nyman, H. Hyde, B. G and Andersson, S.(1984) Acta Cryst. B (40) 441
5. Blumenthal, W.B. (1958) The Chemical Behaviour of Zirconium, Van Nostrand, N.J., U.S.A.,
6. Hyde, B. G. Andersson, S. (1989) Inorganic crystal structures, A Wiley-Interscience publication, New York.

CHAPTER 7

EXPERIMENTAL

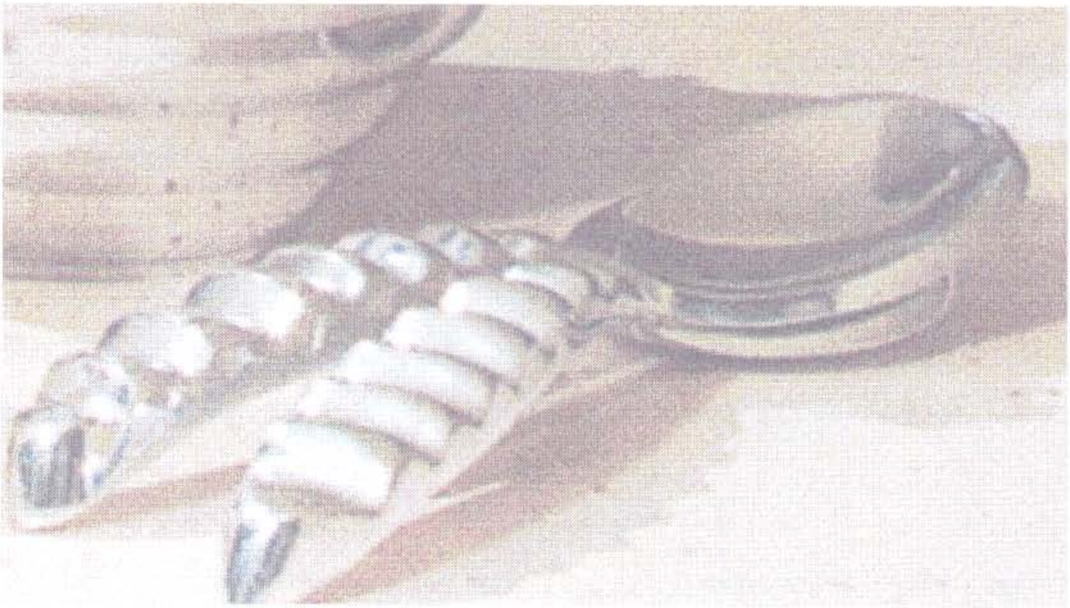

"One table spoon of Zircon, Alumina and Soda a day is what the Doctor ordered."

7.1 INTRODUCTION

This chapter gives a description of the apparatus, planning, reagents, experimental procedures and analysis that were used to investigate the alkali fusion processes.

7.2 APPARATUS

7.2.1 PESTLE AND MORTAR

A pestle and mortar was used in the milling of zircon sand and sodium hydroxide pearls. The mortar was capable of carrying one litre of solution and the pestle was about 300mm in length with a head of diameter c.a. 100 mm.

7.2.2 FIRECLAY CRUCIBLES

Fireclay crucibles were used in the fusion of zircon with sodium hydroxide. The crucibles were capable of carrying a total of about 200 grams of zircon sand. The crucibles were resistant to sodium hydroxide. The fused product was easy to remove from the sides of the crucibles.

7.2.3 HIGH TEMPERATURE OVEN

A High temperature oven was used for calcination and fusion purposes. The oven was a TPF 12/2 model capable of reaching a maximum temperature of about 1 200°C. It was supplied and maintained by Thermopower Furnaces S. A. (Pty.) Ltd. the oven.

7.2.4 CENTRIFUGE

A centrifuge was used to separate solids from the mother liquor. A Beckmann GPR model, capable of reaching a maximum of about 5 000 revolutions per minute, was used.

7.2.5 pH METER

A pH meter, model Mettler Delta 340, was used to follow the variations in pH for the various process steps.

7.3 PLANNING

The objective of this study was to characterise and optimise the De Wet's alkali fusion zirconia extraction processes [1] from zircon sand. These processes are outlined in Figure 7.1 therefore the experiments reported here were designed around this flow diagram. However, at each process step some factors were varied e.g. fusion temperature, stoichiometric ratios, HCl washing concentration and step elimination. Figure 7.2 shows a modification (in terms of ZBS preparation) to the De Wet process.

7.4 METHODS

7.4.1 REAGENTS

All reagents used were of analytical grade supplied by local fine chemical companies. These reagents were sulphuric acid, hydrochloric acid, sodium hydroxide pearls and sodium carbonate decahydrate.

Milled zircon, $d_{50} \approx 9\mu m$, 99.8% (m/m) from Richards' bay, South Africa supplied by Ferro Industrial products, was used for the purpose of these experiments. The chemical and physical analysis is supplied in Table 2.4 and 2.5 respectively.

7.2.3 HIGH TEMPERATURE OVEN

A High temperature oven was used for calcination and fusion purposes. The oven was a TPF 12/2 model capable of reaching a maximum temperature of about 1 200°C. It was supplied and maintained by Thermopower Furnaces S. A. (Pty.) Ltd. the oven.

7.2.4 CENTRIFUGE

A centrifuge was used to separate solids from the mother liquor. A Beckmann GPR model, capable of reaching a maximum of about 5 000 revolutions per minute, was used.

7.2.5 pH METER

A pH meter, model Mettler Delta 340, was used to follow the variations in pH for the various process steps.

7.3 PLANNING

The objective of this study was to characterise and optimise the De Wet's alkali fusion zirconia extraction processes [1] from zircon sand. These processes are outlined in Figure 7.1 therefore the experiments reported here were designed around this flow diagram. However, at each process step some factors were varied e.g. fusion temperature, stoichiometric ratios, HCl washing concentration and step elimination. Figure 7.2 shows a modification (in terms of ZBS preparation) to the De Wet process.

7.4 METHODS

7.4.1 REAGENTS

All reagents used were of analytical grade supplied by local fine chemical companies. These reagents were sulphuric acid, hydrochloric acid, sodium hydroxide pearls and sodium carbonate decahydrate.

Milled zircon, $d_{50} \approx 9\mu m$, 99.8% (m/m) from Richards' bay, South Africa supplied by Ferro Industrial products, was used for the purpose of these experiments. The chemical and physical analysis is supplied in Table 2.4 and 2.5 respectively.

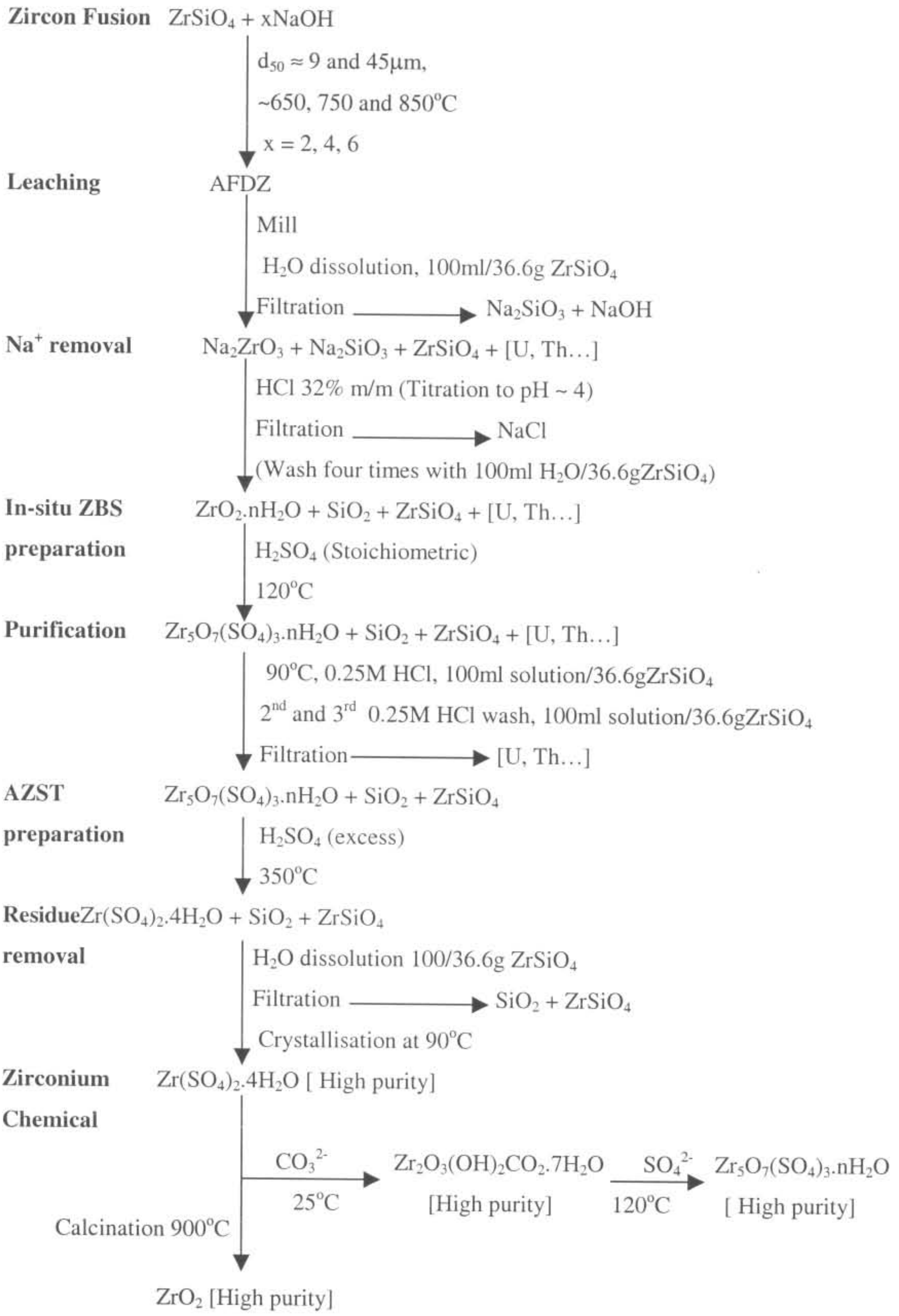

FIGURE 7.1 A diagrammatic representation of the alkali fusion processes (De Wet's process) used to synthesise high purity zirconium sulphate and zirconia

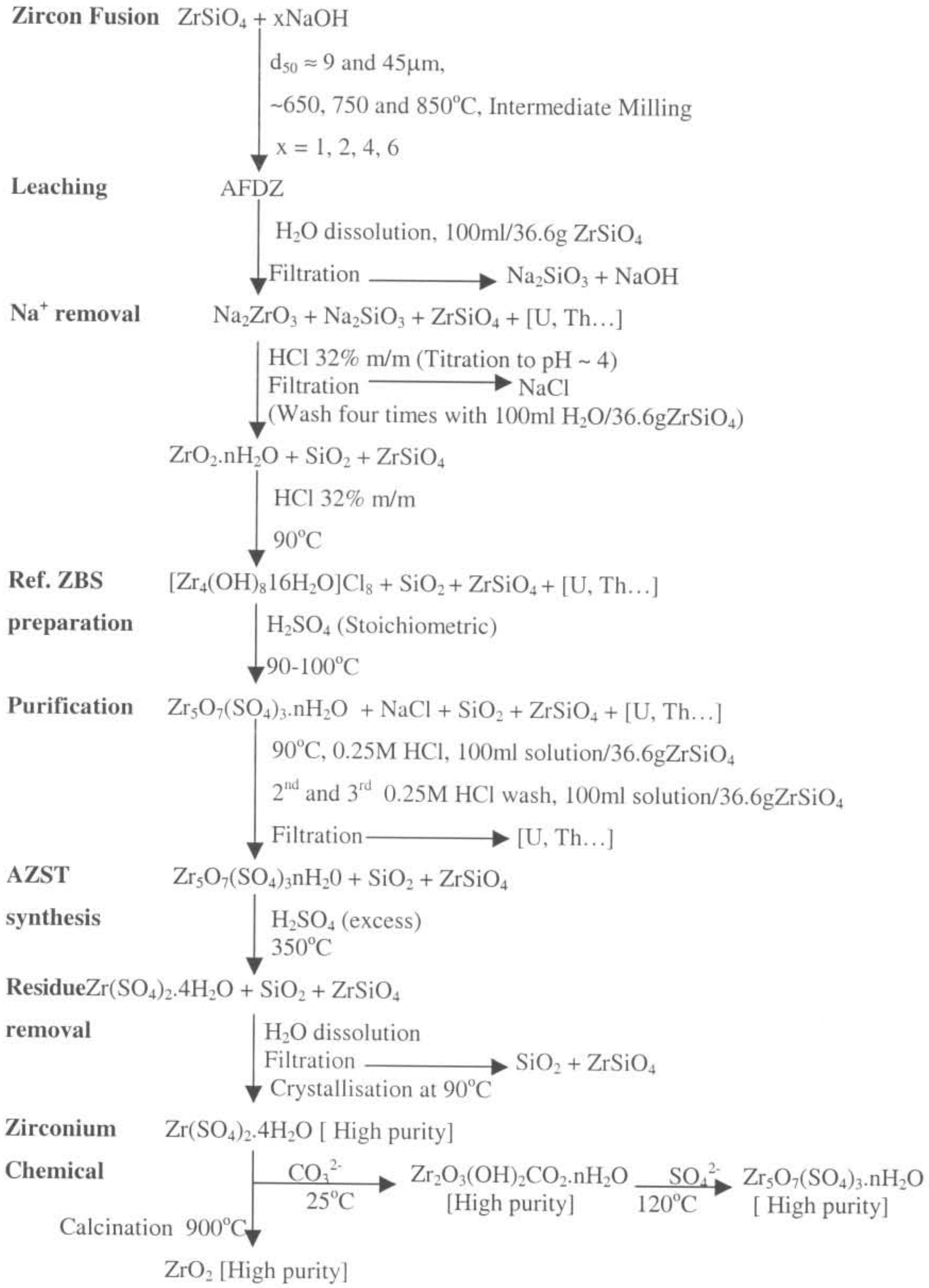

FIGURE 7.2 A diagrammatic representation of the alkali fusion processes (**modified process**) used to synthesise high purity zirconia and zirconium chemicals. The process employs a single precipitation technique to prepare ZBS. The ZBS synthesised by this method is much more stable than the ZBS synthesised from adding sulphuric acid to hydrous zirconia at 120°C (Fig. 7.1).

7.4.2 ZIRCON FUSION (MILLING AFTER FUSION)

Milled zircon, $d_{50} \approx 9\mu m$, 99.8% (m/m) from Richards' bay, South Africa supplied by Ferro Industrial products, was fused with sodium hydroxide in a high temperature oven at varying mole ratios and fusion temperatures. The moles of sodium hydroxide, per mole of zircon, were varied from two to six, at two mole increments. The fusion temperature ranged from 650 to 850°C with 100°C increments. Fusion time was about two hours. For example in one experiment, 36.6g of zircon sand was reacted with 16.0g of sodium hydroxide at 750°C. This reaction represented a mole of zircon fused with two moles of sodium hydroxide fusion at 750°C.

The oven product, commonly called alkali fusion decomposed zircon (AFDZ), was allowed to cool to room temperature, weighed to determine water evaporation during the course of the reaction, milled and weighed again to determine any losses due to experimental error. The milled fused product (MAFDZ), was divided into two parts, this was done to establish the reproducibility of each data point.

7.4.3 ZIRCON FUSION (INTERMEDIATE MILLING)

This step was introduced for the fusion optimisation experiments. The zircon was fused with sodium hydroxide for about 45 minutes. The AFDZ was removed from the oven and allowed to cool to room temperature for 30 minutes. The AFDZ was then milled with a pastel and mortar for about 5 minutes. The AFDZ was fused again for about an hour.

7.4.3 LEACHING OF THE ALKALI FUSED DECOMPOSED ZIRCON

7.4.3.1 ALKALI SILICATE

The MAFDZ was leached in water to remove most of the sodium and soluble silicates from the insoluble zirconium containing species. The liquids were separated from the solids using centrifugation (5 000 r.p.m.). The liquids were then dried in an evaporating oven and sent for elemental analysis.

7.4.3.2 SODIUM AND SILICA DETERMINATION

The MAFDZ was leached in water to remove the soluble sodium and silicates from the insoluble zirconium containing species. The water leach was titrated while stirring with a standardised 32% (m/m) HCl solution. Bromomethyl orange was used as an indicator and a pH meter to determine the equivalence point at pH = 4. The hydrated silica was precipitated with an ammonia and ammonium chloride solution with the pH adjusted to seven. The sodium salts were then separated from the hydrated silica using centrifuge washes (5 000 r.p.m.). About 100ml of water was used for each wash. The hydrated silica was dried overnight in a drying oven at 90°C and calcined at 900°C to silica.

7.4.3.3 THE ALKALI ZIRCONATES

SODIUM REMOVAL (PREPARATION OF IN-SITU HYDROUS ZIRCONIA)

The zirconium containing solids remaining after the silica was leached out, were titrated with 32% (m/m) HCl solution to a pH = 4. The sodium containing salts e.g. NaCl were washed from the hydrous zirconia 4 to 5 times with a centrifuge using 250ml of distilled water for 36.6g $ZrSiO_4$ in each wash.

7.4.4 PREPARATION OF ZBS

7.4.4.1 PREPARATION OF in-situ ZBS FROM in-situ HYDROUS ZIRCONIA

The solids containing the hydrous zirconia were reacted with stoichiometric amounts of sulphuric acid at 150°C to form in-situ ZBS, $Zr_5O_7(SO_4)_3.nH_20$. Care was taken not to dry the paste in the oven. For example in-situ hydrous zirconia obtained from the fusion of 36.6g $ZrSiO_4$ 99.8% (m/m) with 32.0g NaOH 99.8% (m/m) (with intermediate milling at 850°C) was reacted 11.98g of standardised H_2SO_4 98% (m/m) at 90°C for about 20 min. Care was taken not to dry the paste.

7.4.4.2 PREPARATION OF REFERENCE ZBS SYNTHESIS (REF. ZBS)

For the purpose of optimising the HCl purification step, this type of ZBS had to be prepared. The sodium free solids (hydrous zirconia) were digested with HCl at 90°C to form zirconyl chloride $[Zr_4(OH)_8 16H_2O]Cl_8$.

For example in situ hydrous zirconia obtained from the fusion of 36.6g $ZrSiO_4$ 99.8 % (m/m) with 32g NaOH 99.8% (m/m) (with intermediate milling at 850°C) was reacted 61.4 g of standardised 32% (m/m) HCl at 90°C for about 20 min while stirring. The reaction continued until a clear slightly yellow solution was obtained. The ZOC solution was separated from the unreacted solids with centrifugation (5 000 r.p.m.).

The Ref. ZBS was prepared from ZOC solution by adding stoichiometric amounts of a standardised sulphuric acid solution (about 11.98g H_2SO_4 98% m/m) at 90°C while stirring for 30 minutes. The precipitated ZBS was washed 3-4 times with distilled water using a centrifuge (5 000 r.p.m.).

7.4.5 THE PURIFICATION AND ANALYSIS OF THE ZBS PRODUCTS

The impurities in the ZBS product were digested with a hydrochloric acid solution in the first wash at approximately 90°C for about 10 minutes. For the purpose of the De Wet's process, 0.25-1.0M HCl solutions were used. The second and third wash ZBS products were washed using centrifugation (5 000 r.p.m.) with about 100ml of distilled water per 36.6g $ZrSiO_4$ was employed for each washing step. The washing water was collected and evaporated at approximately 80°C in an oven overnight. The solids left from the evaporation were collected and calcined at 900°C. The calcined zirconia was weighed and sent for elemental analysis. The in-situ ZBS was collected from each washing step, converted to AZST, separated from the residue with centrifugation, calcined to zirconia then sent for elemental analysis. A similar procedure for sample collection for Ref. ZBS was used.

7.4.6 PREPARATION OF ZIRCONIUM SULPHATE TETRAHYDRATE

7.4.6.1 AZST PREPARATION FROM IN-SITU ZBS

The in-situ ZBS was reacted with sulphuric acid in a well-ventilated oven at 150°C to form in-situ AZST. The excess sulphuric acid was evaporated at 350°C in a well-ventilated oven. The solids were allowed to cool to room temperature. The in-situ AZST was separated from the unreacted solids by water dissolution and centrifugation (5 000 r.p.m.). The AZST was then crystallised overnight at 90°C by water evaporation

7.4.6.2 AZST PREPARATION FROM IN-SITU HYDROUS ZIRCONIA

This route of preparing AZST from hydrous zirconia was followed when the decomposition step was being optimised. This step ignores the losses experienced in the purification step. The sodium free solids (in-situ hydrous zirconia) were reacted with sulphuric acid 98% (m/m) to form zirconium sulphate tetrahydrate $Zr(SO_4)_2.4H_2O$ (AZST) in a well-ventilated oven, firstly at 150°C then at 350°C to evaporate any excess sulphuric acid.

The solids were allowed to cool to room temperature, and the AZST was dissolved in the water and separated from the unreacted residue. About 100ml of distilled water per 36.6g $ZrSiO_4$ was used. The AZST was then crystallised overnight at 90°C by water evaporation and calcined to zirconia at 900°C.

7.4.7 THE RESIDUE

The solids remaining after the AZST dissolution were dried at 90°C. The solids were also calcined at 900°C. All the calcined products: zirconia, silica and residue were collected and weighed for mass balances and elemental analysis with XRF and ICP spectroscopy

7.4.8 ZIRCONIUM CHEMICALS

7.4.8.1 SYNTHESIS OF ZIRCONIUM BASIC CARBONATE

Zirconium basic carbonate was precipitated at room temperature from solutions of AZST. The AZST, of High purity, was synthesised from the alkali fusion process shown in Figure 7.1. For example, a 0.6 M Na_2CO_3 or $(NH_4)_2CO_3$ solution was added to 100ml of 0.1M AZST solution with continuous stirring until a pH of 6.75. The ZBC precipitate was thoroughly washed with a centrifuge (5 000 r.p.m.). The ZBC was washed four times with 100ml of distilled water to remove the sodium or ammonium and sulphate ions.

7.4.8.2 SYNTHESIS OF ZIRCONIUM BASIC SULPHATE

Zirconium basic sulphate (ZBS) was prepared from ZBC by adding stoichiometric amounts of sulphuric acid. The reaction was allowed to continue at 150°C for about 30 minutes. For instance, about 5.12ml of 18.72 M H_2SO_4 solution was added to a paste of ZBC $Zr_2O_3(OH)_2CO_2.nH_2O$ prepared from 36.6g of zircon decomposed with 32.0g of NaOH.

Differently, about 5.12 ml of 18.72 M H_2SO_4 solution was added to about 34.72g of ZBC. The ZBS $Zr_5O_7(SO_4)_3.nH_2O$ product was washed four times with about 100ml of distilled water with centrifugation (5 000 r.p.m.).

7.5 ANALYSIS

7.5.1 X-RAY POWDER DIFFRACTOMETRY (XRD)

X-ray diffraction (XRD) measurements between 0.8 and 10° 2θ were obtained with Siemens D-501 automated diffractometer Cu-$K\alpha$ (15.418 nm) with the Soller slits at 2° (diffracted beam side), divergence slits at 1° and Receiving slits at 0.05°. A scintillation counter detector was used, over the range 3-65° 2θ and step width 0.02°, at the scan rate of 30s per step.

7.5.2 SCANNING ELECTRON MICROSCOPE (SEM)

The particle morphology was examined by the scanning electron microscope with a JEOL JSM-840 instrument. The probe current was 3×10^{-11} ampere and an acceleration voltage of 5.0 kV kept constant for all measurements.

7.5.3 X-RAY FLUORESCENCE (XRF)

The elemental analysis was done with an ARL 9 400 XP + wavelength dispersive XRF spectrophotometer. The samples were ground to < 75µm in a Tungsten carbide milling vessel and pressed in a powder briquette using a saturated Movial solution as binder. Analysis was executed on the samples using a wide confidence limit program i.e. analysis was carried-out for every possible element present in the samples.

7.5.4 THE RAMAN AND INFRARED SPECTROPHOTOMETER

The Raman spectra were recorded in the region 200-3 600 cm^{-1} using the microprobe on the XY Dilor Multichannel instrument. Excitation was accomplished with the 514.5 nm line of an Argon ion laser. Incident power was approximately 100 mW. Infrared spectra were recorded on the Bruker IFS 113 v FTIR spectrometer as KBr pellets in the region 400-4 000 cm^{-1}.

REFERENCE:

1. Wet, W.J. (1999) Method for treating zircon, S. A. Patent 2000/2797

CHAPTER 8

CHARACTERISATION OF ALKALI FUSION PROCESSES

8.1 INTRODUCTION

De Wet's patent has the advantage of synthesising a stable basic sulphate at a fast rate. The sulphate is so stable such that it can be washed with mineral acids [4], for example HCl, to remove radioactive impurities. The characterisation of the process will now be given. Figure 7.1 shows a diagrammatic representation of the process for zirconia recovery and the methods used for analysis in bold.

The alkali fusion process was followed stepwise with characterisation methods. The characterisation focused on identifying the phases present and quantifying their composition. The by-products and effluents were also investigated using elemental analysis. The final products are further characterised with spectroscopic methods and SEM.

8.2 RESULTS

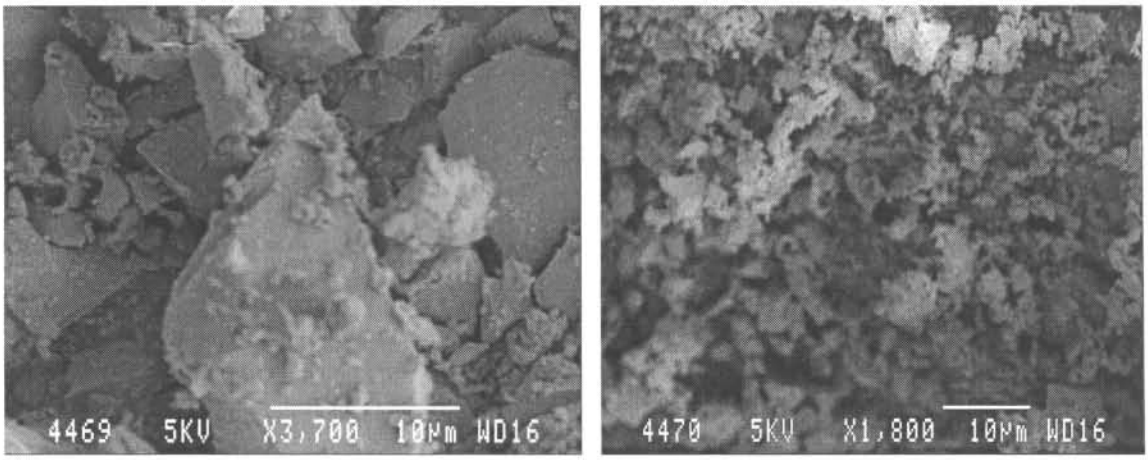

(a) *b)*

FIGURE 8.1: SEM photographs of milled zircon sand mined at Richards Bay, (a) the 45μm and (b) the 9μm mean particle size. The difference in particle size can be seen.

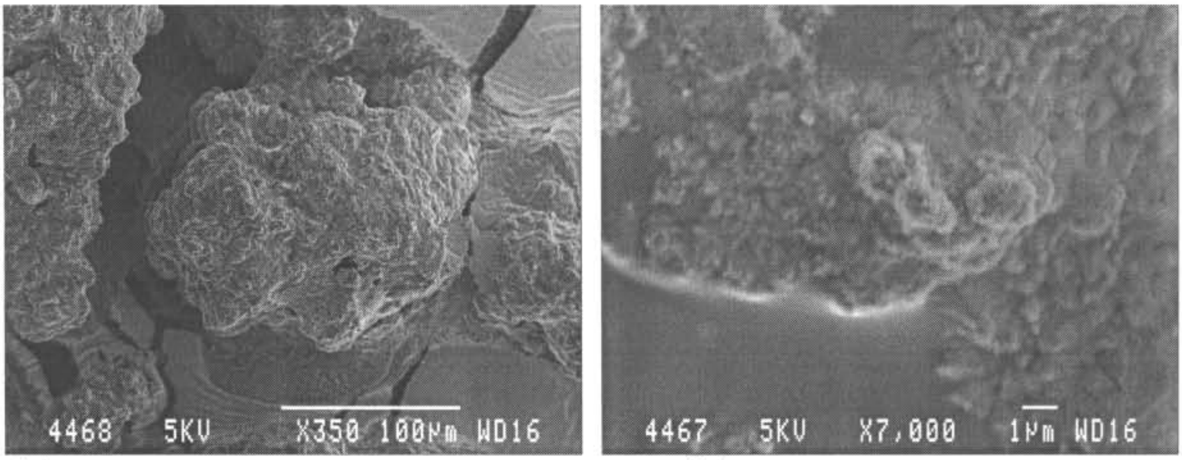

(a) *(b)*

FIGURE 8.2: SEM photographs of decomposed zircon sand (AFDZ). The AFDZ was obtained by zircon with sodium hydroxide for an hour. The particle size of the agglomerate of the fused product is shown in (a). On the surface of (b), some unreacted NaOH can be seen as the homogenised area. The unreacted NaOH was common for all the fusion without the intermediate milling.

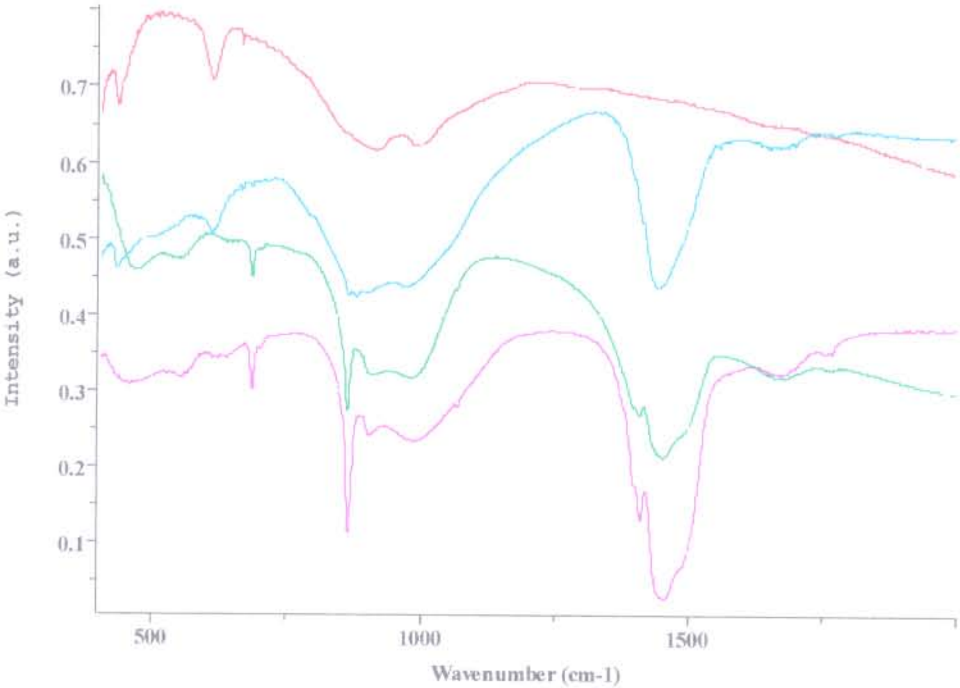

FIGURE 8.3: A super-positioning of the infrared spectra of alkali fused decomposed zircon at 650°C. The spectrum at the top represents milled zircon sand. Following consecutively are the spectra for 2, 4, and 6 moles NaOH fused with a mole of zircon sand for about an hour.

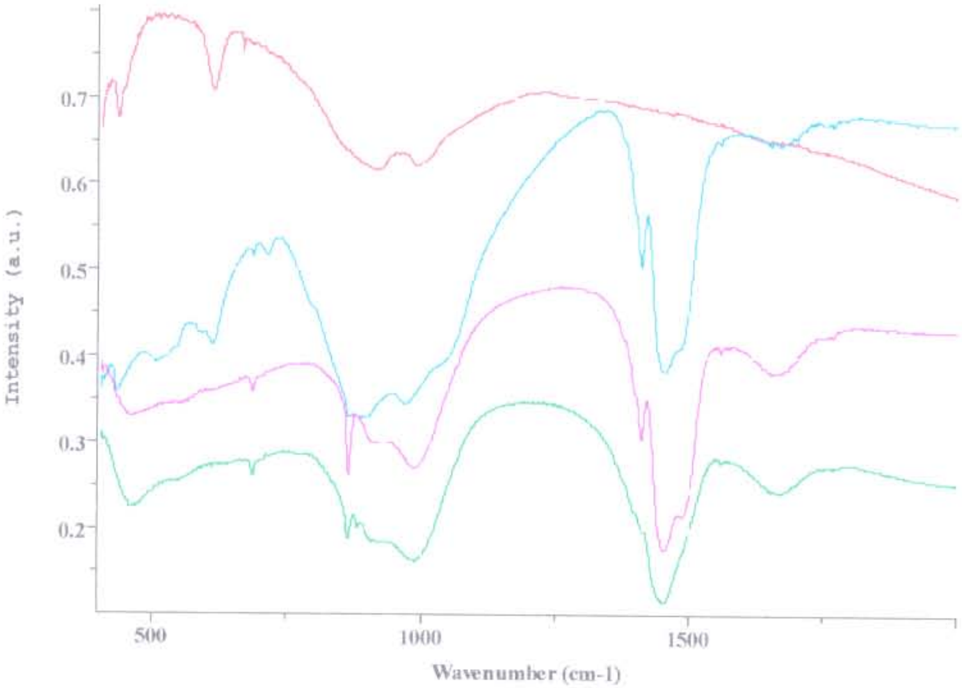

FIGURE 8.4: A super-positioning of the infrared spectra of alkali fused decomposed zircon at 750°C. The spectrum at the top represents milled zircon sand. Following consecutively are the spectra for 2, 4, and 6 moles NaOH fused with a mole of zircon sand for about an hour.

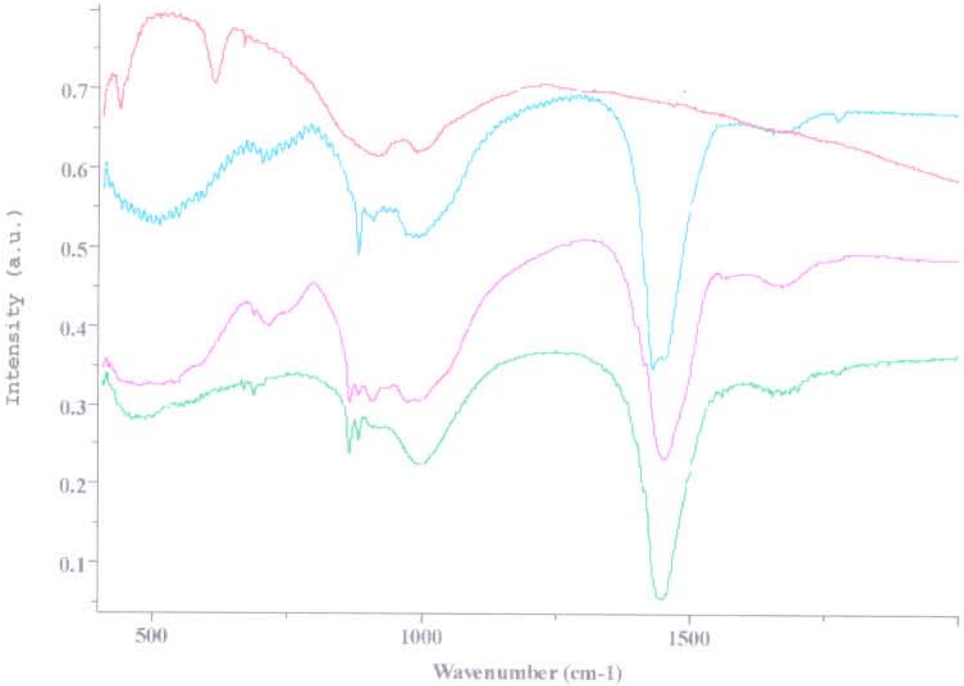

FIGURE 8.5: A super-positioning of the infrared spectra of alkali fused decomposed zircon at 850°C. The spectrum at the top represents milled zircon sand. Following consecutively are the spectra for 2, 4, and 6 moles NaOH fused with a mole of zircon sand for about an hour.

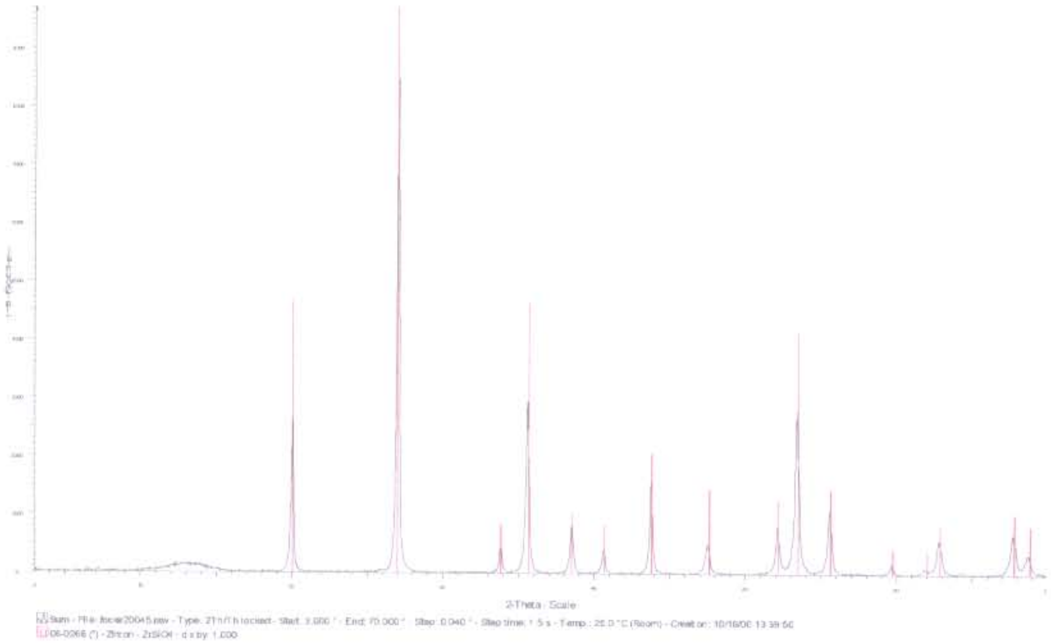

FIGURE 8.6: X-ray spectra of milled zircon sand, $d_{50} \approx 9\mu m$, from Richard's bay.

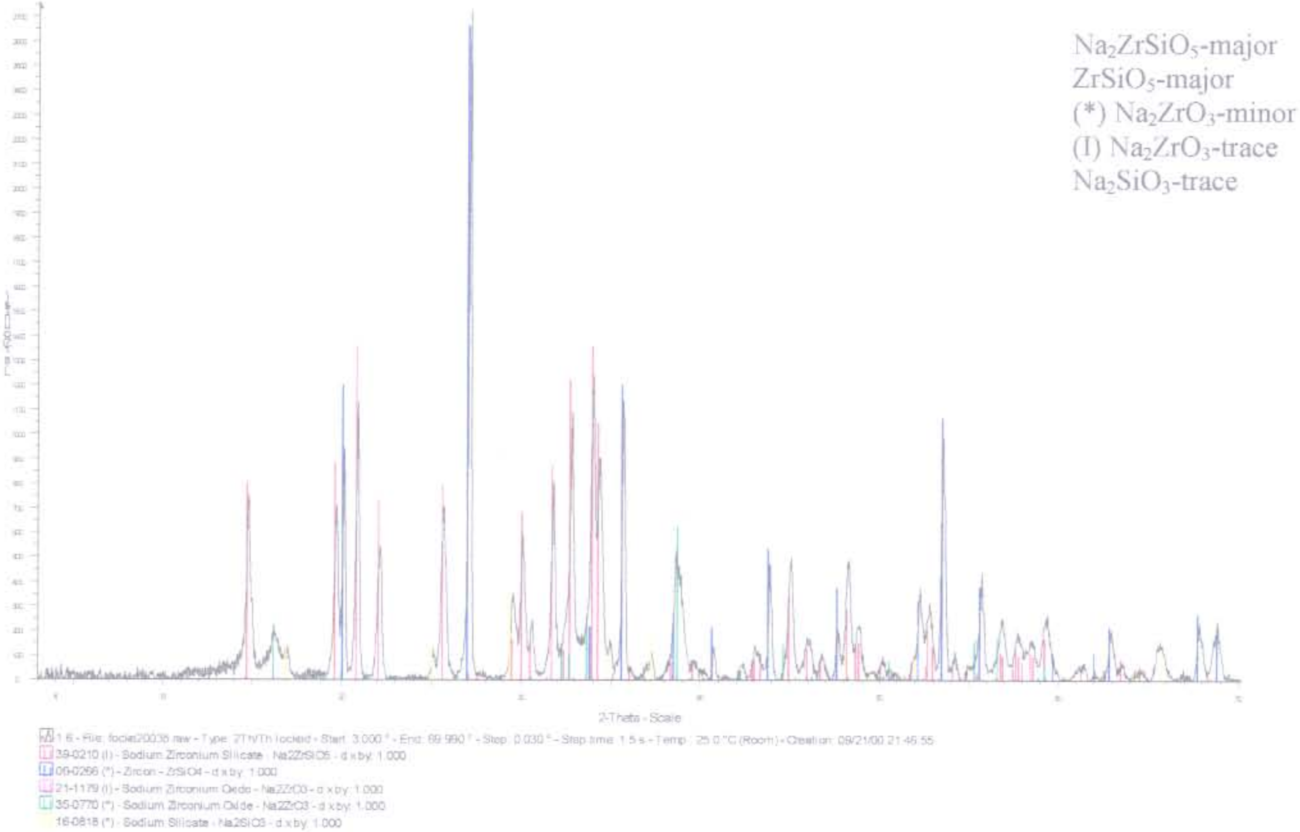

FIGURE 8.7: X-ray diffraction pattern of alkali fused decomposed zircon. A mole of $d_{50} \approx 9\mu m$ zircon was decomposed with two moles of sodium hydroxide at 850°C for about 2 hours with intermediate milling.

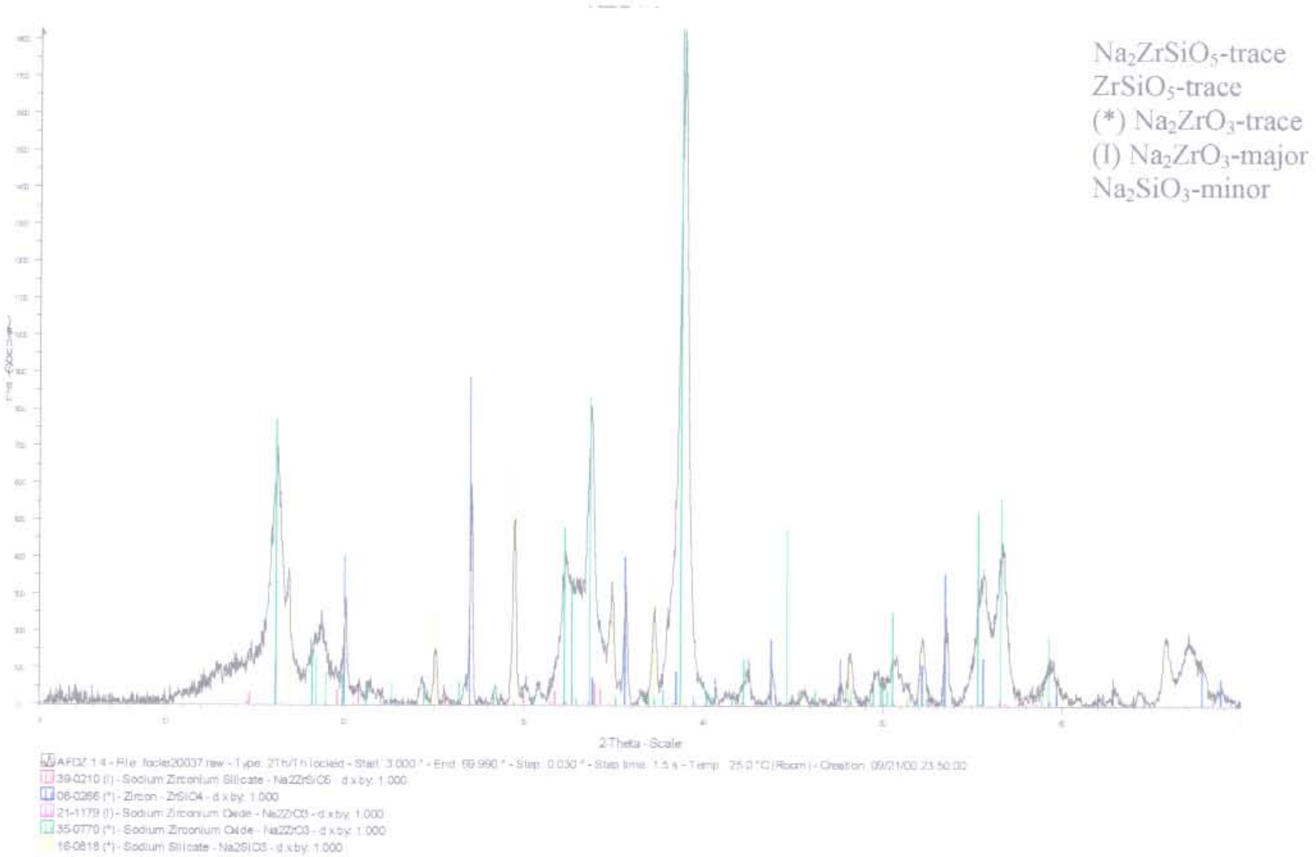

FIGURE 8.8: X-ray diffraction pattern of alkali fused decomposed zircon. A mole of $d_{50} \approx 9\mu m$ zircon was decomposed with four moles of sodium hydroxide at 850°C for 2 hours with intermediate milling.

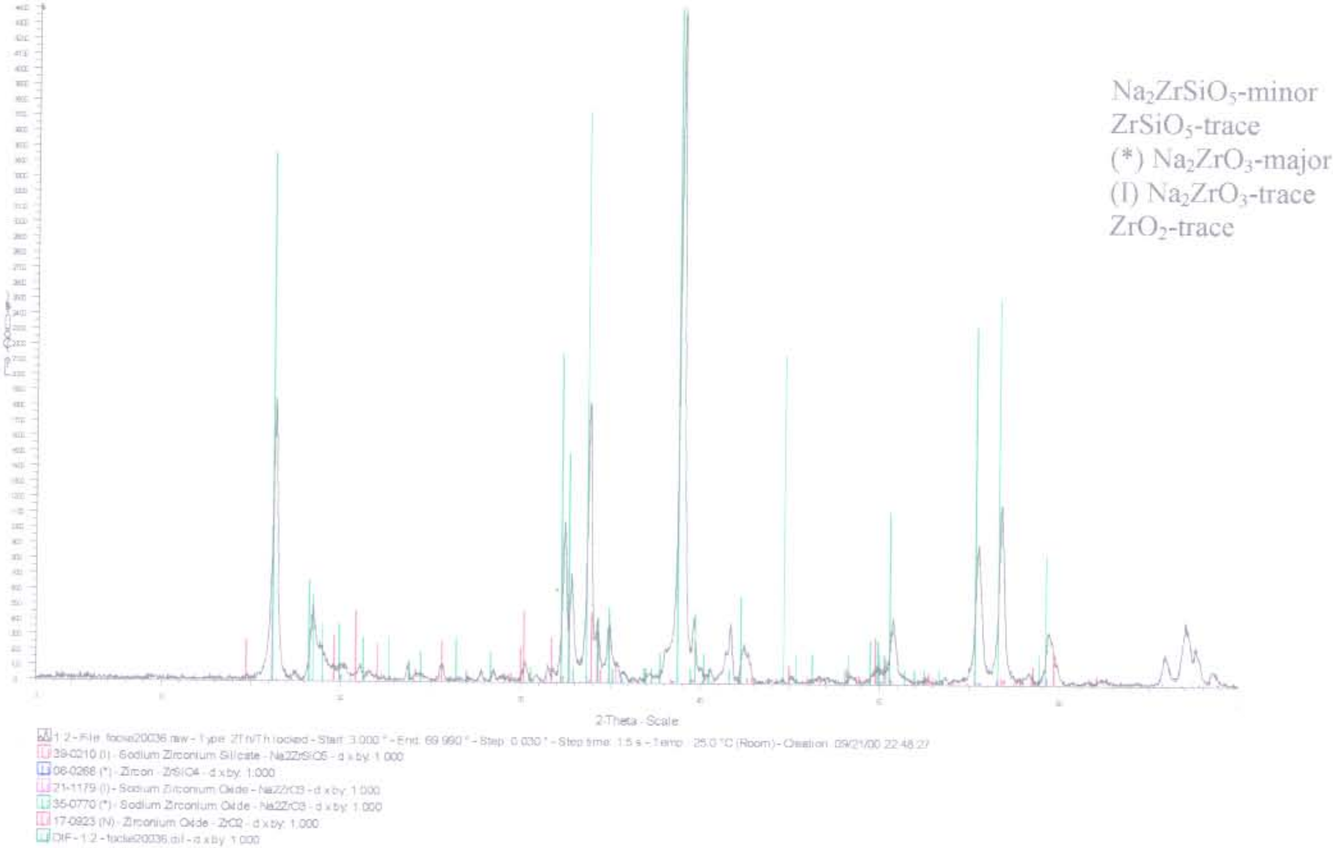

FIGURE 8.9: X-ray diffraction pattern of alkali fused decomposed zircon. A mole of $d_{50} \approx 9\mu m$ zircon was decomposed with six moles of sodium hydroxide at 850°C for 2 hours with intermediate milling.

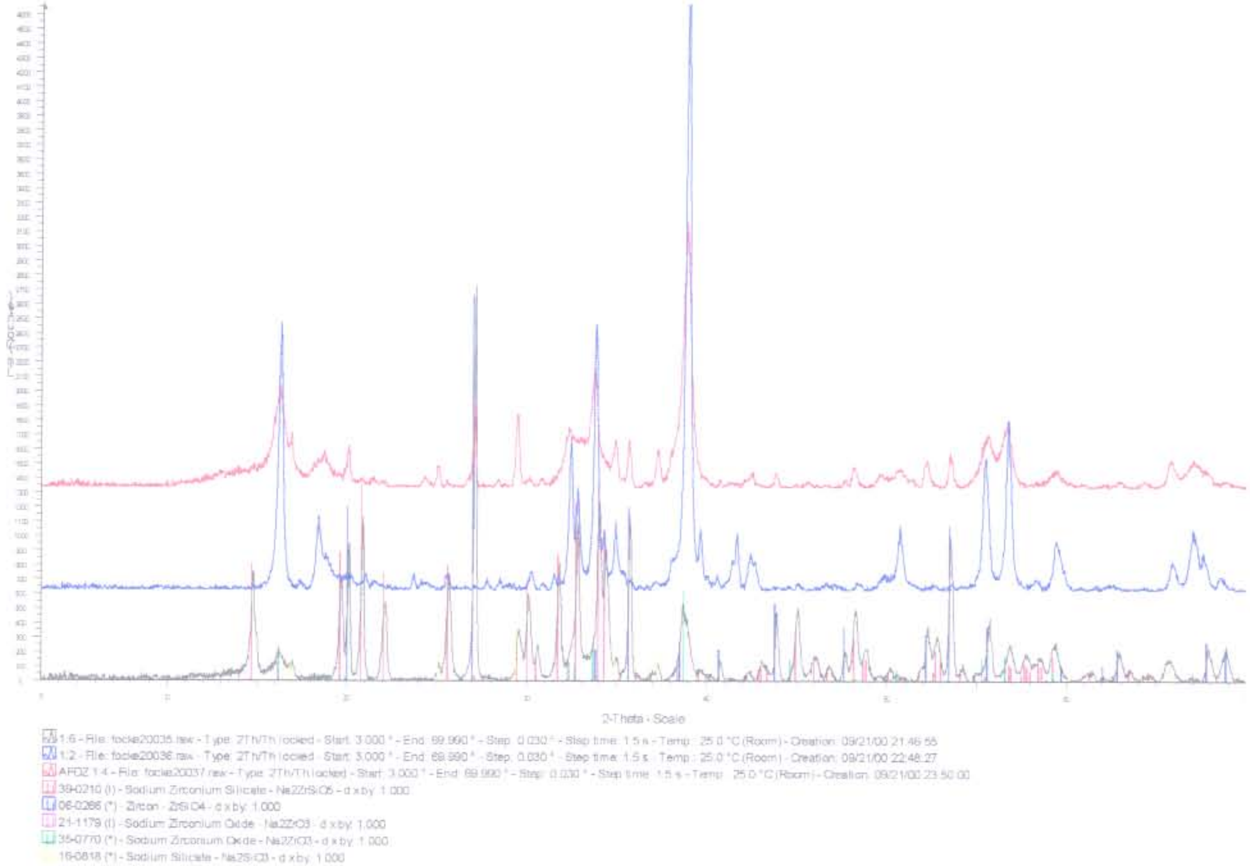

FIGURE 8.10: A super-positioning of the X-ray diffraction pattern of alkali fused decomposed zircon. The spectra at for the various mole ratios at 850°C were superimposed. At the top is the spectra when fusing with six moles of NaOH. Following consecutively is the spectra when fusing with four and two moles of NaOH.

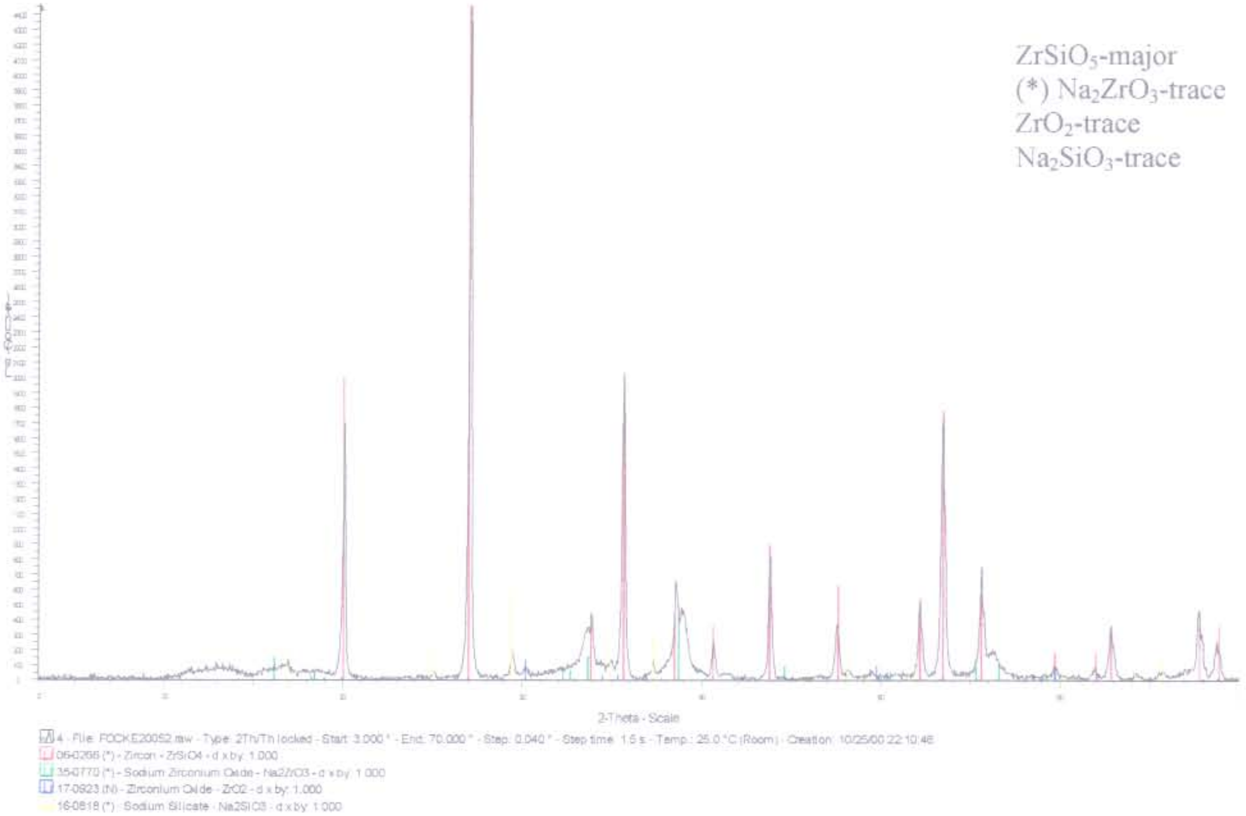

FIGURE 8.11: X-ray diffraction pattern of alkali fused decomposed zircon. A mole of $d_{50} \approx 9\mu m$ zircon was decomposed with two moles of sodium hydroxide at 650°C for 2 hours with intermediate milling.

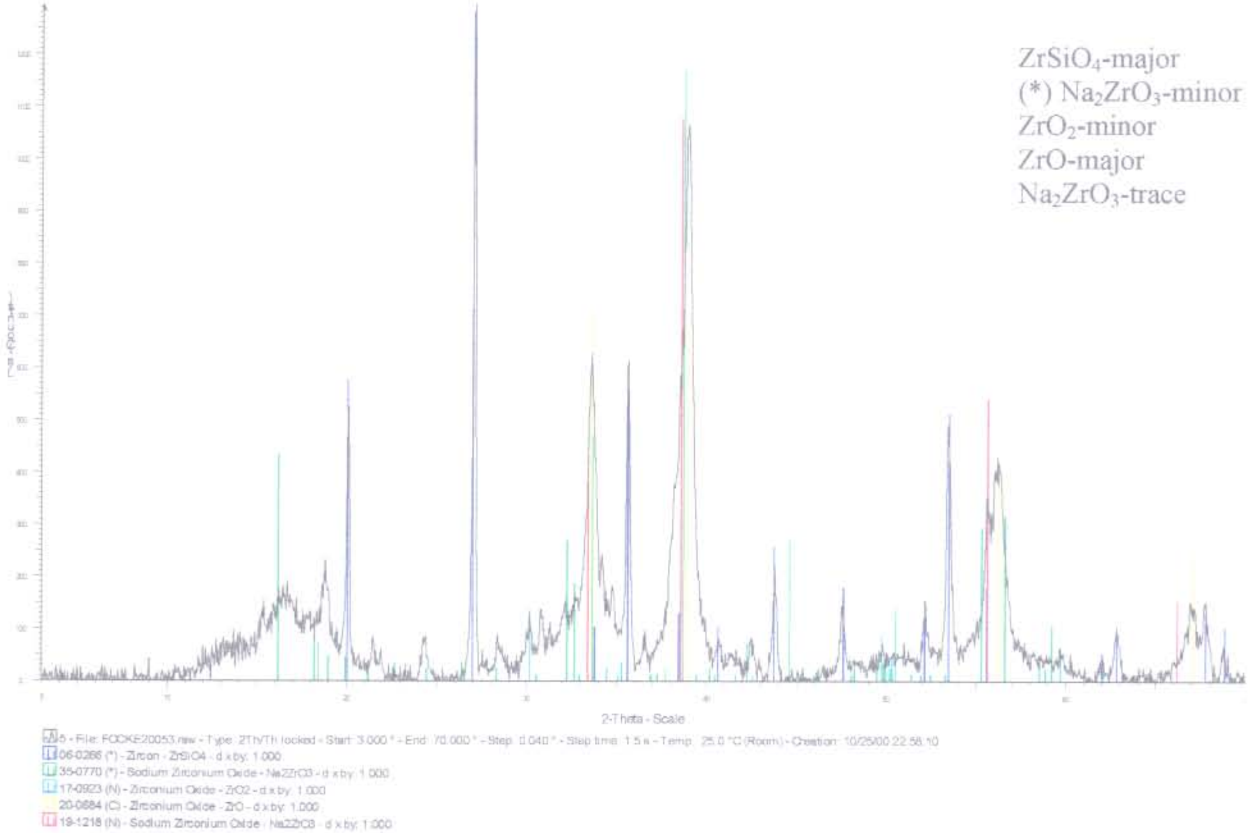

FIGURE 8.12: X-ray diffraction pattern of alkali fused decomposed zircon. A mole of $d_{50} \approx 9\mu m$ zircon was decomposed with four moles of sodium hydroxide at 650°C for 2 hours with intermediate milling.

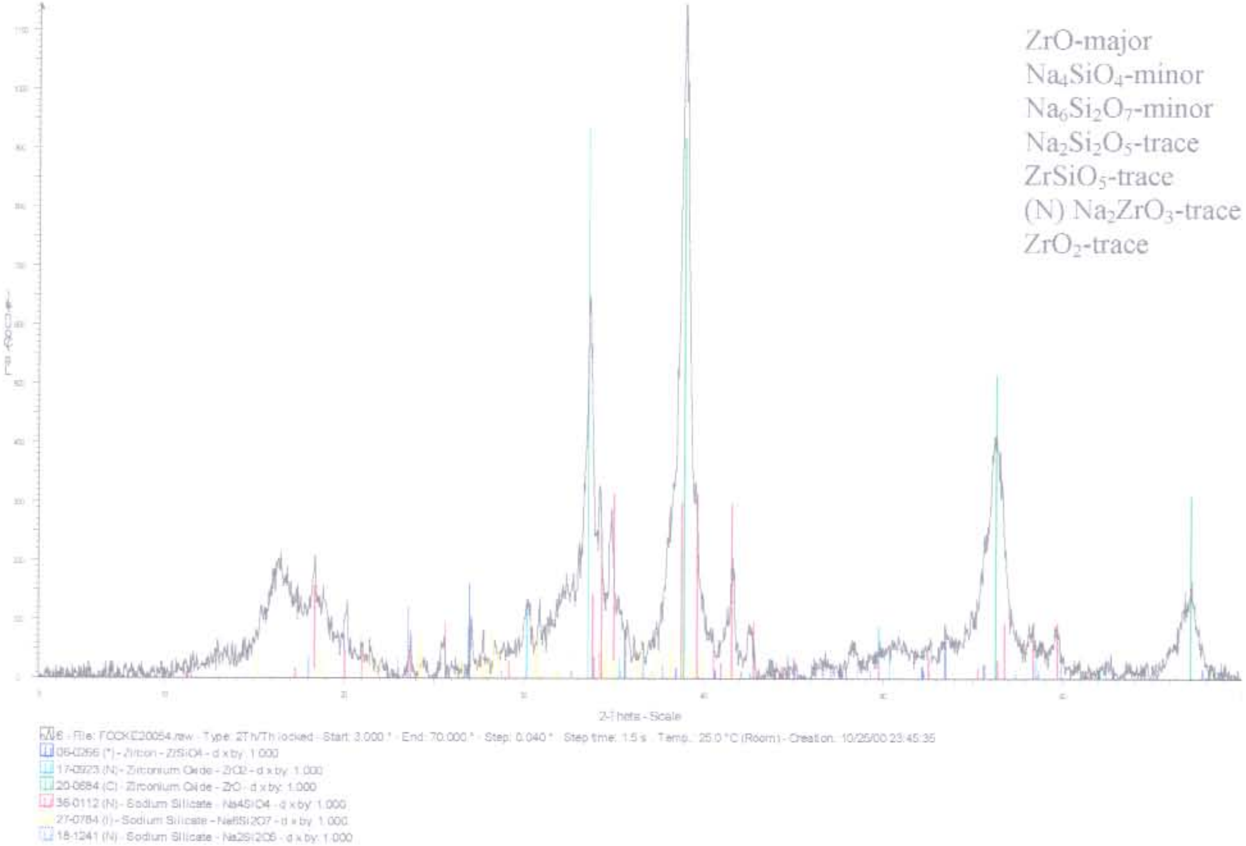

FIGURE 8.13: X-ray diffraction pattern of alkali fused decomposed zircon. A mole of $d_{50} \approx 9\mu m$ zircon was decomposed with six moles of sodium hydroxide at 650°C for 2 hours with intermediate milling.

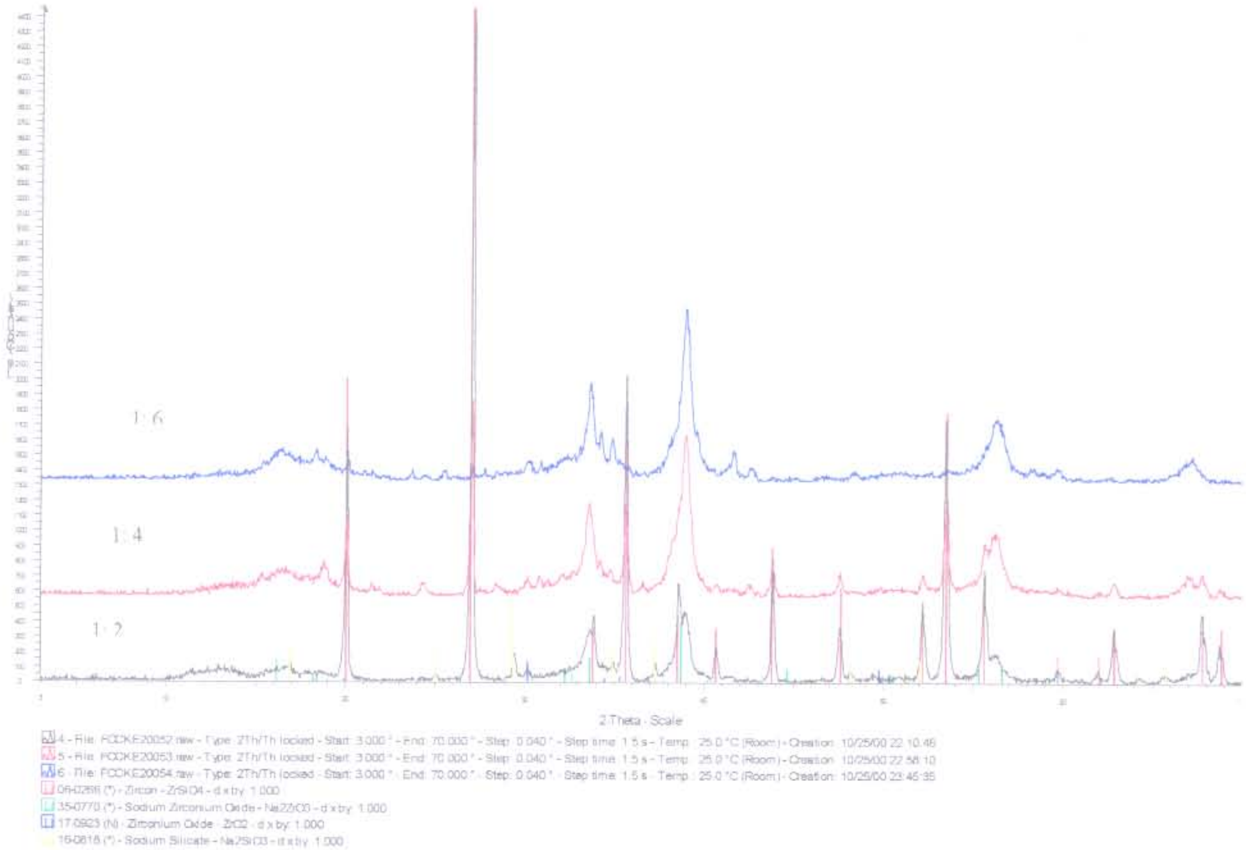

FIGURE 8.14: A super-positioning of the X-ray diffraction pattern of alkali fused decomposed zircon. The spectra at for the various mole ratios at 650°C after two hours with intermediate milling were superimposed.

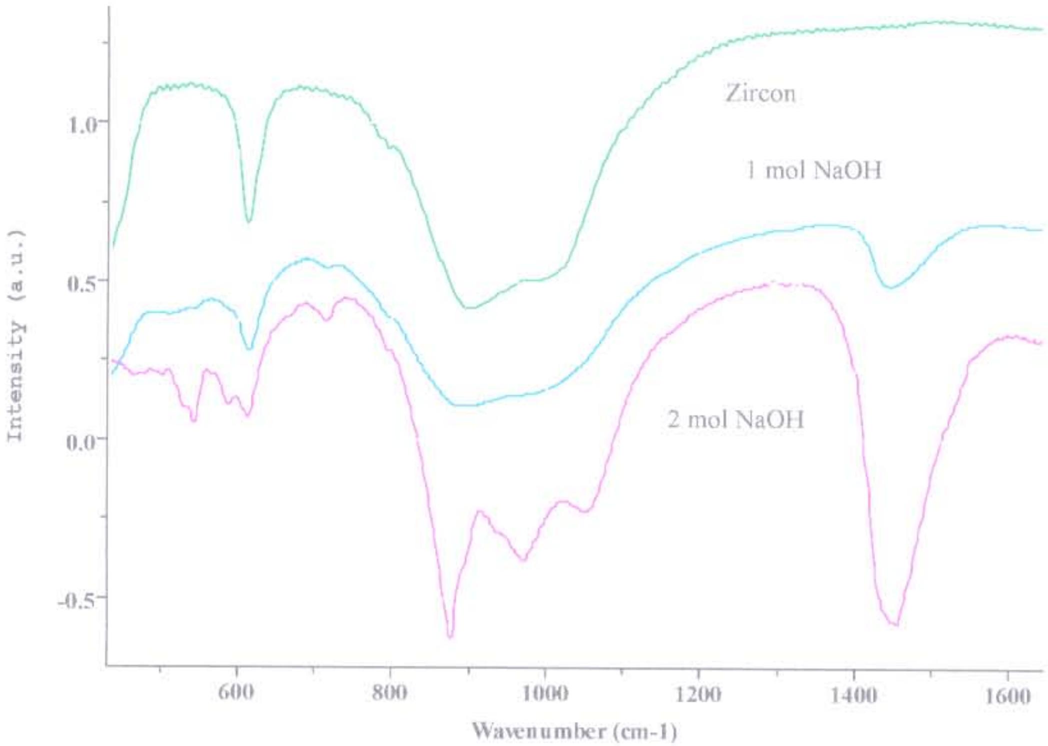

Figure 8.15: A super-positioning of the Infra red spectra of alkali fused decomposed zircon. The spectra at for the various mole ratios (as shown in the diagram) at 650°C after 336 hours of decomposition were superimposed.

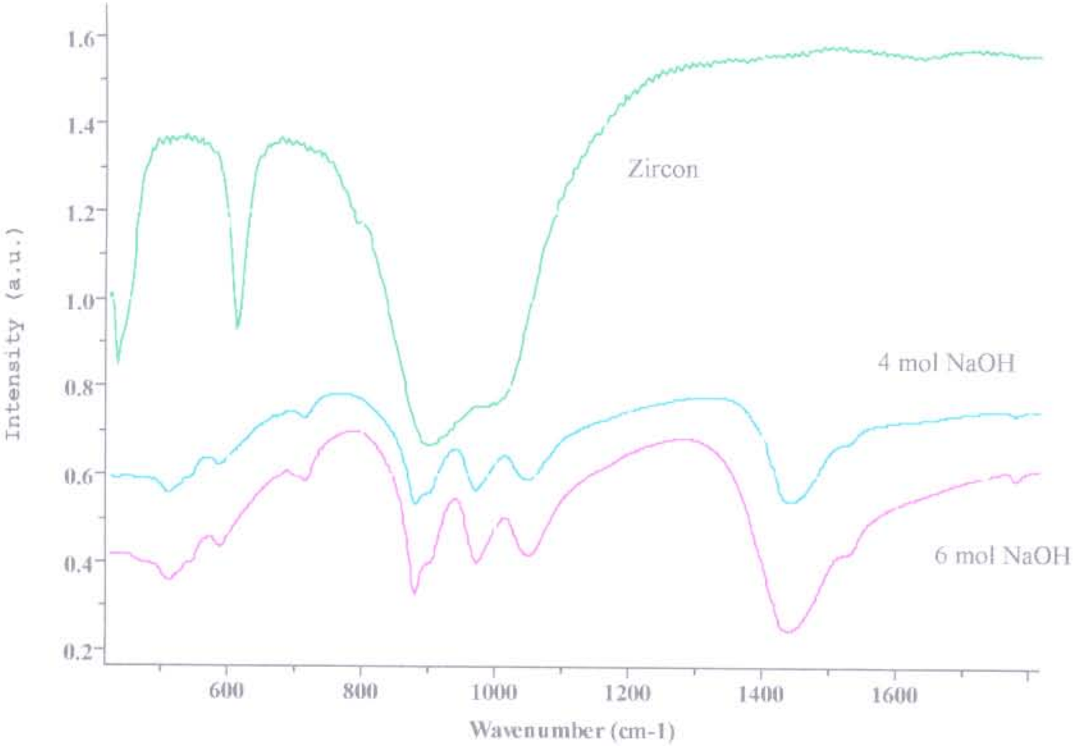

Figure 8.16: A super-positioning of the Infra red spectra of alkali fused decomposed zircon. The spectra at for the various mole ratios (as shown in the diagram) at 650°C after 336 hours of decomposition were superimposed.

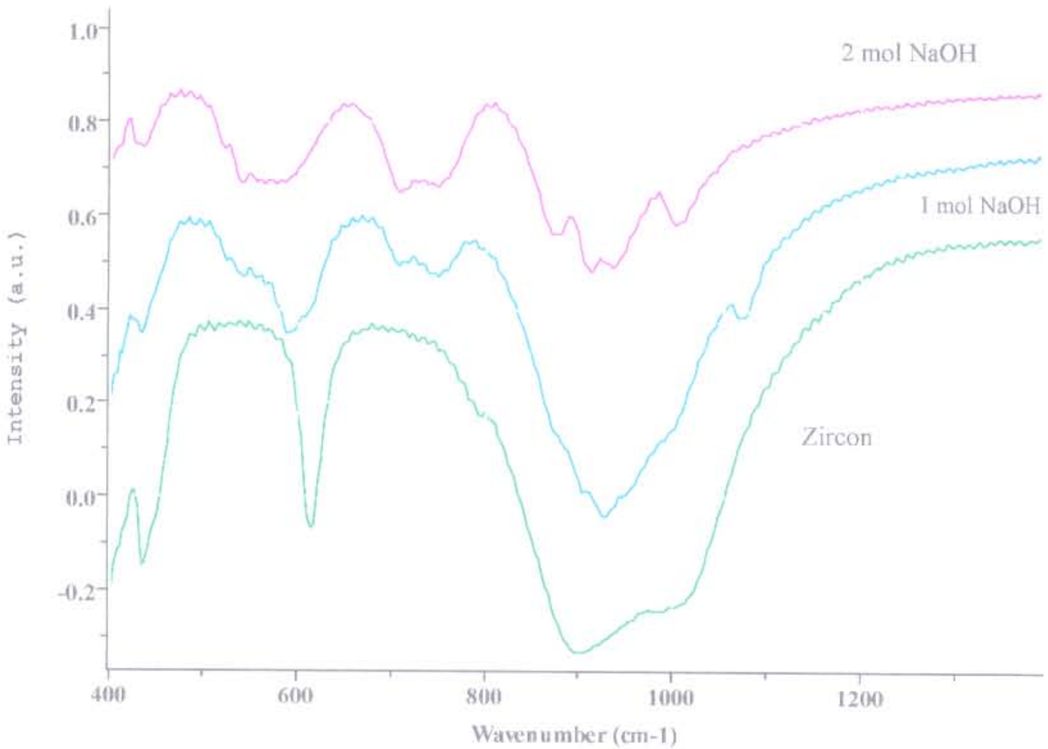

Figure 8.17: A super-positioning of the Infra red spectra of alkali fused decomposed zircon. The spectra at for the various mole ratios (as shown in the diagram) at 850°C after 336 hours of decomposition were superimposed.

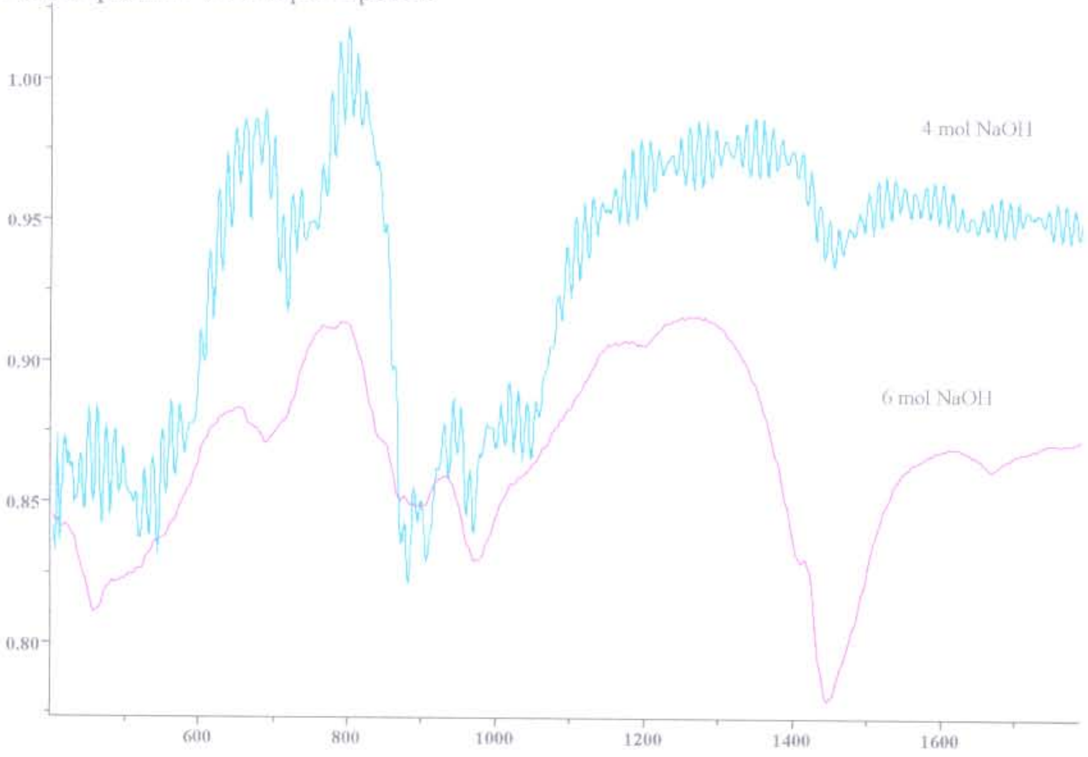

Figure 8.18: A super-positioning of the Infra red spectra of alkali fused decomposed zircon. The spectra at for the various mole ratios (as shown in the diagram) at 850°C after 336 hours of decomposition were superimposed.

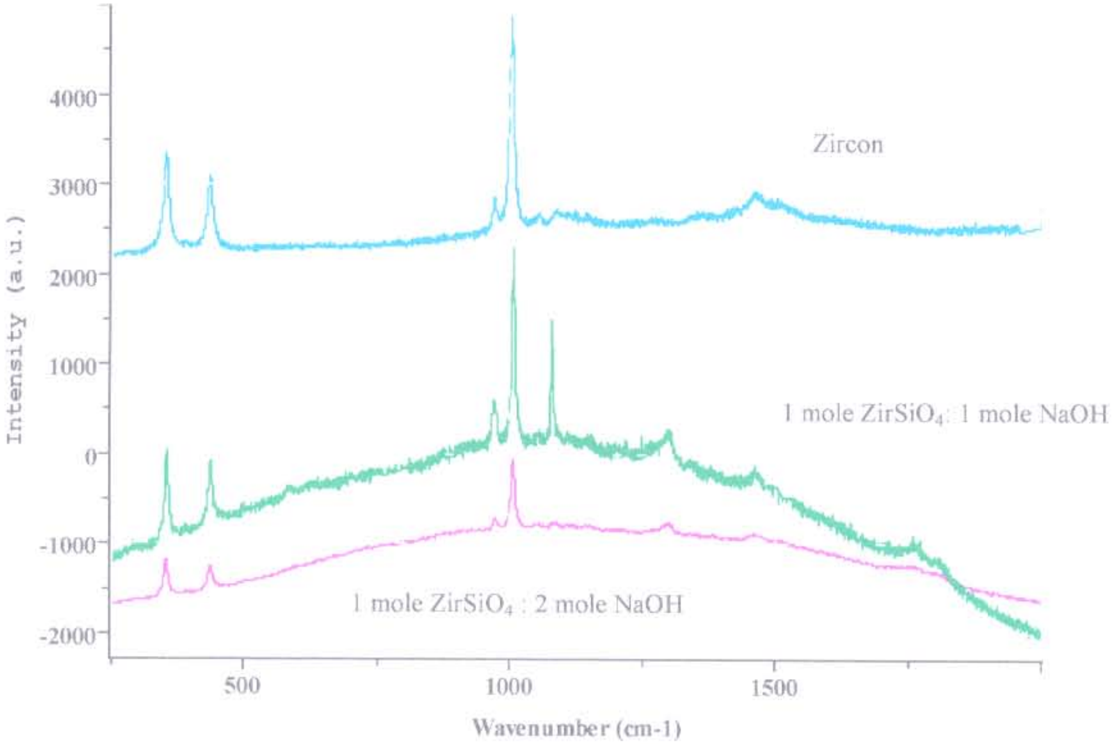

FIGURE 8.19: A Super-positioning of the Raman spectra of alkali fused decomposed zircon. A mole of $d_{50} \approx 9$ μm zircon was decomposed with various moles (as shown on diagram) of sodium hydroxide at 650°C for 336 hours.

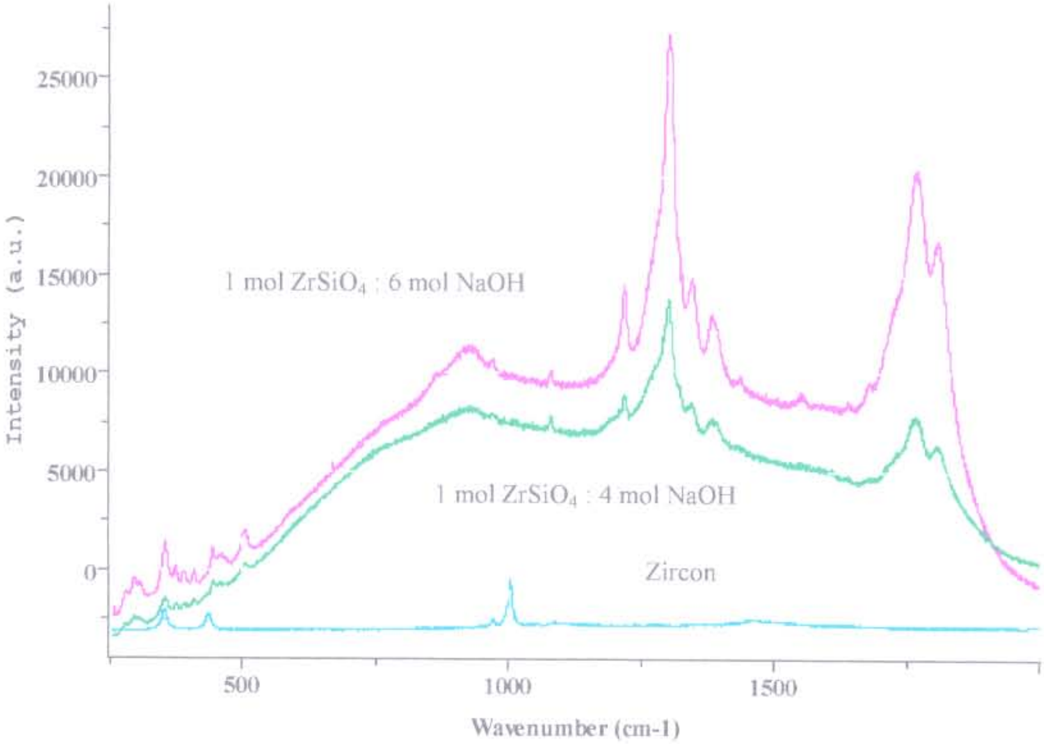

FIGURE 8.20: A Super-positioning of the Raman spectra of alkali fused decomposed zircon. A mole of $d_{50} \approx 9$ μm zircon was decomposed with various moles (as shown on diagram) of sodium hydroxide at 650°C for 336 hours.

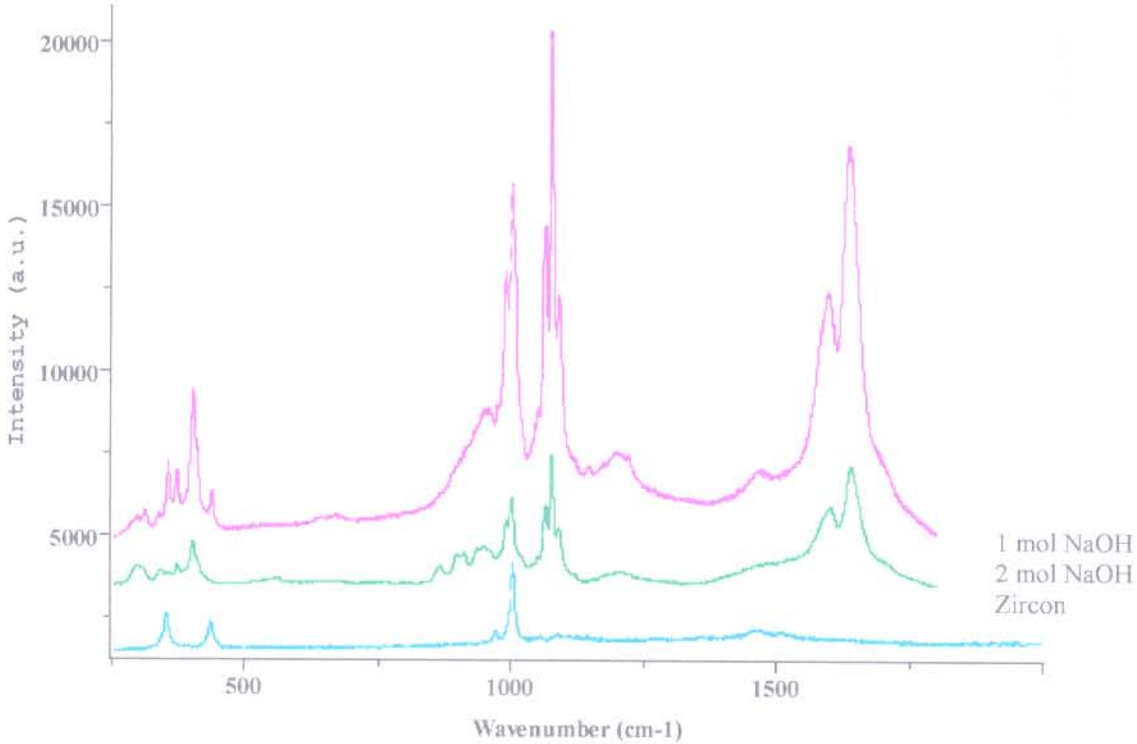

FIGURE 8.21: A Super-positioning of the Raman spectra of alkali fused decomposed zircon. A mole of $d_{50} \approx 9$ µm zircon was decomposed with various moles (as shown on diagram) of sodium hydroxide at 850°C for 336 hours.

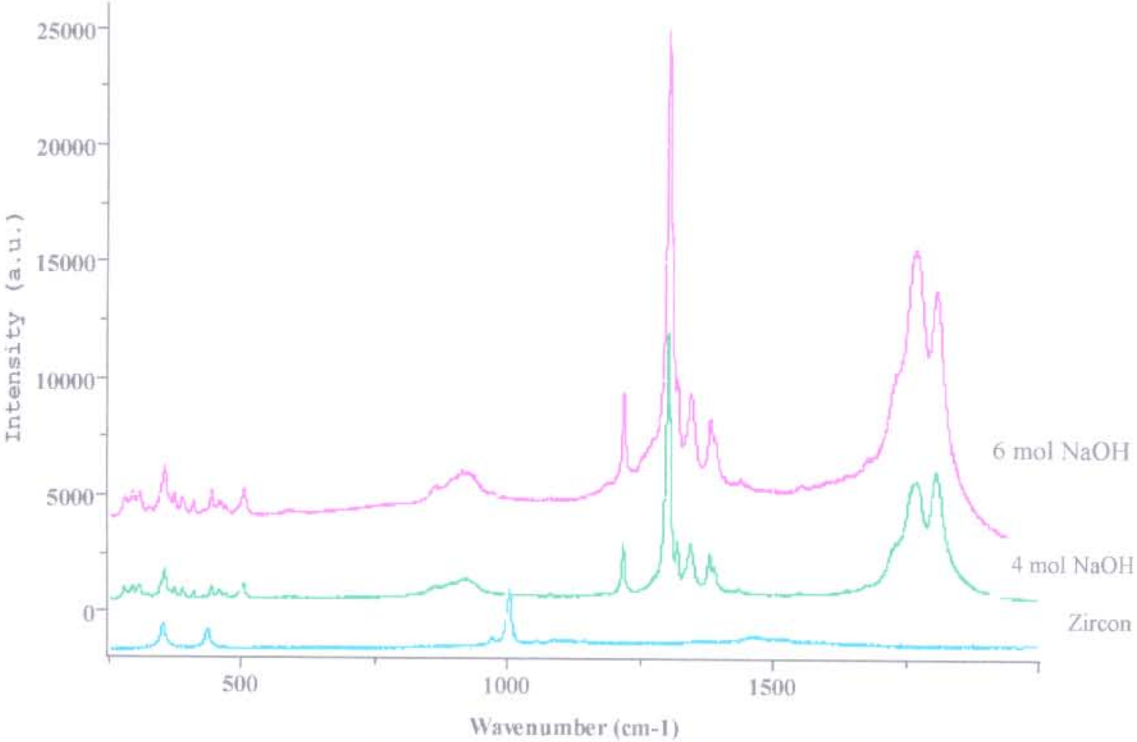

FIGURE 8.22: A Super-positioning of the Raman spectra of alkali fused decomposed zircon. A mole of $d_{50} \approx 9$ µm zircon was decomposed with various moles (as shown on diagram) of sodium hydroxide at 850°C for 336 hours.

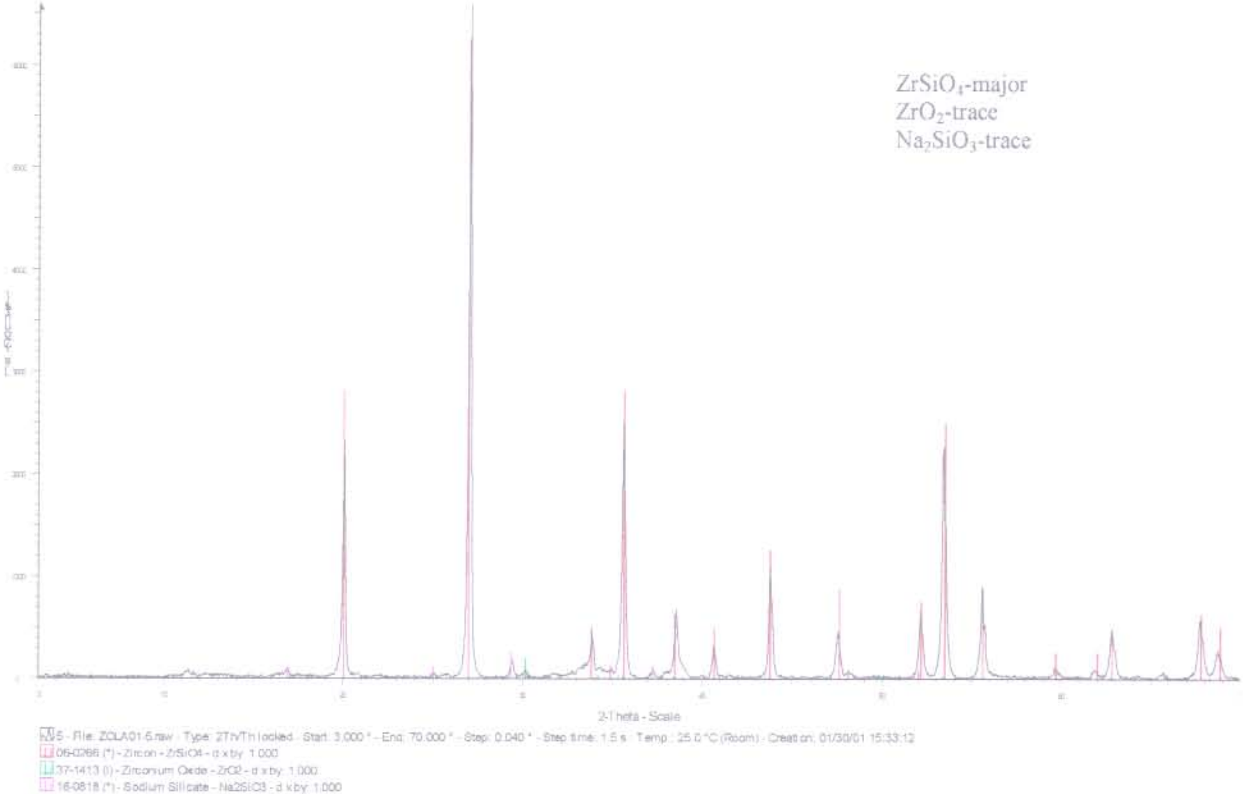

FIGURE 8.23: X-ray diffraction pattern of alkali fused decomposed zircon. A mole of $d_{50} \approx 9\mu m$ zircon was decomposed with a mole of sodium hydroxide at 650°C for 336 hours with intermediate milling after every 24 hours.

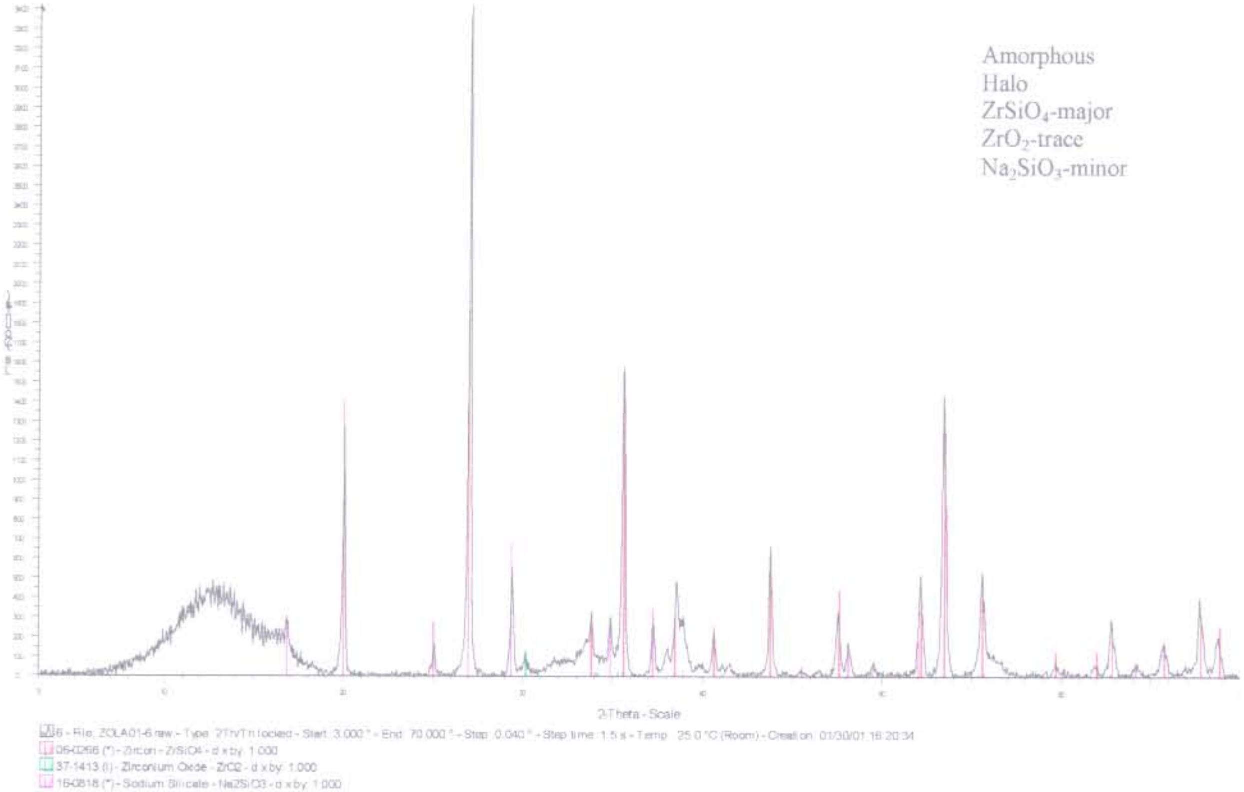

FIGURE 8.24: X-ray diffraction pattern of alkali fused decomposed zircon. A mole of $d_{50} \approx 9\mu m$ zircon was decomposed with two moles of sodium hydroxide at 650°C for 336 hours with intermediate milling after each 24 hours .

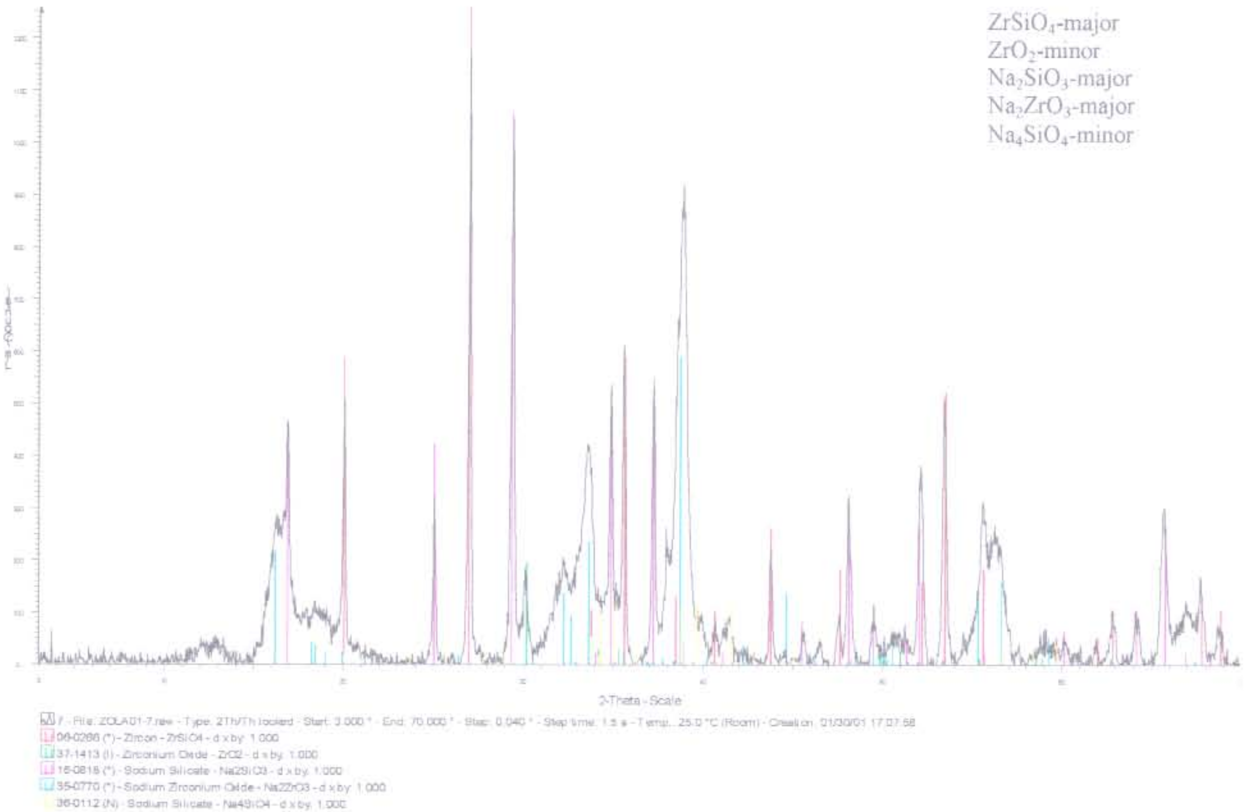

FIGURE 8.25: X-ray diffraction pattern of alkali fused decomposed zircon. A mole of $d_{50} \approx 9\mu m$ zircon was decomposed with four moles of sodium hydroxide at 650°C for 336 hours.

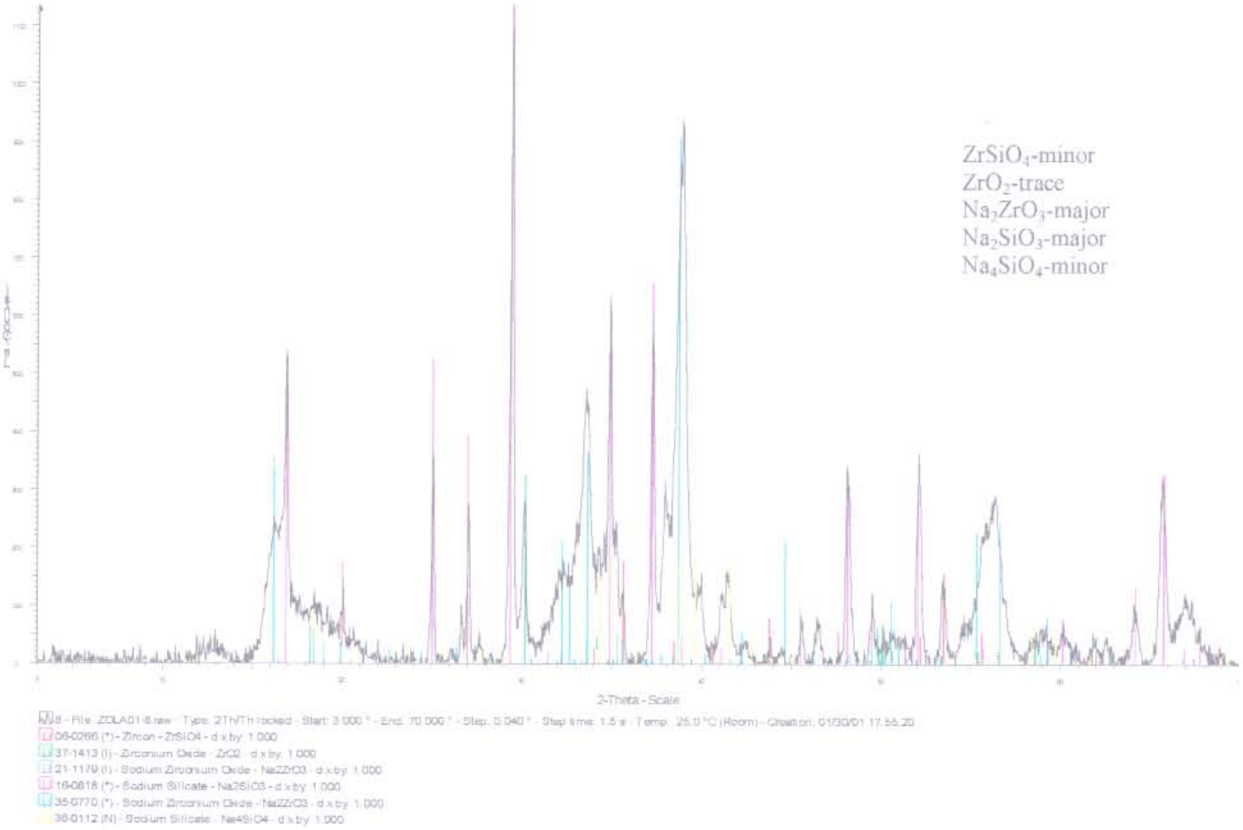

FIGURE 8.26: X-ray diffraction pattern of alkali fused decomposed zircon. A mole of $d_{50} \approx 9\mu m$ zircon was decomposed with six moles of sodium hydroxide at 650°C for 336 hours.

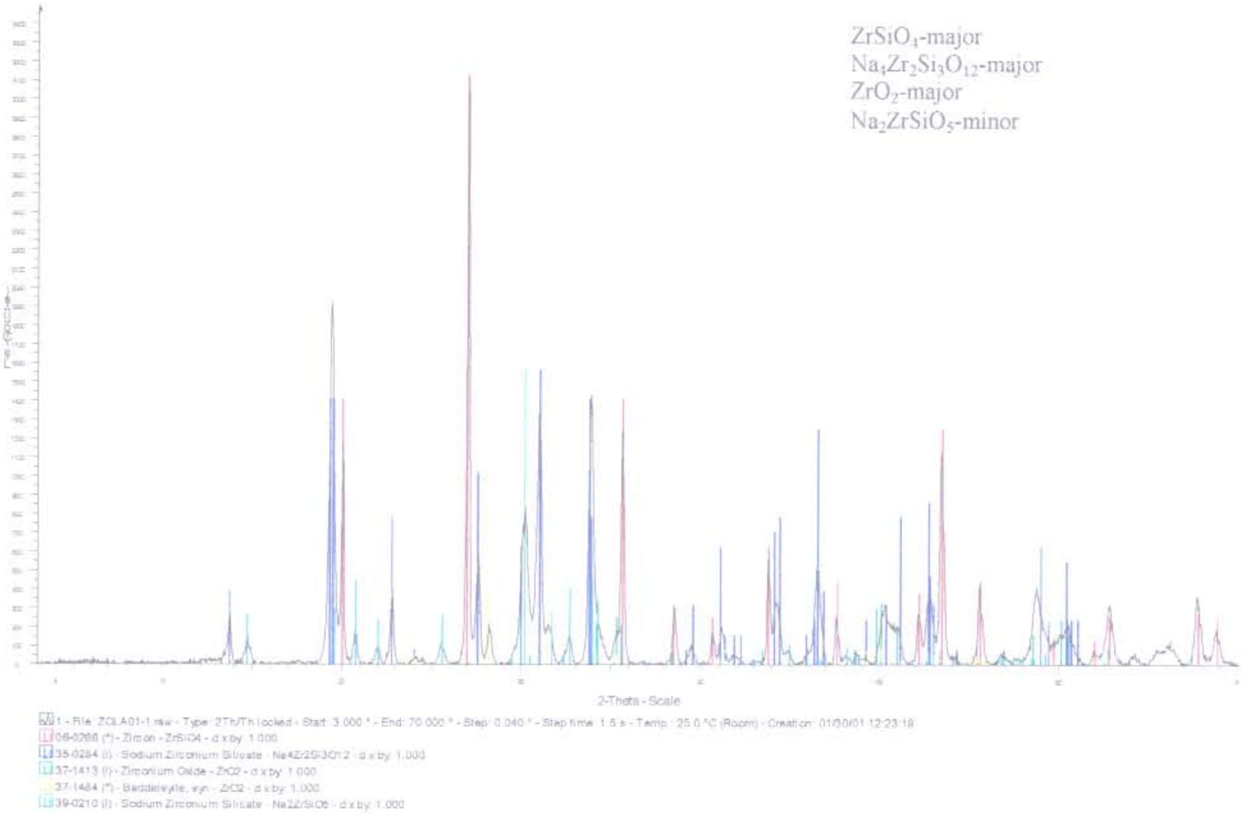

FIGURE 8.27: X-ray diffraction pattern of alkali fused decomposed zircon. A mole of $d_{50} \approx 9$ µm zircon was decomposed with a mole of sodium hydroxide at 850°C for 336 hours.

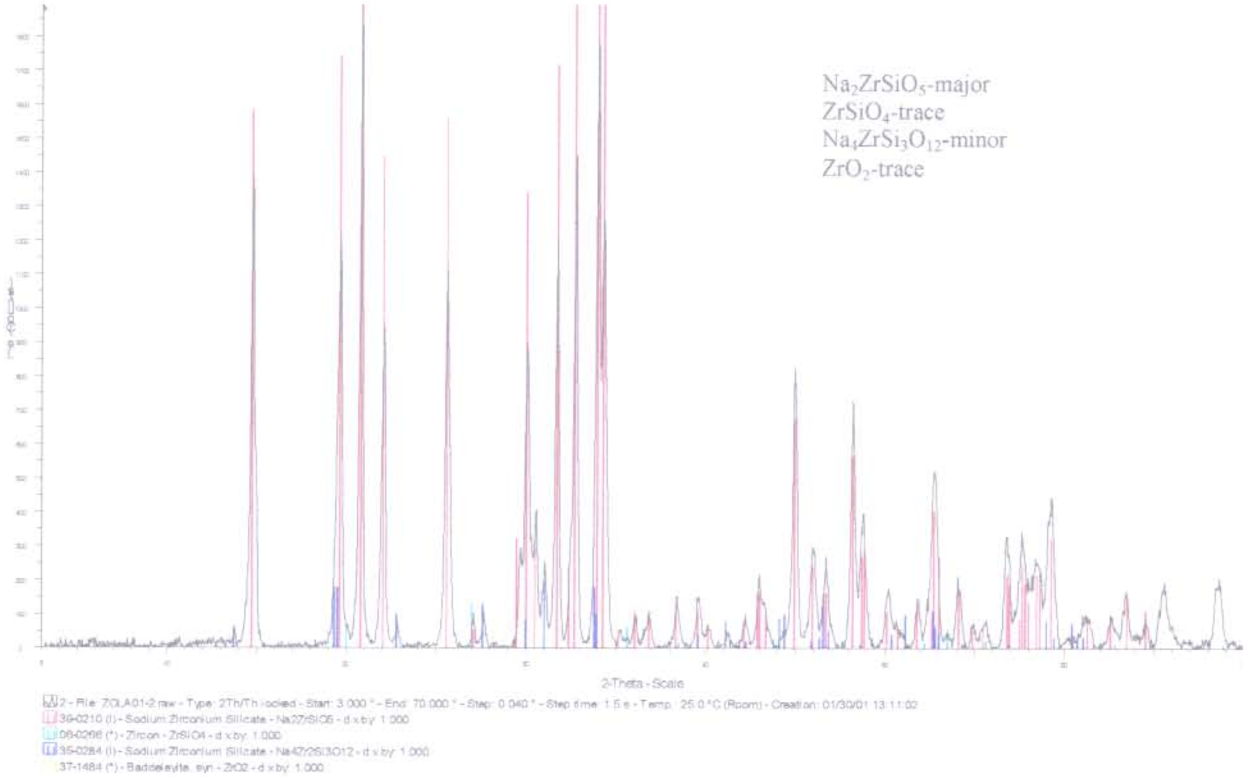

FIGURE 8.28: X-ray diffraction pattern of alkali fused decomposed zircon. A mole of $d_{50} \approx 9$ µm zircon was decomposed with two moles of sodium hydroxide at 850°C for 336 hours with intermediate milling after every 24 hours.

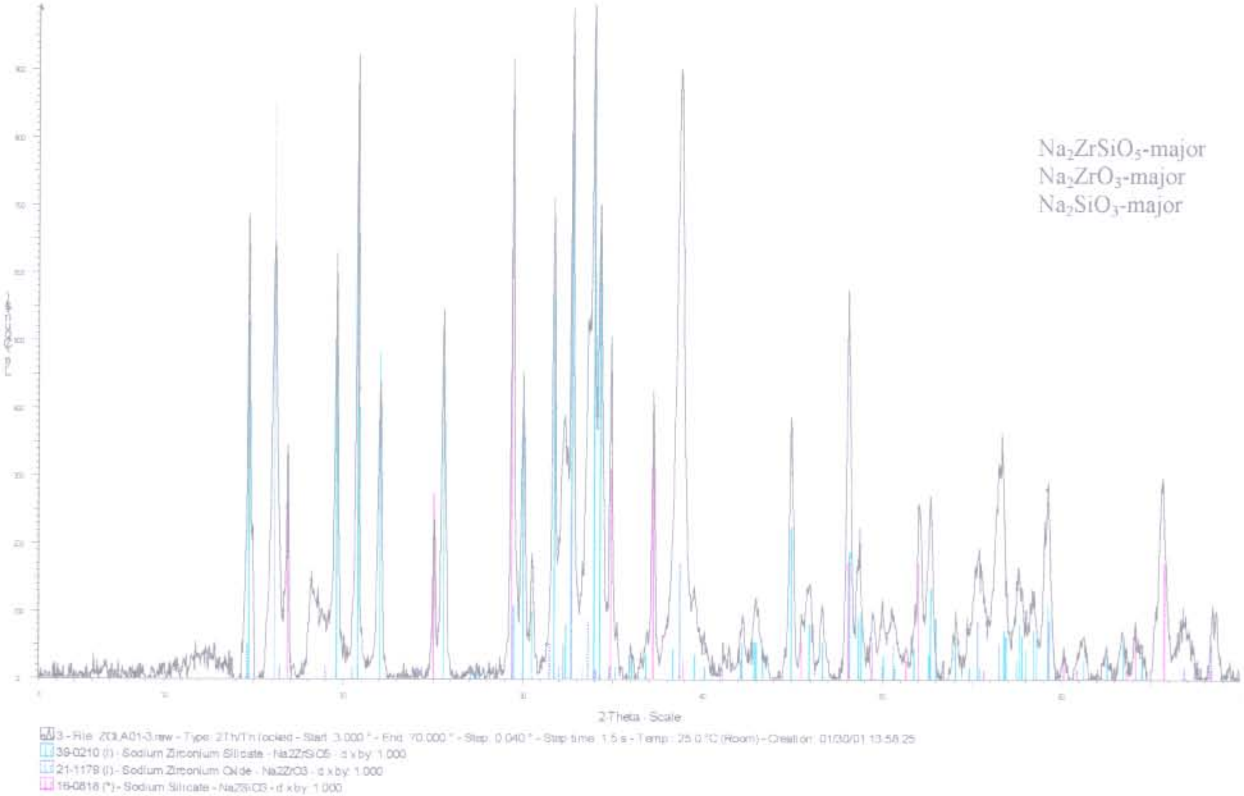

FIGURE 8.29: X-ray diffraction pattern of alkali fused decomposed zircon. A mole of $d_{50} \approx 9\mu m$ zircon was decomposed with four moles of sodium hydroxide at 850°C for 336 hours

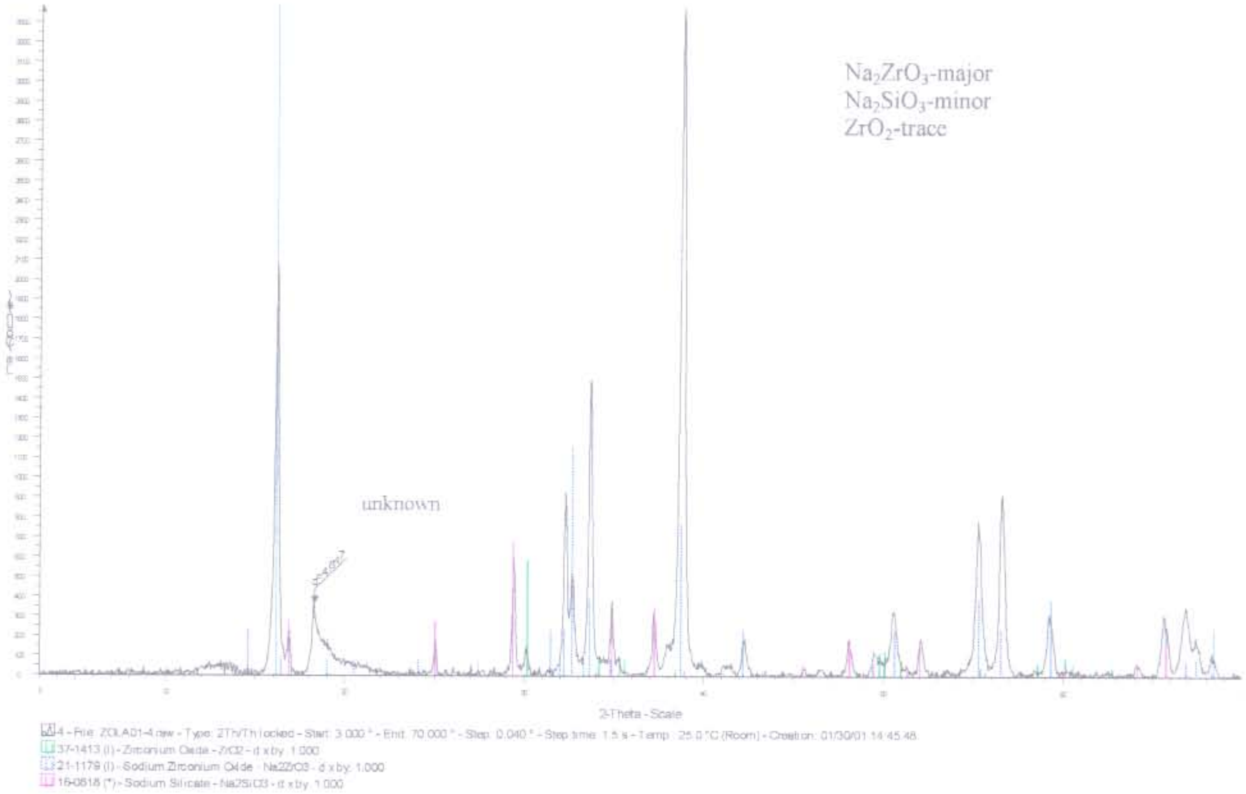

FIGURE 8.30: X-ray diffraction pattern of alkali fused decomposed zircon. A mole of $d_{50} \approx 9\mu m$ zircon was decomposed with six moles of sodium hydroxide at 850°C for 336 hours with intermediate milling after every 24 hours.

FIGURE 8.31: A super-positioning of the X-ray diffraction pattern of alkali fused decomposed zircon. The spectra at for the various mole ratios at 850°C after 336 hours of decomposition were superimposed.

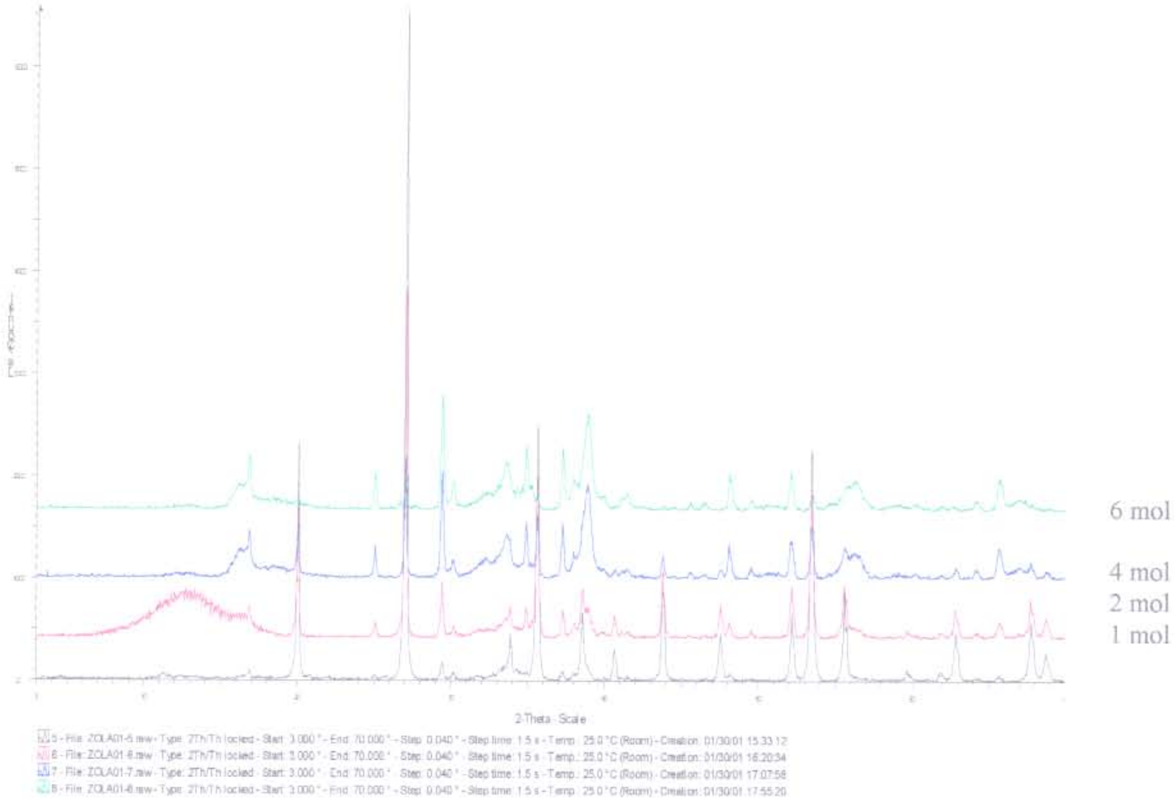

FIGURE 8.32: A super-positioning of the X-ray diffraction pattern of alkali fused decomposed zircon. The spectra for the various mole ratios at 650°C after 336 hours of decomposition were superimposed.

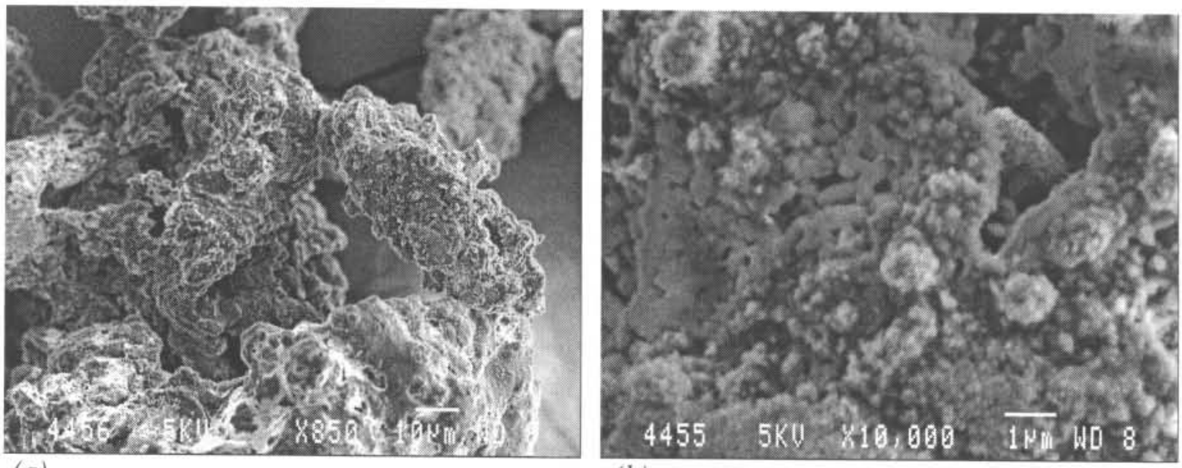

(a) *(b)*

FIGURE 8.33: SEM photographs of the unmilled by-product sodium metasilicate crystallised overnight by water evaporation in an evaporation oven at 90°C. The by-product was obtained after the water dissolution of AFDZ at 90°C for 5 minutes.

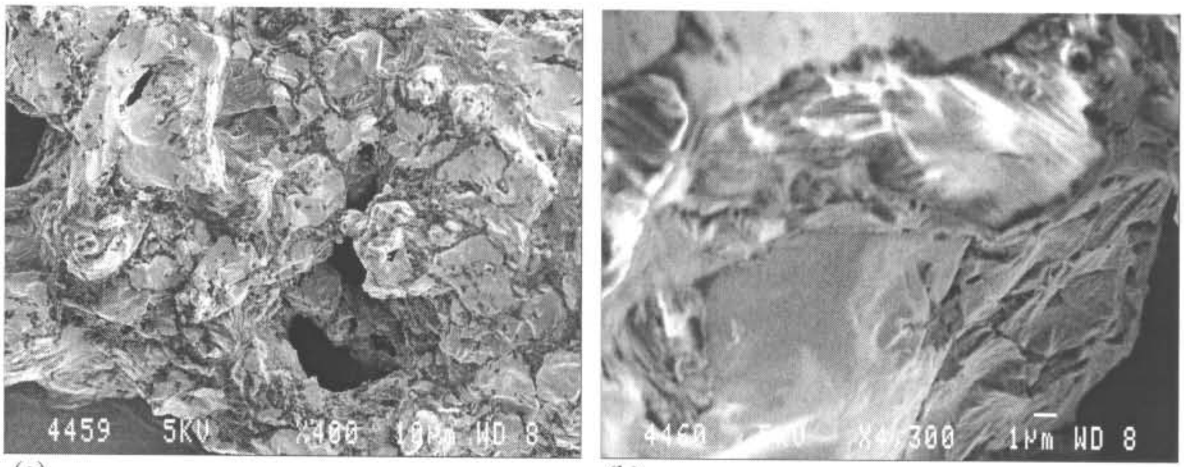

(a) (b)

FIGURE 8.34: SEM photograph of zirconium sulphate tetrahydrate crystallised by water evaporation in a drying oven at 90°C.

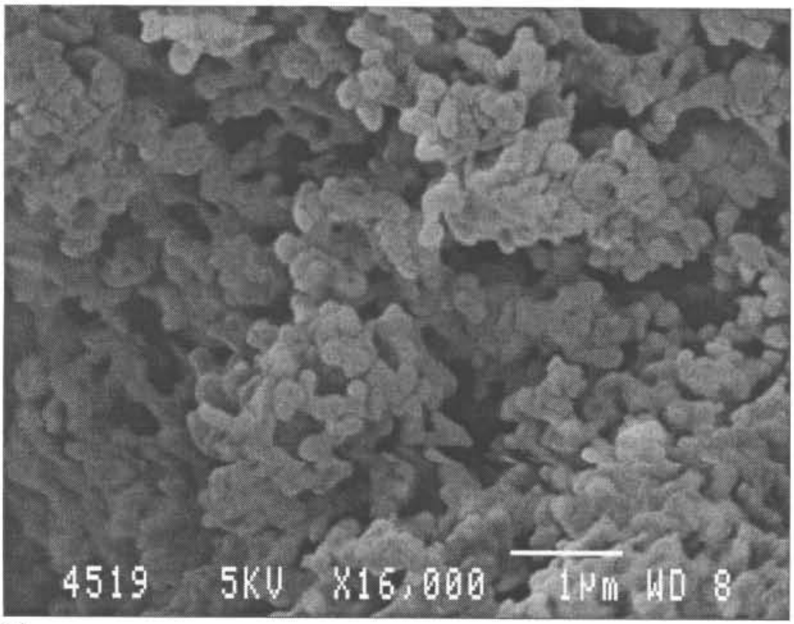

(a)

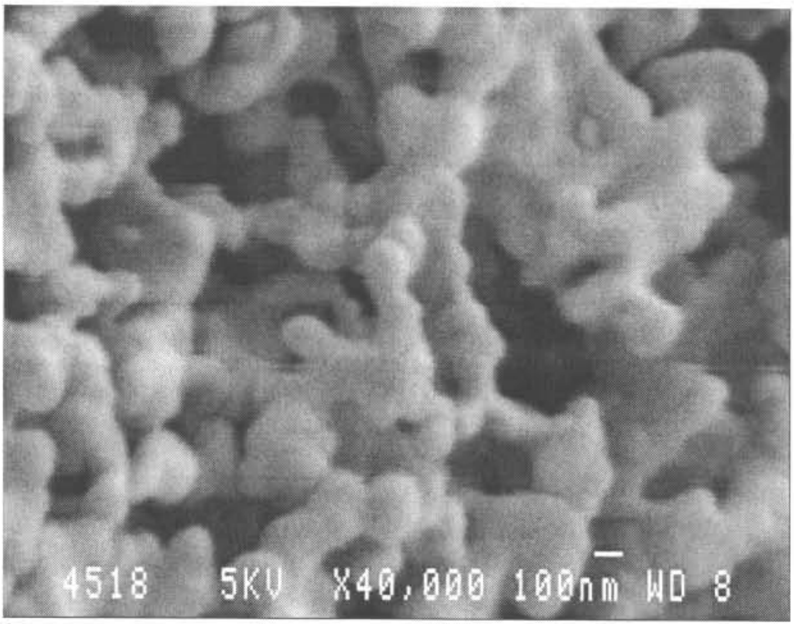

(b)

FIGURE 8.35: SEM photographs of monoclinic zirconia that was obtained by calcining AZST at 900°C for about an hour.

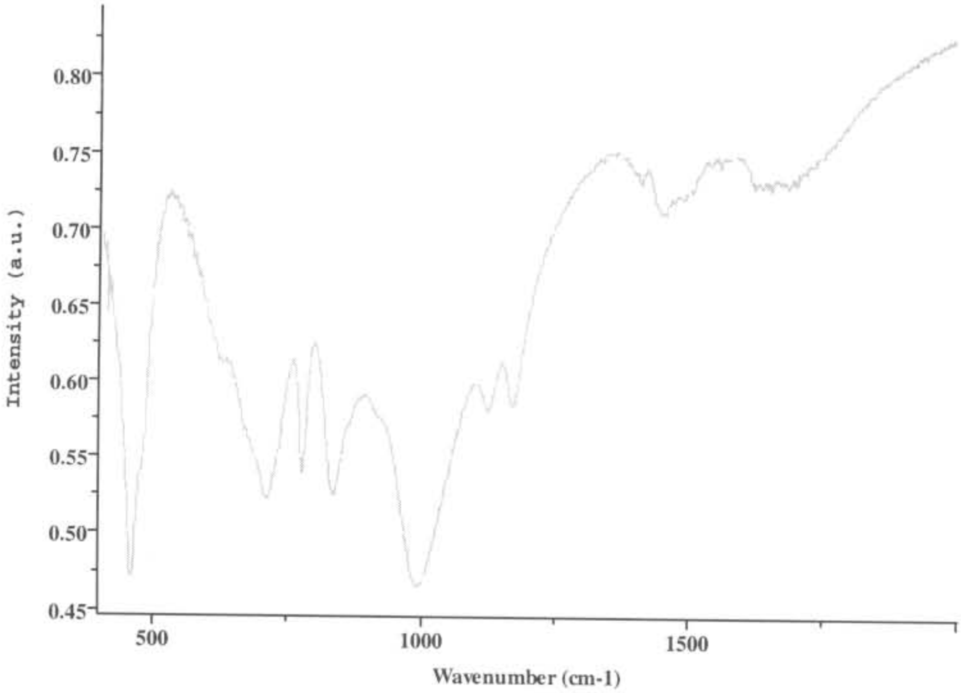

FIGURE 8.36: The infrared spectrum of the sodium silicate by-product. The alkali silicate was crystallised by water evaporation at 90°C overnight.

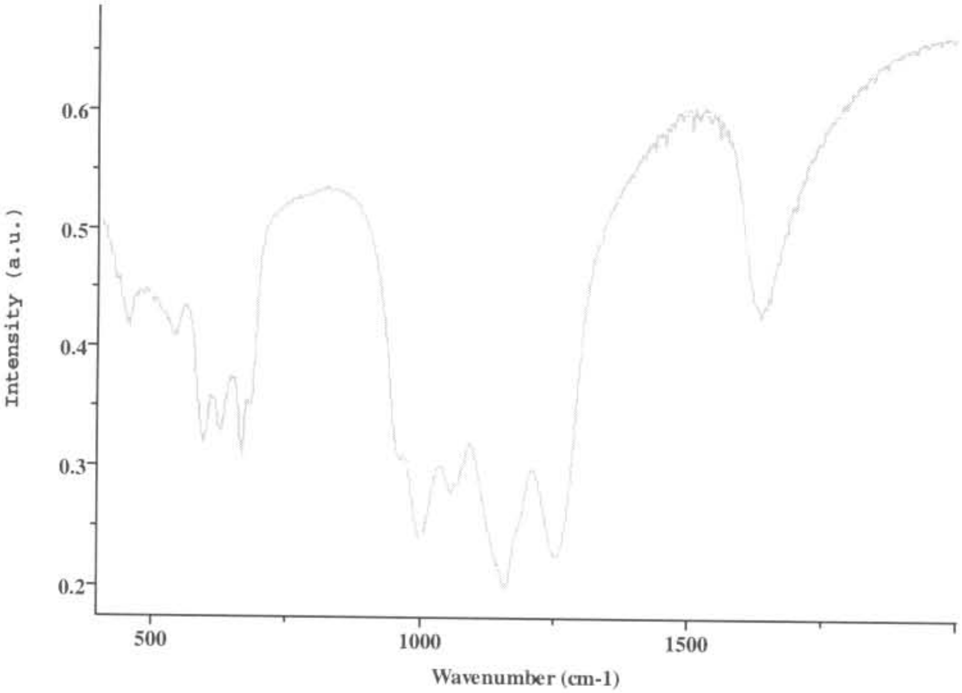

FIGURE 8.37: The infrared spectrum of zirconium sulphate tetrahydrate. The sulphate was crystallised by water evaporation at 90°C overnight.

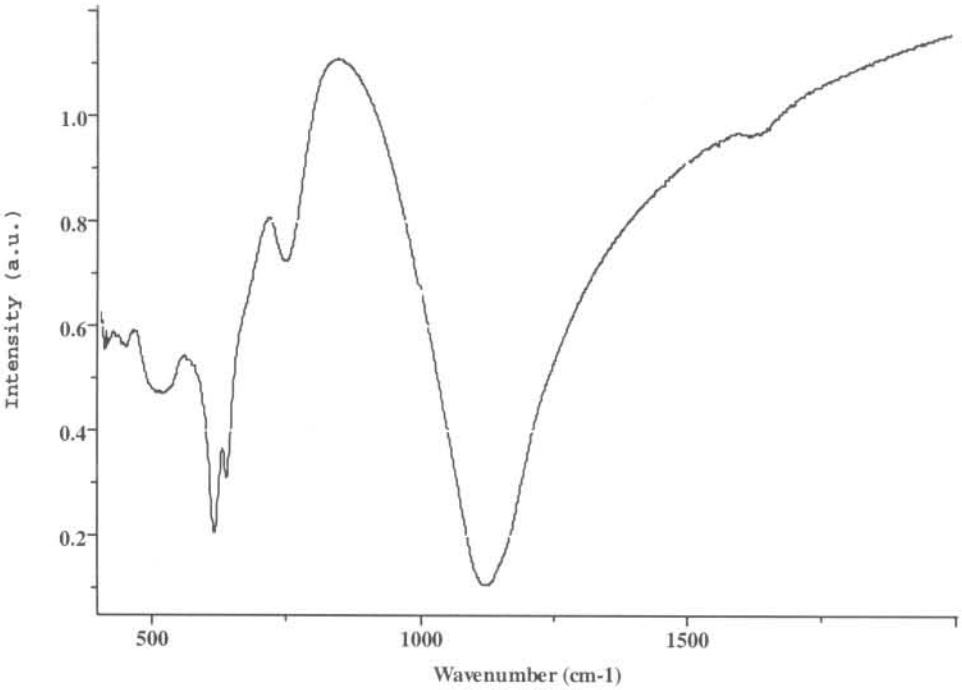

FIGURE 8.38: The infrared spectrum of zirconia. The zirconia was obtained by calcining AZST at 900°C for an hour.

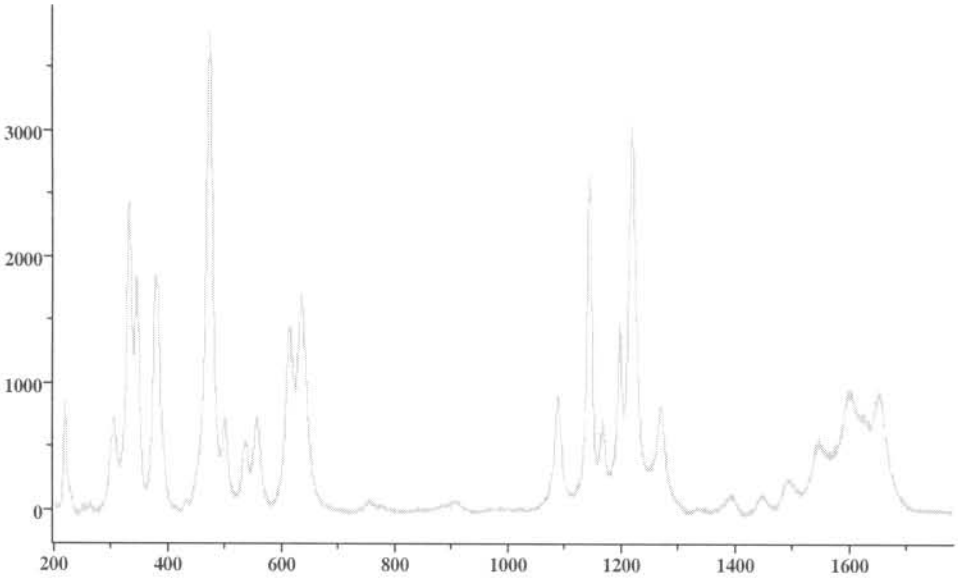

FIGURE 8.39: The Raman spectrum of monoclinic zirconia. The zirconia was obtained by calcining AZST at 900°C for an hour.

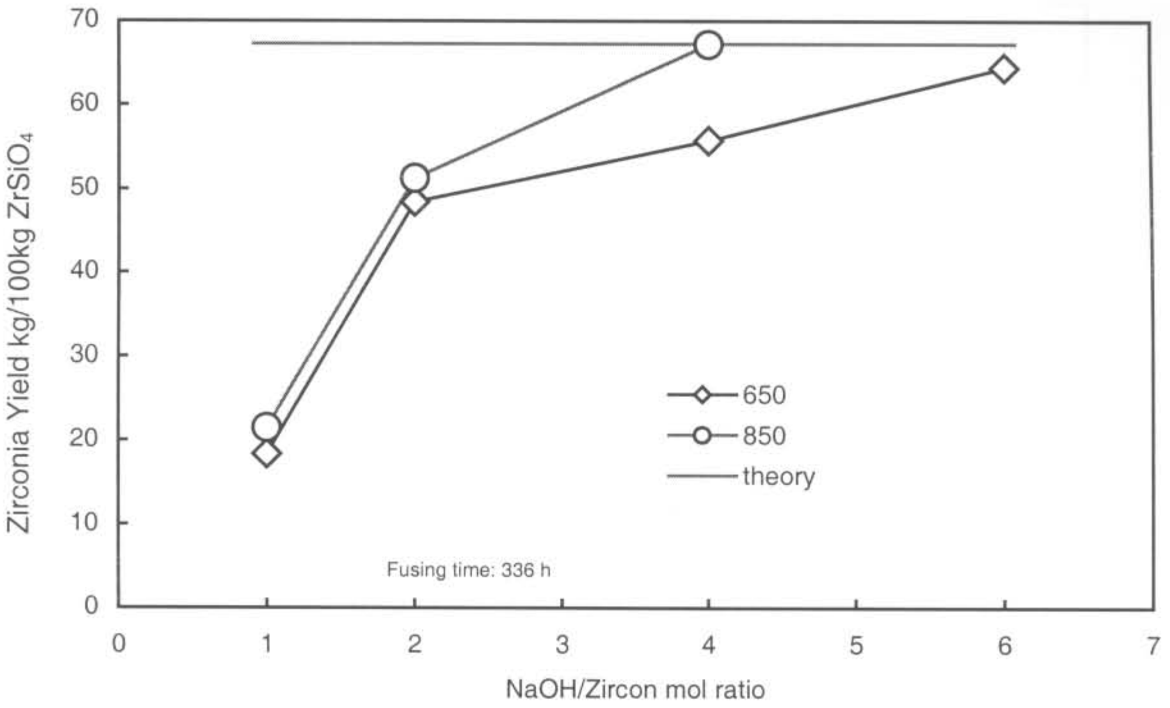

FIGURE 8.40: The influence of the moles of sodium hydroxide on the yield of zirconia. The values given are those used in a mass balance; the zirconia was obtained from AFDZ that was fused for 336 hours with intermediate milling.

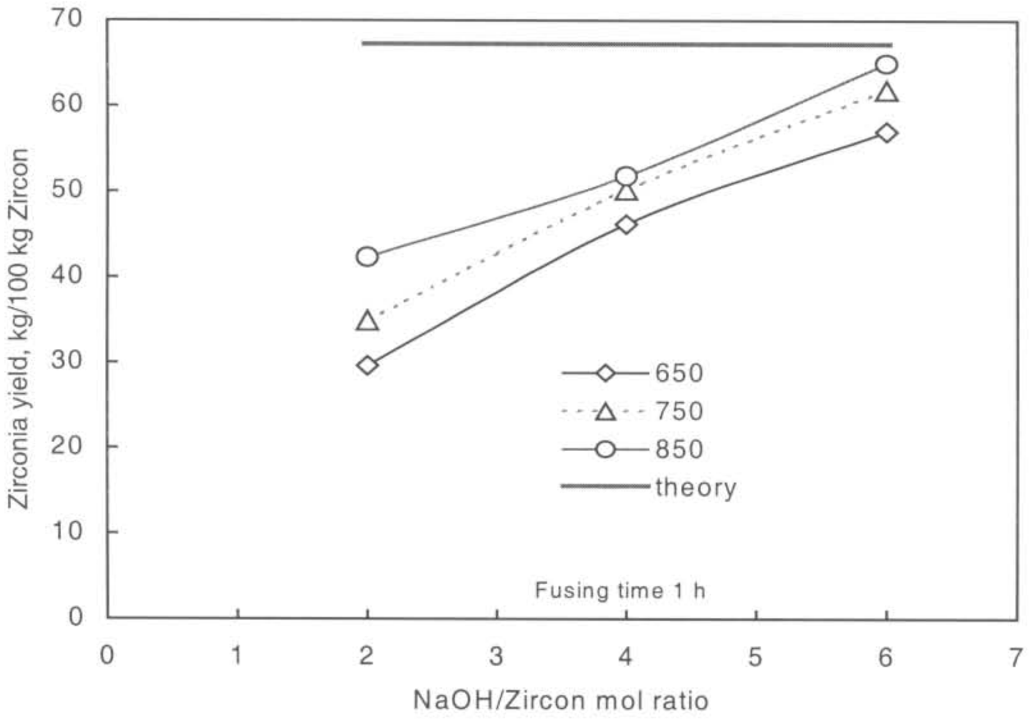

FIGURE 8.41: The influence of the moles of sodium hydroxide on the yield of zirconia. The values given are those used in a mass balance; the zirconia was obtained from AFDZ that was fused for one hour with intermediate milling.

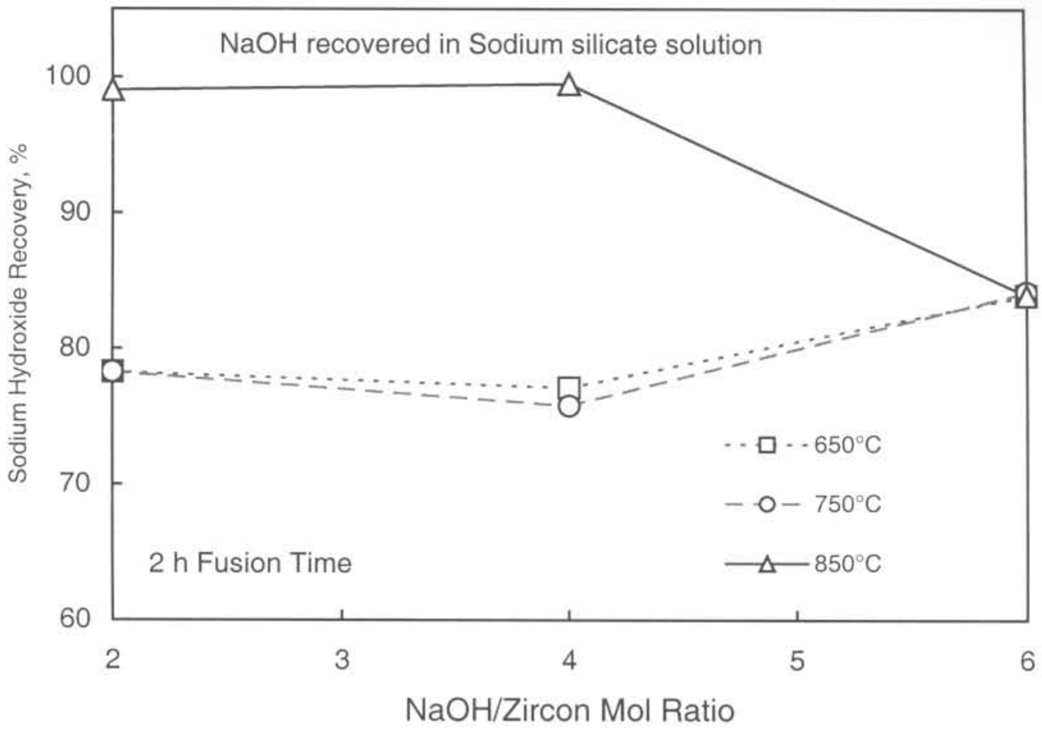

FIGURE 8.42: The influence of sodium hydroxide to zircon mole ratio on the amount of sodium recovered from solids fused for 2 hours. The sodium was recovered with soluble sodium silicates.

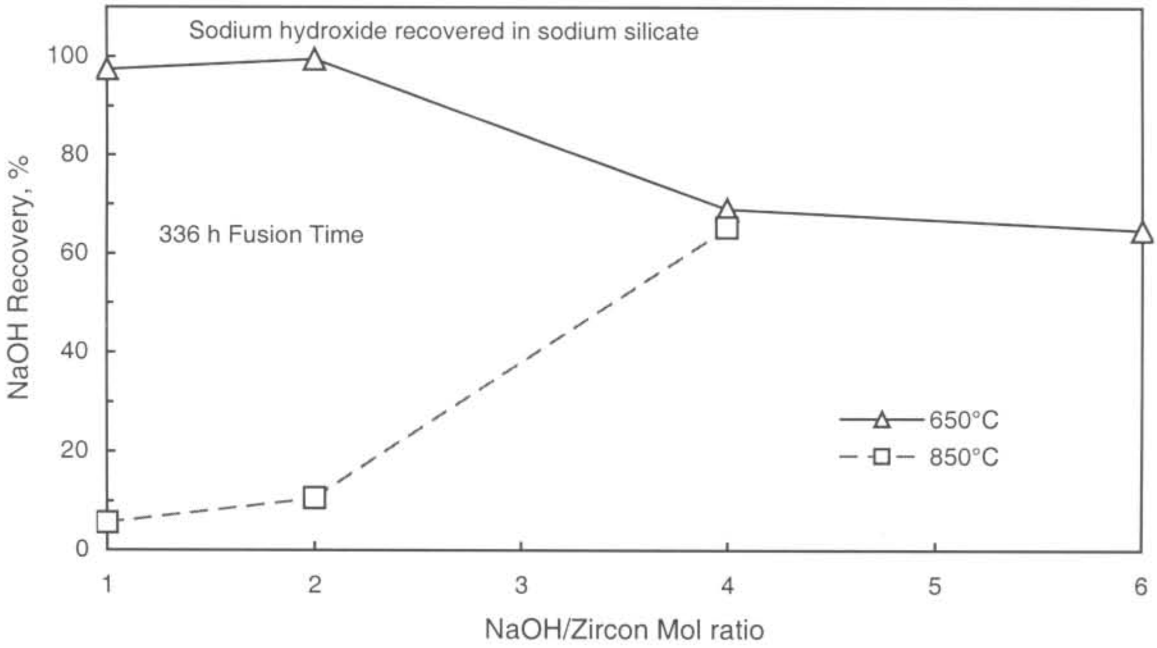

FIGURE 8.43: The influence of sodium hydroxide to zircon mole ratio on the amount of sodium recovered from solids fused for 336 hours. The sodium was recovered with soluble sodium silicates.

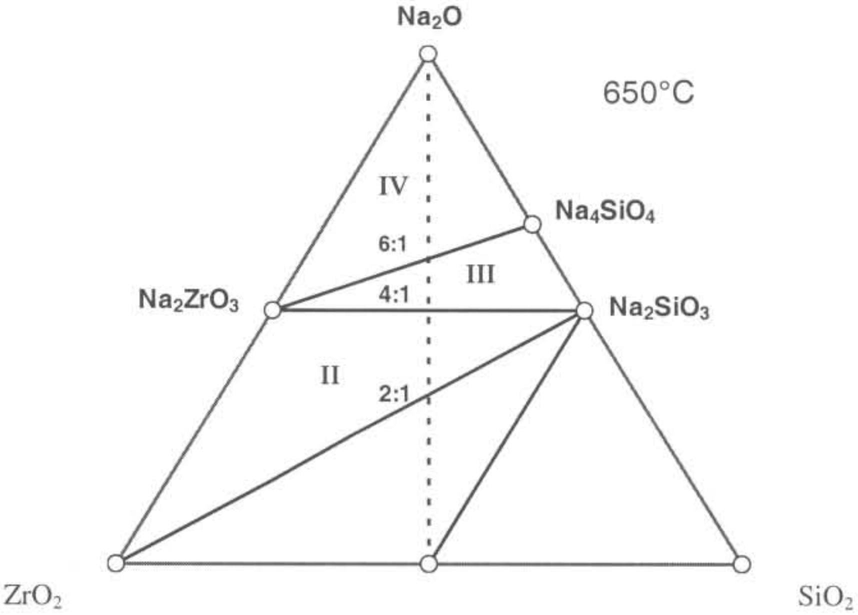

FIGURE 8.44: A diagrammatic representation of the phase diagram obtained for the decomposition of zircon with sodium hydroxide at 650°C. The phases Na_2ZrSiO_5 and $Na_4Zr_2Si_3O_{12}$ were not observed.

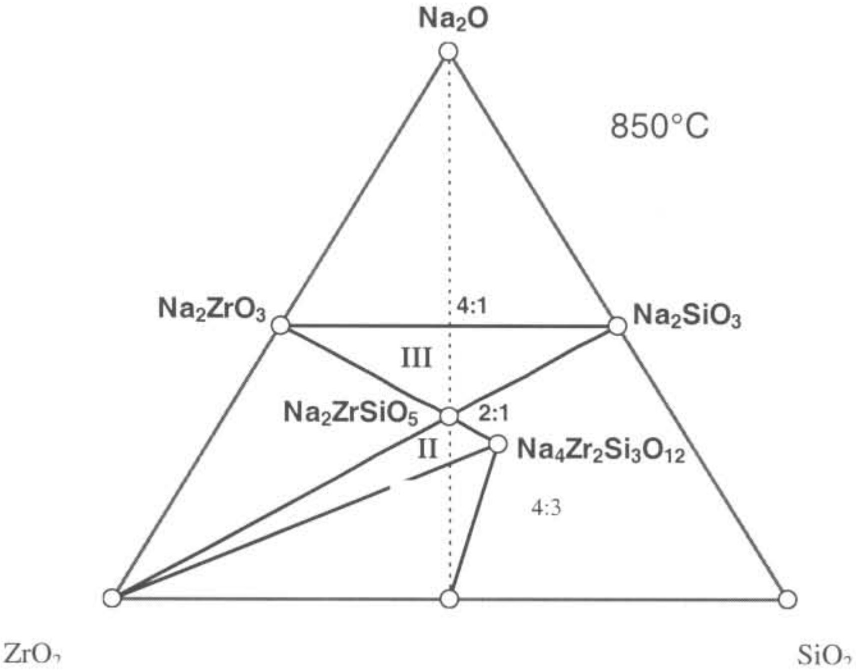

FIGURE 8.45: A diagrammatic representation of the phase diagram obtained for the decomposition of zircon with sodium hydroxide at 850°C. The phases Na_2ZrSiO_5 and $Na_4Zr_2Si_3O_{12}$ were observed. The diagram is comparable to that by D' Ans and Loeffer (1930).

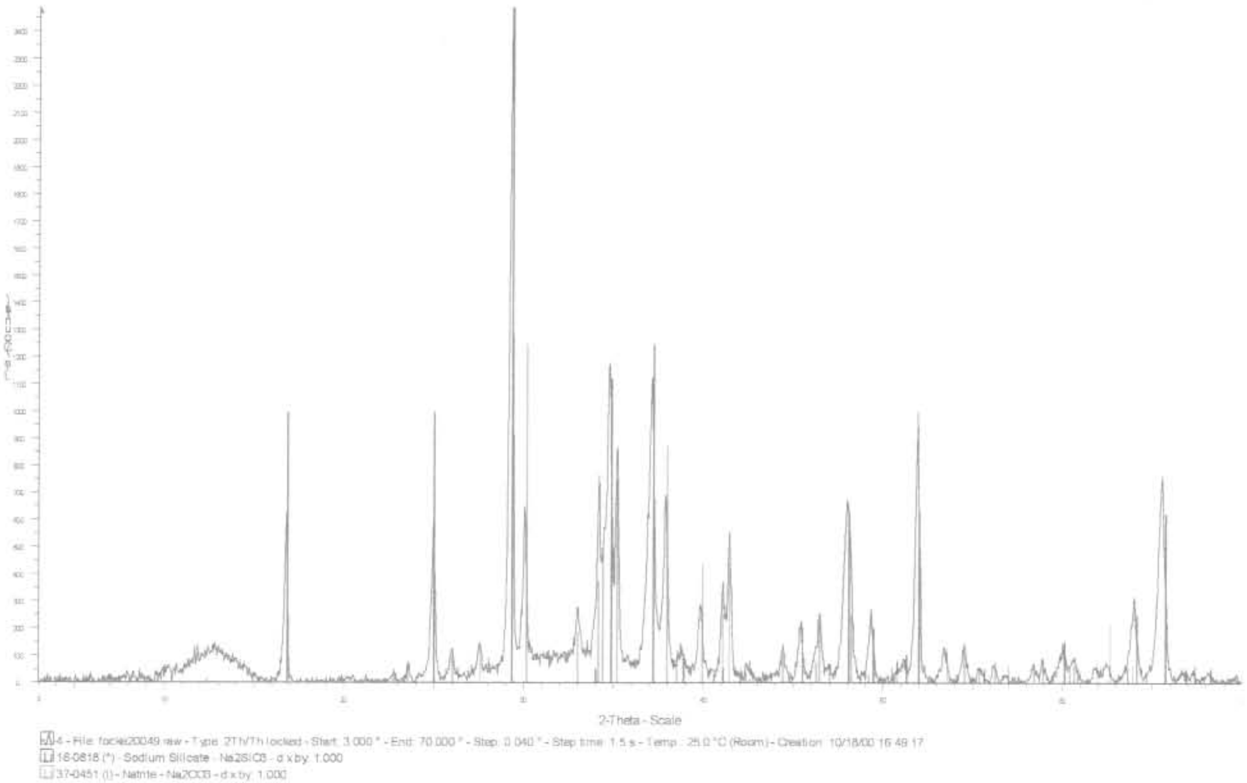

FIGURE 8.46: X-ray diffraction pattern of the alkali silicate by-product. The silicate was crystallised by water evaporation at 90°C overnight.

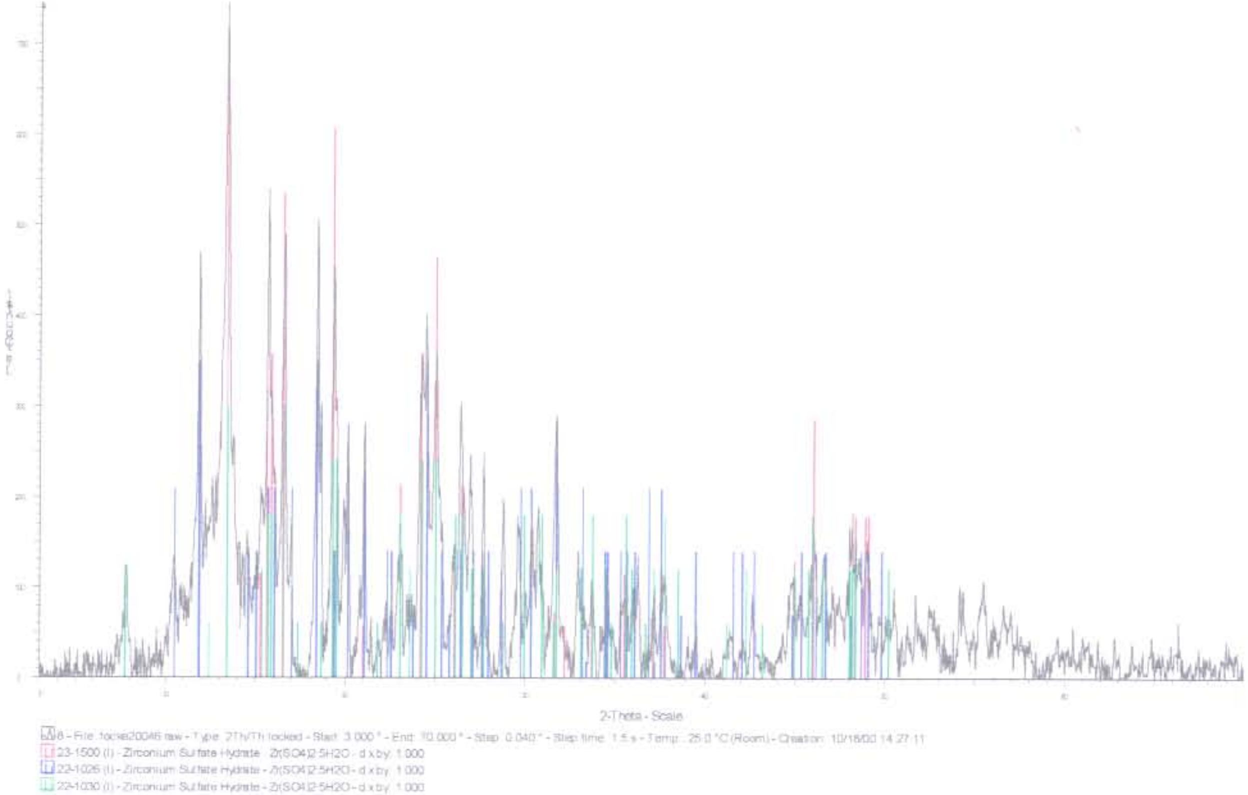

FIGURE 8.47: X-ray diffraction pattern of zirconium sulphate, AZST. The hydrated normal sulphate was crystallised by water evaporation at 90°C overnight.

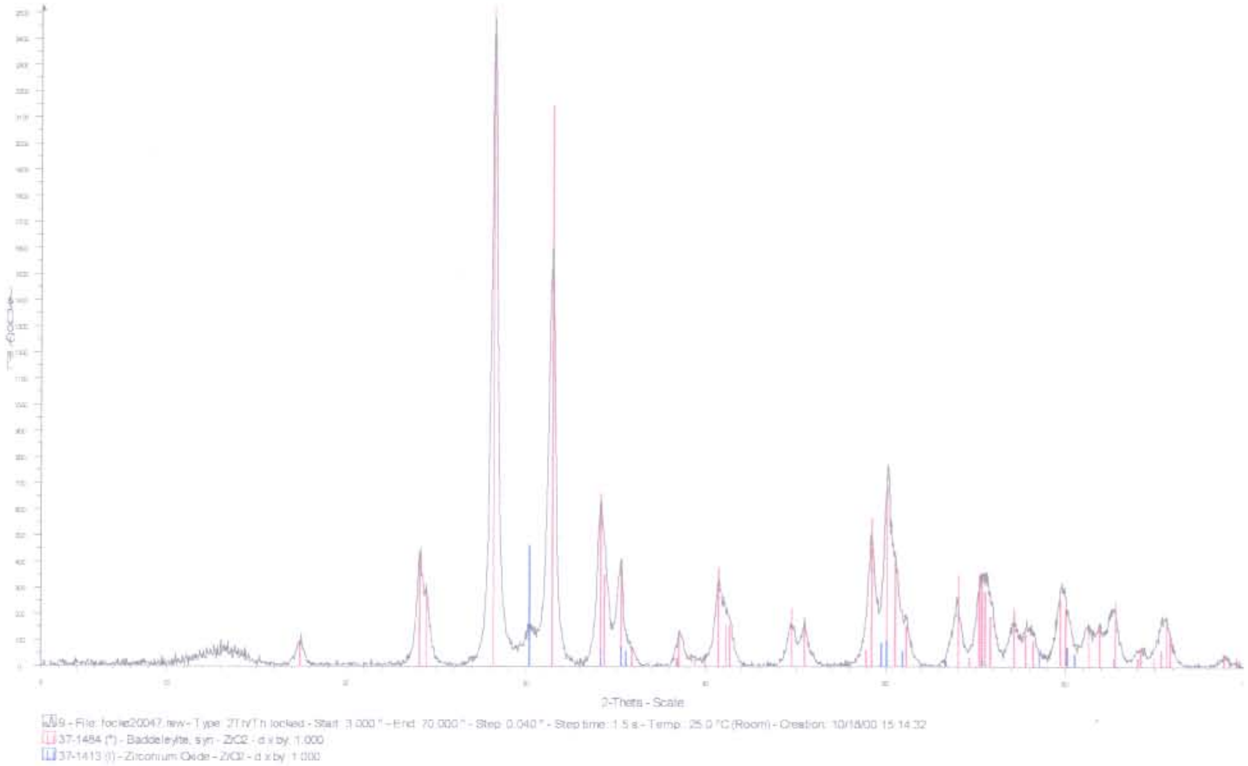

FIGURE 8.48: X-ray diffraction pattern of zirconia. The zirconia was obtained by calcining AZST at 900°C for about an hour.

8.3 DISCUSSIONS

8.3.1 ZIRCON DECOMPOSITION AFTER TWO HOURS OF FUSION

Figure 8.1 shows SEM photographs of milled zircon sand from Richard's bay, South Africa. Figure 8.1 (a) is a photograph of the $d_{50} \approx 45\mu m$ zircon sand and Figure 8.1 (b) is the $d_{50} \approx 9\mu m$ sand. The difference in the particle size can be seen in the SEM photographs. Appendix K provides the XRF determined elemental analysis of this product.

Figure 8.2 shows the fusion product commonly called alkali fusion decomposed zircon (AFDZ). The $d_{50} \approx 9\mu m$ zircon sand was decomposed with sodium hydroxide at various mole ratios and temperature. Figure 8.2 (a) shows the size of an agglomerate of AFDZ. A closer look at the surface of the agglomerate, Figure 8.2 (b), shows a large (c.a. 25μm) molten region (melt). The melt could possibly be unreacted Na_2O. The SEM suggests that there was segregation of reactants during fusion. The NaOH melts at approximately 324°C before zircon at approximately 2 200°C. The higher sodium content of the melt was verified by X-ray analysis with the aid of the SEM. This region was seen for all AFDZ samples that were not *intermediately* milled.

This segregation can be minimised by milling followed by a second fusion step. The advantage is improved zircon decomposition (zirconia yields improved by 10-15%). The disadvantages are long process times and the additional processing step (milling).

Figures 8.3 to 8.5 show the infrared spectra of AFDZ at various reaction conditions. New bands appear at 686, 864, 1 410, 1 669 and 1 756 cm^{-1}. These bands increase in intensity as the sodium hydroxide to zircon mole ratio is increased. With increase of temperature, the intensity of the new bands decreases. For the fusion of a mole of zircon with six moles NaOH, the bands observed at 650°C had minimal intensity at 850°C. As shown below, XRD aided the interpretation of the infrared spectra.

Figure 8.6 shows the XRD spectra of milled zircon sand from Richard's bay. The spectra for the 9 and 45 μm are similar. There appears to be a small amorphous halo in the spectra.

Figures 8.7 to 8.14 show the XRD patterns of the AFDZ at 850°C and 650°C for the various mole ratios when fused for two hours. The AFDZ went through a single cycle of milling and fusion to obtain a homogenous mixture. The relative intensities in the XRD spectra are given in brackets.

Figure 8.7 shows the XRD pattern for the fusion of a mole of zircon with two moles of sodium hydroxide at 850°C. The phases Na_2ZrSiO_5 (major), Na_2ZrO_3 (minor) unreacted $ZrSiO_4$ (major) and traces of Na_2SiO_3 were observed. Zircon is the major component, suggesting that its decomposition is incomplete. The infrared spectrum is also dominated by bands due to zircon.

Figure 8.8 shows the XRD pattern for the fusion of a mole of zircon with four moles of sodium hydroxide at 850°C. The phases Na_2ZrSiO_5 (trace), Na_2SiO_3 (minor), different phases of Na_2ZrO_3 (major) were observed. The zircon ($ZrSiO_4$) was identified in trace amount only indicating virtually complete zircon decomposition.

Figure 8.9 shows the XRD pattern for the fusion of a mole of zircon with six moles of sodium hydroxide at 850°C. The phases Na_2ZrSiO_5 (minor), different phases of Na_2ZrO_3 (major), and traces of ZrO_2 and $ZrSiO_4$ were observed. The zircon was identified in trace amounts only. It indicates that this reaction condition provides for complete zircon decomposition.

At the 2 hour stage of fusion at 850°C, the XRD spectra suggest that increments of NaOH improve the decomposition of zircon. Near complete zircon decomposition is obtained when fusing a mole of zircon with four moles of NaOH. When fusing a mole of zircon with two moles of NaOH the phase Na_2ZrSiO_5 is obtained in majority, but with increments of NaOH the phase is formed in minority. The quantity of Na_2ZrO_3 and Na_2SiO_3 are seen to increase with increments of NaOH.

Figure 8.11 shows the XRD pattern for the fusion of a mole of zircon with two moles of sodium hydroxide at 650°C. The phases Na_2ZrO_3 (trace), $ZrSiO_4$ (major), Na_2SiO_3 (trace) and ZrO_2 (trace) were observed. Zircon was the major phase; this amount suggests a small extent of decomposition.

Figure 8.12 shows the XRD pattern for the fusion of a mole of zircon with four moles of sodium hydroxide at 650°C. The phases Na_2ZrO_3 (minor), ZrO_2 (minor), ZrO (major) and $ZrSiO_4$ (major) were observed. No sodium silicates were detected. The presence of the amorphous halo indicates that the sample was amorphous, possibly explaining the poor detection of sodium silicates. The detection of the phase ZrO in majority suggests the preference of sodium to attack the less stable silica tetrahedral linkages. The zirconia could have been reduced by the decomposition by-product, water.

Figure 8.13 shows the XRD pattern for the fusion of a mole of zircon with six moles of sodium hydroxide at 650°C. The XRD spectrum indicates the presents of sodium silicates high in sodium content Na_4SiO_4 (minor), $Na_6Si_2O_7$ (minor) and traces of $Na_2Si_2O_5$ (low in sodium). The phase ZrO is identified in majority. Zircon and zirconia are other phases identified in minority. The presents of the sodium silicate phase Na_4SiO_4, and ZrO indicate the preference for sodium to attack the silica tetrahedra. The phases $Na_6Si_2O_7$ and $Na_2Si_2O_5$ indicate the possibility of a secondary reaction. The monomers, the sodium orthosilicate Na_4SiO_4, are polymerised to the dimers $Na_6Si_2O_7$ and possibly, ultimately to the sheets $Na_2Si_2O_5$. The metasilicate chains Na_2SiO_3 were not detected by the XRD, but could possibly be the intermediate between the dimers $Na_6Si_2O_7$ and sheets $Na_2Si_2O_5$. The phase $Na_2Si_2O_5$ was identified in traces, suggesting that the polymerisation at this stage is not the dominant reaction.

The new infrared band at 686 cm^{-1} (Fig. 8.3-8.5) is an indication of the δ(Si-O-Si) bending vibrations in a polymerised silicate structure e.g. $Na_2Si_2O_5$ or Na_2SiO_3 [7-9]. The XRD only revealed the phase $Na_2Si_2O_5$ at 650°C when fusing with six moles of sodium hydroxide. The presence of the infrared band at 686 cm^{-1}, between the frequency range 600-720 cm^{-1}, is taken as evidence of the presence of polymeric silicates [6-10]. This infrared band is seen for samples obtained at all the fusion temperatures. At 850°C the infrared band appears to be much broader. This could be an indication of the size of the silicate ring. The dependence of the position of this band on the number of ring members and the extent of its deformation has been determined: In the spectrum of glassy $Na_2Si_2O_5$ it has been shown that the infrared band is expected to be in the range of 740-600 cm^{-1} [9-10].

The infrared band at 864 cm^{-1} (Fig. 8.3-8.5) increases in intensity with increasing sodium hydroxide, but only for a fusion temperature of 650°C. This band can be assigned to the $\nu(Si-O^{-})$ stretching vibrations of a non-bridging silico-oxygen found in a polymeric silicate [6-10].

When fusing a mole of zircon with six moles of sodium hydroxide at 650°C, the band is most intense. The XRD reveals traces of the phases $Na_6Si_2O_7$ and the silicate sheets $Na_2Si_2O_5$. The infrared band can be attributed to the $\nu(Si-O^{-})$ stretching vibrations of a non-bridging silico-oxygen that is found in the XRD identified silicates [6-10].

The infrared stretching vibrations $\nu(Si-O-Si)$ at 900-960 cm^{-1} overlap with those due to zircon, but variations in intensity can be seen. These infrared bands were observed to increase in intensity with increments in sodium hydroxide (Fig 8.3-8.5). The bands indicate the development of Si-O-Si bridges [6-10].

The infrared spectra therefore suggest the presence of a polymerisation reaction. Under favourable conditions the orthosilicate monomers Na_4SiO_4, pyrosilicate dimers $Na_6Si_2O_7$ high in sodium and metasilicate chains Na_2SiO_3 can be polymerised to the disilicate sheets $Na_2Si_2O_5$ (scheme 8.1). The polymerisation reaction is *pseudo*-catalysed by the sodium, because it is first consumed to form the monomer and subsequently released as the oxide Na_2O to further decompose the zircon lattice.

$$2\,Na_4SiO_4 \longrightarrow Na_6Si_2O_7 + Na_2O \qquad (8.1A)$$

$$Na_6Si_2O_7 \longrightarrow 2Na_2SiO_3 + Na_2O \qquad (8.2B)$$

$$2Na_2SiO_3 \longrightarrow Na_2Si_2O_5 + Na_2O \qquad (8.3C)$$

SCHEME 8.1: A reaction scheme on the possible polymerisation reactions of the silicates during the prolonged decomposition of zircon at 650°C.

The presence, and the increasing intensity of the infrared band $\nu(Si-O^{-})$ at 864 cm^{-1} with increase in NaOH, shows the preference for sodium to form sodium silicates (high in sodium) at 650°C rather than to attack the edge cell connected bisdisphenoids to form sodium zirconates. This suggests that the high stability of zircon is mainly due to the ZrO_8 bisdisphenoids edge cell connections.

The infrared band at 864 cm^{-1} was observed to decrease in intensity as the temperature was increased (Fig. 8.4-8.5); for instance at 850°C fusion with six moles of sodium hydroxide, the intensity of this band was negligible. This suggests that at high temperatures the sodium was not selective in its decomposition of the zircon lattice but attacked both SiO_4 silica tetrahedra and ZrO_8 bisdisphenoid linkages. This is corroborated by the phases identified in the XRD: sodium metasilicate, sodium zirconates and zircon (Figure 8.7-8.14).

8.3.2 ZIRCON DECOMPOSITION AFTER 336 HOURS OF FUSION

In order to determine the thermodynamically stable phases at the different reagent ratios, fusions were carried out for 336 hours with intermediate milling after every twenty-four hours. Fusion of a mole of zircon with one mole of sodium hydroxide was also considered.

Figures 8.15 to 8.18 show the infrared spectra obtained from the fusion products obtained after two weeks of fusion with periodic milling. The infrared stretching vibrations ν(Si-O-Si) at 900-960cm^{-1} and the bending vibrations δ(Si-O-Si) at 550-800 cm^{-1} (associated with rings/polymeric silicates) [6-10] are much more distinct at this stage and cannot be confused with that of zircon anymore.

The infrared bands at 742, 710 and 600cm^{-1} support the presence of silicate rings. The infrared band at 742cm^{-1} can also be attributed to monoclinic zirconia as seen in the raw spectra (Figure 8.38). The bands are now much broader that previously (at two hours of fusion). The 710 cm^{-1} band position corresponds to three membered rings. The infrared band at 600 cm^{-1}supports the presence of silicates with six membered rings. The band broadening supports the presence of silicate rings with more than six members.

Figure 8.23-24 shows the XRD pattern for the fusion of a mole of zircon with a mole of sodium hydroxide at 650°C for 336 hours. The phases ZrO_2 (trace), Na_2SiO_3 (trace) and $ZrSiO_4$ (major) were detected. Similar phases (and not their amounts) were detected when fusing a mole of zircon with two moles of sodium hydroxide (Figure 8.24). The zircon phase was detected in majority and the other phases in minority. The phases support the preference of sodium for the SiO_4 tetrahedra and the secondary reaction (Scheme 8.1). The secondary reaction is seen to progress only as far as the metasilicate chains.

The equilibrium phases (Scheme 8.2) were previously observed to form at much higher temperatures (~1480°C) [11-12]. The implied equilibrium reaction at 650°C and low $NaOH/ZrSiO_4$ mole ratios is:

$$ZrSiO_4 + Na_2O \longrightarrow ZrO_2 + Na_2SiO_3$$

SCHEME 8.2: The equilibrium reaction between zircon and sodium hydroxide at 850°C for $NaOH/ZrSiO_4 \leq 2$ mole ratio.

Figure 8.25 shows the XRD pattern for the fusion of a mole of zircon with four moles of sodium hydroxide at 650°C for 336 hours. The phases Na_2ZrO_3 (major), Na_2SiO_3 (major), Na_4SiO_4 (trace), ZrO_2 (trace) and $ZrSiO_4$ (minor) were observed. The presence of phases Na_4SiO_4 (trace), ZrO_2 (trace) suggest that the reaction was not yet at equilibrium. The presence and quantity of Na_2SiO_3 (major) supports the secondary reaction as seen in Scheme 8.1. The reaction is seen to only progress as far as the metasilicate chains. The presence and quantity of Na_2ZrO_3 suggests that the amount of sodium hydroxide is another thermodynamic parameter that governs the stability of the zircon structure. The quantity of the XRD phases suggests that reaction in Scheme 8.3 is predominant. Under favourable conditions the equilibrium reaction is:

$$ZrSiO_4 + 2Na_2O \longrightarrow Na_2ZrO_3 + Na_2SiO_3$$

SCHEME 8.3: The equilibrium reaction between sodium hydroxide and zircon at 650°C for $NaOH/ZrSiO_4 \geq 4$ mole ratio.

Figure 8.26 shows the XRD pattern for the fusion of a mole of zircon with six moles of sodium hydroxide at 650°C for 336 hours. The phases Na_2ZrO_3 (major), Na_2SiO_3 (major), Na_4SiO_4 (minor), ZrO_2 (minor) and $ZrSiO_4$ (minor) were observed. The presence of phases Na_4SiO_4 and ZrO_2 are seen to increase in amount when compared with those at four moles of NaOH. This suggests that equilibrium was not attained.

The presence of zircon suggests that this cannot be a point of complete decomposition. This can be attributed to the Na_4SiO_4 orthosilicate monomers that consume high amounts of sodium when decomposing the zircon lattice and the extent of polymerisation.

Figures 8.27 shows the XRD pattern for the fusion of a mole of zircon with one mole of sodium hydroxide at 850°C for 336 hours (intermediate milling). The phases $Na_4Zr_2Si_3O_{12}$ (major), Na_2ZrSiO_5 (minor), ZrO_2 (major) and $ZrSiO_4$ (major) were detected.

The phase $Na_4Zr_2Si_3O_{12}$ was reported to form after prolonged fusion [11]. It is a consequence of the reaction between Na_2ZrSiO_5 and Na_2SiO_3 with the liberation of Na_4SiO_4 (Scheme 8.4 reaction 8.4C). The orthosilicate Na_4SiO_4 when liberated should undergo the reaction in scheme 8.1 only as far as the metasilicate. The quantity of the phase $Na_4Zr_2Si_3O_{12}$ suggests that the reaction 8.4B in Scheme 8.4 predominates under these conditions.

Figures 8.28 shows the XRD pattern for the fusion of a mole of zircon with two moles of sodium hydroxide at 850°C for 336 hours (intermediate milling), the phases $Na_4Zr_2Si_3O_{12}$ (trace), Na_2ZrSiO_5 (major), ZrO_2 (trace) and $ZrSiO_4$ (trace) were identified. The amount of Na_2ZrSiO_5 is seen to increase and that of $Na_4Zr_2Si_3O_{12}$ and ZrO_2 decrease. The reactions suggested under favourable conditions are:

$$ZrSiO_4 + Na_2O \longrightarrow Na_2ZrSiO_5 \qquad (8.4A)$$

$$3ZrSiO_4 + 2Na_2O \longrightarrow Na_4Zr_2Si_3O_{12} + ZrO_2 \qquad (8.4B)$$

$$2Na_2ZrSiO_5 + 2Na_2SiO_3 \longrightarrow Na_4Zr_2Si_3O_{12} + Na_4SiO_4 \qquad (8.4C)$$

SCHEME 8.4: The equilibrium reaction between zircon and sodium hydroxide at 850°C for $NaOH/ZrSiO_4 \leq 2$ mole ratio. Reaction 8.4A predominates when fusing a mole of zircon with two moles of NaOH. The reaction 8.4B predominates at amounts less than two moles of fusion (e.g. one mole of NaOH per mole of zircon).

Figure 8.29 shows the XRD pattern for the fusion of a mole of zircon with four moles of sodium hydroxide at 850°C for 336 hours. The phases Na_2ZrO_3 (major), Na_2SiO_3 (minor), Na_2ZrSiO_5 (major) were detected. The quantity of Na_2ZrSiO_5 suggests that reaction 8.5A in Scheme 8.5 predominates. The phases were detected at much higher temperatures but at comparable amounts of sodium hydroxide. No zircon phase was detected, suggesting that this is possibly a point of complete decomposition. The infrared (Figure 8.18) further supports this point by the absence of the zircon characteristic band at 614 cm^{-1}.

The phase Na_2ZrSiO_5 was identified in majority, suggesting that the improved zircon decomposition is due to this phase.

Unlike the Na_4SiO_4 orthosilicates, this phase consumes low amounts of sodium (two moles less) while liberating a mole of zirconia form the zircon lattice.

Under favourable conditions the following reactions are possible:

$$ZrSiO_4 + Na_2O \longrightarrow Na_2ZrSiO_5 \qquad (8.5A)$$

$$ZrSiO_4 + 2Na_2O \longrightarrow Na_2ZrO_3 + Na_2SiO_3 \qquad (8.5B)$$

SCHEME 8.5: The reaction between zircon and sodium hydroxide at 850°C for $NaOH/ZrSiO_4 \geq 4$ mole ratio. Reaction 8.4A and 8.4B predominate when fusing a mole of zircon with four moles of NaOH. Reaction 8.5B predominates when fusing a mole of zircon with six moles of NaOH.

Figure 8.30 shows the XRD pattern for the fusion of a mole of zircon with six moles of sodium hydroxide at 850°C for 336 hours. The phases Na_2ZrO_3 (major), Na_2SiO_3 (minor) and ZrO_2 (trace) were detected. The quantity of Na_2ZrO_3 phase suggests that reaction 8.5B in Scheme 8.5 predominates. No zircon phase was detected, suggesting that this is possibly a point of complete decomposition. The infrared (Figure 8.18) further supports this point by the absence of the zircon characteristic band at 614 cm^{-1}.

Figures 8.19 to 8.22 show the Raman spectra obtained from the fusion products after 336 hours of fusion and periodic milling. Raman bands due to zircon (353, 435, 996, 1002, 1054 and 1458 cm^{-1}) dominate the Raman spectra at 650°C. This is further evidence (together with the XRD and IR) of the incomplete decomposition in this temperature region.

The Raman spectrum (Fig. 8.21) when fusing at 850°C with four or six moles of sodium hydroxide shows no bands due to zircon. The XRD and IR further support this observation. Raman bands at 400 to 510 cm^{-1} can be attributed to inter tetrahedral linkages Si-O-Si. The shift towards lower wavenumbers can be attributed to the heavy Zr^{4+} ion especially in the XRD identified phase $Na_4Zr_2Si_3O_{12}$ [14].

The Raman bands at 850 cm^{-1}, characteristic of the orthosilicate monomers, those at 900cm^{-1} for the pyrosilicate dimers, the 1000-950 cm^{-1} band of the metasilicate chains and the 1100-1050cm^{-1} band due to disilicate sheets were all not observed.

Griffith (1969) [13] suggests that the Raman bands due to the groups (SiO_n) are very weak owing to the small degree of π-bonding in the Si-O linkages. A mathematical deconvolution (to resolve a spectrum into its constituent bands) of the Raman spectra could be more descriptive as to the presence or absence of these bands. Thus their absence could be attributed to their low intensities [13-14].

8.4 EXPERIMENTAL DETERMINATION (MASS BALANCE APPROACH)

8.4.1 SODIUM DETERMINATION

The possibility of the reactions suggested by the XRD, IR and Raman were checked experimentally. The amount of sodium in the in-situ zirconates and silicates was determined with the aid of titration with standardised HCl. Experimental procedure described in Section 7.4.3 were employed. The yields of zirconia, silica and unreacted zircon were determined. A mass balance for reactions was done for two hour fusion time with no intermediate milling step is provided (Appendix A-F). Appendix G provides a mass balance of yields obtained after 336 hours of fusion and intermediate milling. Theoretically calculated values of the expected zirconia and silica yields are provided in Appendix H; theoretically expected amounts of sodium are provided in Appendix I.

8.4.2 SODIUM RECOVERY AT 650°C

Determination of the sodium (Figure 8.43, Appendix F) after 336 hours at 650°C when fusing with $NaOH/ZrSiO_4 \leq 2$ mole ratio, showed that most of the sodium (~99% Na_2O m/m) was dissolved with the silicates. This suggests that the zirconium compound in the AFDZ was low in sodium or hydrolysed easily.

The results are consistent with:

- sodium zirconate releasing half its sodium when hydrolysed in the water wash, and
- The sodium silicates being completely soluble in water.

Thus the expected NaOH recovery should be 100, 75 and 66,7% for $NaOH/ZrSiO_4$ mole ratios of 2, 4 and 6 respectively. In actual fact the values observed were 99, 69 and 65%.

When fusing for 2 hours at 650°C with a $NaOH/ZrSiO_4 \leq 4$ mole ratio most of the sodium (~79% Na_2O m/m) was recovered with the silicates (Figure 8.42, Appendix B). Besides the formation of the phases Na_2SiO_3 or Na_4SiO_4 and the hydrolysis of zirconates, the increased sodium content could be due to unreacted Na_2O. The NaOH recovery increases to a value of approximately 85.0 % Na_2O m/m in the soluble solids when fusing with $NaOH/ZrSiO_4 = 6$ mole ratio; this effect is attributed is also attributed to the unreacted Na_2O.

8.4.3 SODIUM RECOVERY AT 850°C

When fusing with $NaOH/ZrSiO_4 \leq 2$ mole ratio at 850°C for 336 hours most of the sodium (~99% Na_2O m/m) was retained as insoluble zirconates or sodium zirconium silicates (Figure 8.43, Appendix J). This implies that soluble sodium silicates were not formed. When the reagent mole ratio is increased to $NaOH/ZrSiO_4 = 4$ the sodium recovery increases to 65.0 %. This is attributed to the formation of Na_2SiO_3, Na_4SiO_4 and Na_2ZrO_3. Thus the increase can be attributed to the solubility of the sodium silicates and the partial hydrolysis of the zirconates to hydrous zirconia.

The determination of sodium to predict what phases have formed remains an inaccurate approach. This method is limited by the hydrolysis of the zirconates or sodium zirconium silicates and unreacted sodium hydroxide, but the method is useful in indicating the sodium content of the by-product.

8.5 THE SODIUM SILICATE BY-PRODUCT

Figure 8.33 shows the SEM photograph of the alkali silicate by-product. The by-product was tacky and adhered strongly to the borosilicate glass beakers. Figure 8.36 shows the infrared spectrum of the alkali silicate. Bands due to sodium metasilicate dominate the spectrum but bands due to sodium carbonate at 1 448 and 1 411cm^{-1} were also observed [6]. Figure 8.46 shows the X-ray diffraction pattern of the alkali silicate the presents of the carbonate is further supported. The elemental analysis is given in Appendix K. The by-product was very high in sodium when compared to the metasilicate Na_2SiO_3.

8.6 ZIRCONIUM SULPHATE TETRAHYDRATE

Figure 8.34 shows the SEM photograph of AZST obtained by water evaporation of an aqueous solution of the normal sulphate salt. Large crystalline particles with no particular morphology can be seen. Figure 8.37 shows the infrared spectrum of AZST.

The spectrum shows bands predominantly due to the AZST molecular vibrations [4, 6]. Figure 8.47 shows the X-ray diffraction pattern of AZST. Many phases of the salt $Zr(SO_4)_2.5H_2O$ were identified [5]. This can be attributed to the complex crystallisation of the normal sulphate and conditions at room temperature, which encourage the crystallisation of the pentahydrate. The elemental analysis is given in Appendix K. The product is of very high purity.

8.7 ZIRCONIA

Figure 8.35 shows the SEM photographs of zirconia. Regular, but agglomerated, oblong particles are visible. Figure 8.38 and 8.39 show the infrared and Raman spectra of zirconia; bands due to monoclinic zirconia dominate the spectra. The strong absorption band that was confused with the zirconyl group at 1 100cm^{-1} can be clearly seen [4]. The band at 748 cm^{-1} can be attributed to Zr-O-Zr vibrations. Figure 8.48 shows the X-ray diffraction pattern of zirconia.

The intensity of the spectrum suggests the predominance of monoclinic zirconia and that tetragonal zirconia formed in trace amounts. The elemental analysis is given in Appendix K. The product purity exceeds 98,4% ZrO_2 with $HfO_2 > 1{,}1\%$.

8.8 CONCLUSIONS

The decomposition of zircon was carried out in open reaction vessels. A mole of zircon was decomposed using from one to six moles of sodium hydroxide and fusion temperatures of 650, 750 and 850°C. When the fusion time is limited to two hours non-equilibrium phases form and the products formed depend on reaction kinetics. For prolonged fusion times (e.g. 336 hours) the reaction products tend towards the expected equilibrium phases. These are the two factors that determine phase formation.

The tetragonal structure of zircon is stabilised by the bisdisphenoids linkages. The silicate phases that are formed can be polymerised to silicates low in sodium (e.g. Na_2SiO_3 or $Na_2Si_2O_5$). This allows the sodium to be released for further decomposition reactions. At 850°C and long fusion times the phases observed are thermodynamically stable one to those reported for higher temperatures by D'Ans and Loeffler (1930) [11]. However, the phase diagram observed at 650°C differs from that obtained by them: The phases Na_2ZrSiO_5 and $Na_4Zr_2Si_3O_{12}$ were not observed.

8.8.1 DECOMPOSITION AT 650°C

Prolonged fusion at 650°C with $NaOH/ZrSiO_4 \leq 2$ mole ratio leads to the formation of sodium metasilicate and zirconia (Scheme 8.2). The XRD reveals the presence of metasilicate and zirconia in trace- or in minor amounts. The low level of detection of these compounds could be due to an amorphous state of the samples (Figure 8.24). The IR bands at 710 and 600 cm^{-1}, support the presence of polymerised silicates (e.g. the sodium metasilicate).

Prolonged fusion (336 hours) at 650°C with $4 \leq NaOH$ moles ≤ 6 leads to the formation of sodium silicates high in sodium and the polymerisation (Scheme 8.1) of the orthosilicate monomers to metasilicate chains. The IR supports this conclusion showing the presence of the δ(Si-O-Si) band at 686 cm^{-1} (for the fusion done in two hours). The split in the band at 686 to ones at 710 and 600 cm^{-1} is indicative of the presence of highly polymerised silicates. The band at 600 cm^{-1}indicates the presents of silicates with rings with more than six members [6-10].

When fusing for two hours, increasing the amount of sodium hydroxide leads to the formation of silicates high in sodium (e.g. Na_4SiO_4) and zirconia. Zirconia, in its reduced state, is formed rather than sodium zirconate. This is a consequence of the stability of the ZrO_8 bisdisphenoids and the instability of the SiO_4 tetrahedra linkages at this temperature.

For prolonged fusion with $NaOH/ZrSiO_4 \leq 2$ mole ratio, most of the sodium followed the silicates. This suggests that the zirconium compound in the AFDZ was low in sodium or hydrolysed easily.

8.8.2 DECOMPOSITION AT 850°C

When zircon is decomposed with sodium hydroxide at higher temperatures e.g. 850°C, the formation of sodium silicates and sodium zirconates is observed. This is an indication that at this temperature the ZrO_8 bisphenoid linkages are not resistant to Na_2O attack.

Prolonged fusion (e.g. 336 hours) at 850°C with $NaOH/ZrSiO_4 < 2$ mole ratio leads to the formation of the phase $Na_4Zr_2Si_3O_{12}$ and ZrO_2 (Scheme 8.4). Prolonged fusion at 850°C with $NaOH/ZrSiO_4 = 2$ mole ratio leads to the formation of the phase Na_2ZrSiO_5 (Scheme 8.4). The formation of these phases ($Na_4Zr_2Si_3O_{12}$ and Na_2ZrSiO_5) was not detected at 650°C.

8.8.3THE PRODUCTS

The by-product contains sodium metasilicate as well as sodium carbonate. The presence of the latter is attributed to the reaction of atmospheric carbon dioxide with excess sodium during crystallisation. The observed Na_2O/SiO_2 mol ratio, in the sodium silicate stream, exceeded three for all reagent ratios for a 2 hour fusion time.

The zirconium sulphate tetrahydrate (AZST) prepared in this study consists of many phases owing to the nature of the crystallisation process. Similar observations were made by Bear and Mumme (1971) [6]. Appendix K confirms that a product of very high purity can be obtained.

The zirconia prepared in this study is predominantly monoclinic. It consisted of oblong, spherical particles with a dimension of about 90 nm. The zirconia obtained was also of high purity as shown in Appendix K.

8.9 REFERENCES

1. Nielsen, R. Chang, T. W. (1996) Ullman's Encyclopaedia of Industrial Chemistry, A (28) 543-567.
2. Hancock, J. D. (1977) A review of conventional and novel processes for the extraction of zirconia from zircon. Mineral Science and Engineering, (9) 25-31.
3. Houchin, M. R. Jenkins, B. E. Sinha, H. N. (1990) Production of high quality zirconia for ceramics, Mineral, Materials and Industry 14th congress of the council of mining and metallurgy Institute, organised by IMM.
4. Clearfield, A. (1964) Structural aspects of Zirconium Chemistry. Rev. Pure and Appl. Chem. (14) 9
5. Bear, I. J. and. Mumme, W. G. (1971) Normal Sulphates of Zirconium and Hafnium, Rev. Pure and Appl. Chem., (21) 189.
6. Nakamoto, K. (1986) The infrared and Raman spectroscopy of inorganic and coordination compounds, 4th edition. A John Wiley and Sons publication, New York.
7. Sitarz, M. Mozgawa, W. Handke, M. (1999) Rings in the structure of silicate glasses, Journal of Molecular Structure, (511-512) 281-285.
8. Mysen, B. O. Virgo, D. Seifert, F. A. (1982) Am. Min. (67) 686-695.
9. Sitarz, M. Moozgawa, W. Handke, M. (1997) Vibrational spectra of complex ring silicate anions-method of recognition, Journal of Molecular structure, (404), 193-197.
10. Huang, Y. Zhimei, J. and Schwieger, W. (1999) Vibrational spectroscopic studies of layered silicates, Chem. Mater. (11), 1210-1217.
11. D' Ans, J. and Loeffler, J. (1930) Z. Anorg. Allg. Chem., (191) [1-2], 22.
12. Sircar, A. and Brett, N. H. (1970) Trans. Brit. Ceram. Soc., (69) [3], 133.
13. Macmillan, P. (1984) Structural studies of silicate glasses and melts-application and limitations of Raman spectroscopy, Am. Min, (69) 622-644.
14. Griffith, W. P. (1969) Raman Studies on rock-forming minerals. Part 1. Orthosilicates and Cyclosilicates, J. Chem. Soc. (A), 1372-1377.
15. Furukawa, T. Fox, E. K. White, W. B. (1981) Raman spectroscopic investigation of silicate glasses. III. Raman intensities and structural units in sodium silicate glasses, J. Chem. Phys., (75) No 7, 3227-3237.
16. Atkins, P.W. (1990) Physical chemistry, Oxford Univ. press, Oxford.

CHAPTER 9

THE OPTIMISATION OF ZIRCON DECOMPOSITION WITH SODIUM HYDROXIDE

9.1 INTRODUCTION

Decomposition of zircon with alkali hydroxides is a well-known procedure [1, 6]. Zircon is very stable, due to the high coordination of the bisdisphenoid ZrO_8 in the tetragonal structure with the low coordinated SiO_4 tetrahedra [7-8]. Thus zircon requires aggressive reactions for decomposition [1, 4, 6].

Decomposition of milled zircon, $d_{50} \approx 9\mu m$, with sodium hydroxide pearls was carried out in open reaction vessels at temperatures between 650°C and 850°C for about two hours, without the intermediate milling step. Mole increments of sodium hydroxide increased the yield significantly. For a reaction at 850°C the use of 6.0 moles of sodium hydroxide for a mole of zircon was optimal for almost complete decomposition. For a reaction at 650°C the use of 2 moles sodium hydroxide for a mole of zircon was enough for approximately 45% zirconia yield. This chapter provides zirconia, silica and residue yields for the various reaction conditions. These should provide an indication of the extent of decomposition and allow the optimisation of reaction conditions with respect to reagent use. The results given here are sub-optimal because they were obtained before the introduction of the intermediate milling step during fusion. Results after the introduction of the intermediate milling step are also provided.

From the characterisation of zircon decomposition (Chapter 8), the following products can be expected to be the most likely to form. The following reactions are not necessarily balanced.

For the fusion of a mole of zircon with one or two moles of sodium hydroxide at 650 or 850°C, under favourable conditions the following reactions can be expected:

$$3ZrSiO_4 + 4NaOH \xrightarrow{850^\circ C} Na_4Zr_2Si_3O_{12} + ZrO_2 + 2H_2O \tag{9.1A}$$

$$ZrSiO_4 + 2NaOH \xrightarrow{850^\circ C} Na_2ZrSiO_5 \tag{9.1.B}$$

$$ZrSiO_4 + 2NaOH \xrightarrow{650^\circ C} Na_2SiO_3 + ZrO_2 + H_2O \tag{9.1C}$$

SCHEME 9.1: A representation of a possible reaction when fusing a mole of zircon with two moles of sodium hydroxide at 650°C and 850°C. Reaction 9.1A and 9.1B predominate when fusing with one or two moles of NaOH at 850°C respectively. Reaction 9.1C predominates at 650oC when fusing with one or two moles of NaOH.

When fusing a mole of zircon with four or six moles of sodium hydroxide at 650 or 850°C, under favourable conditions the following reaction products can be expected:

$$ZrSiO_4 + 4NaOH \xrightarrow{650^\circ C} Na_2SiO_3 + Na_2ZrO_3 + 2H_2O \tag{9.2A}$$

$$ZrSiO_4 + 6NaOH \xrightarrow{650^\circ C} Na_4SiO_4 + Na_2ZrO_3 + 2H_2O \tag{9.2B}$$

$$ZrSiO_4 + 4NaOH \xrightarrow{850^\circ C} 2Na_2ZrSiO_5 + 2H_2O \tag{9.2C}$$

$$ZrSiO_4 + 4NaOH \xrightarrow{850^\circ C} Na_2SiO_3 + Na_2ZrO_3 + Na_2O + 2H_2O \tag{9.2D}$$

SCHEME 9.2: A representation of the possible reactions when fusing a mole of zircon with four or six moles of sodium hydroxide at 650 or 850°C. The conditions under which each reaction dominates are given in the reaction Scheme 9.2.

Now that the reactions, which take place during the decomposition of zircon, are known the theoretical limit can be defined. For this purpose a fraction defined with the aid of reaction 9.1A should give the theoretical limit. Reaction 9.1A consumes the least amount of NaOH when liberating the zirconia form the zircon lattice. Reaction 9.1A consumes four moles of NaOH while liberating three moles of zirconia, thus the fraction has a magnitude of 1.33 NaOH (mol) / ZrO_2 (mol).

9.2 RESULTS

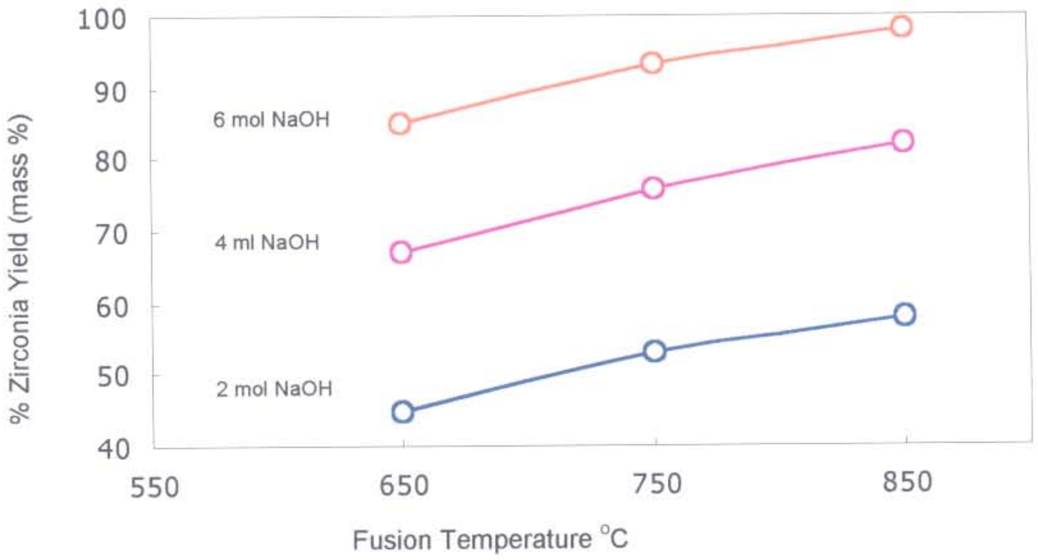

FIGURE 9.1: Influence of Fusion temperature on the yield of zirconia. Fusion time was two hours for the $d_{50} \approx 9\mu m$ zircon sand (no intermediate milling).

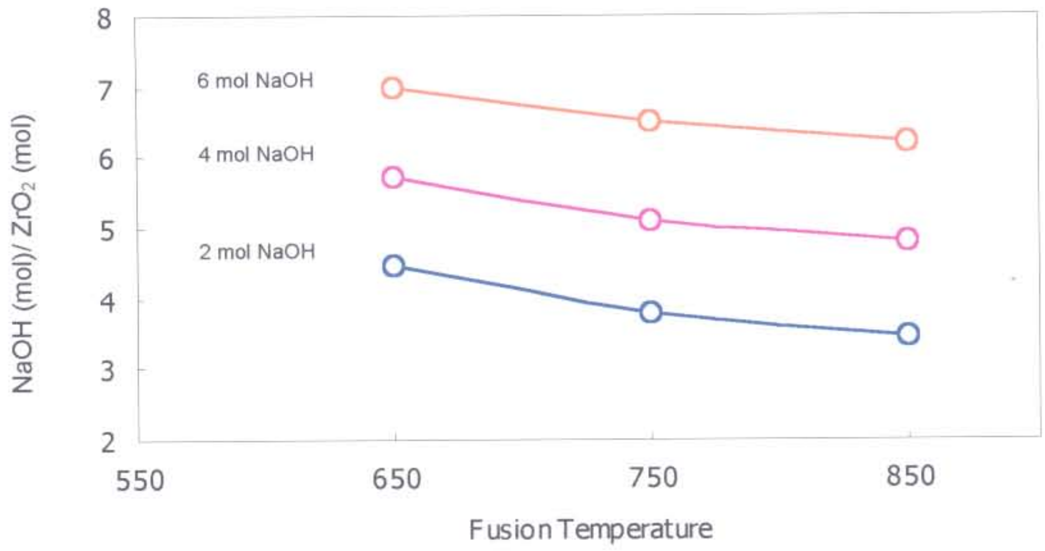

FIGURE 9.2: Influence of temperature on the efficiency of zirconia yield. Fusion time was two hours for the $d_{50} \approx 9\mu m$ zircon sand (no intermediate milling).

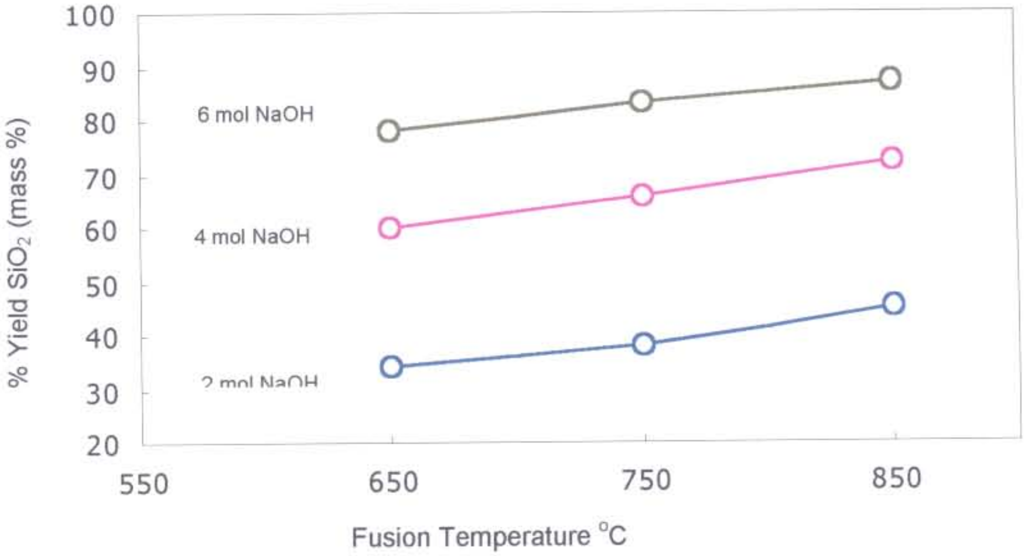

FIGURE 9.3: The influence of temperature on the yield of silica. Fusion time was two hours for the $d_{50} \approx 9\mu m$ zircon sand (no intermediate milling).

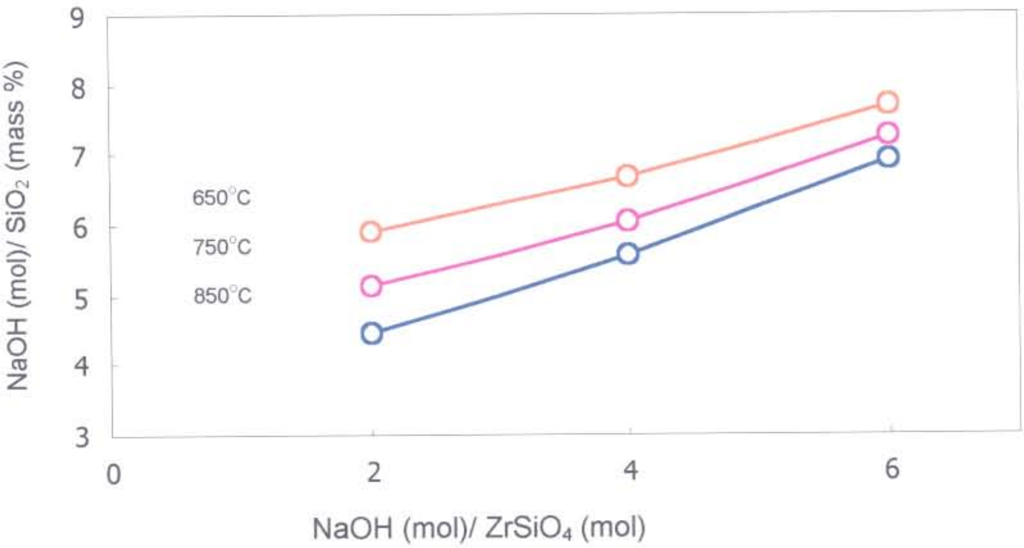

FIGURE 9.4: The influence of sodium hydroxide on the efficiency of silica yield. Fusion time was two hours for the $d_{50} \approx 9\mu m$ zircon sand.

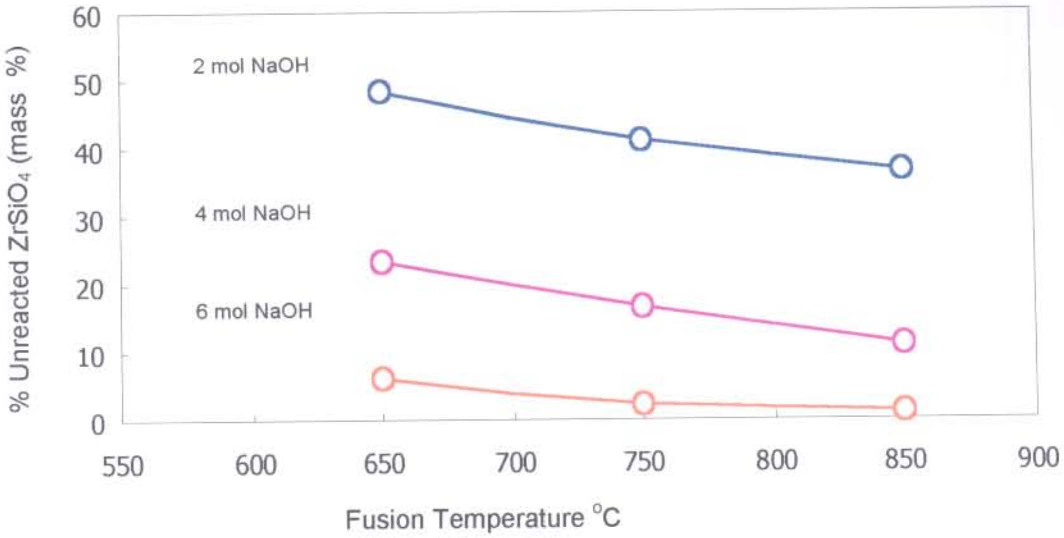

FIGURE 9.5: Influence of Temperature on the yield of Solids. Fusion time was two hours for the $d_{50} \approx 9\mu m$ zircon sand.

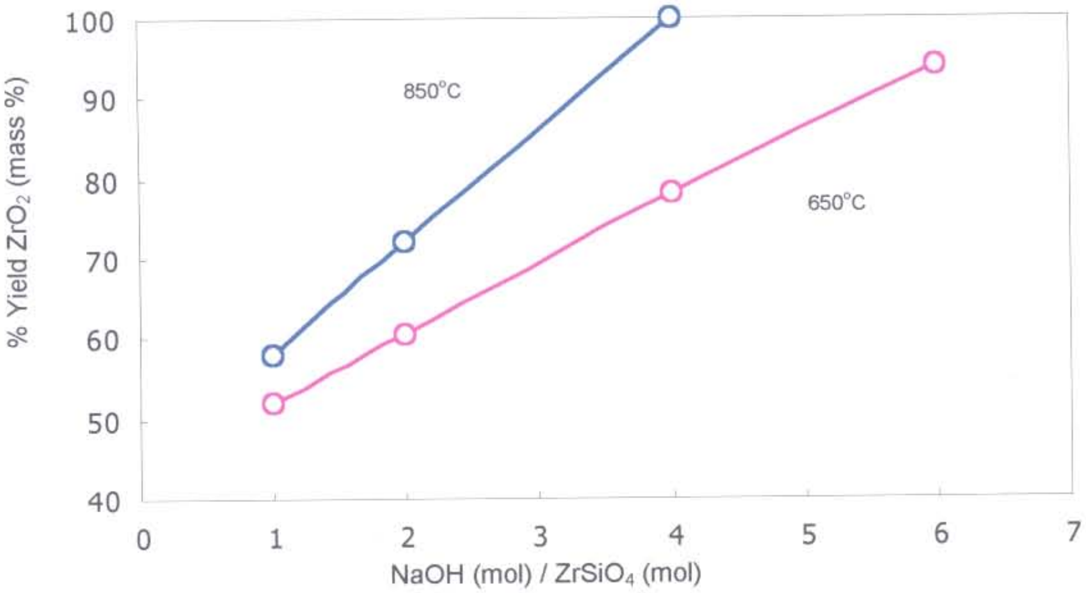

FIGURE 9.6: Influence of the moles of sodium hydroxide per mole of zircon on the yield of zirconia form zircon sand. Fusion time was 336 hours for the $d_{50} \approx 9\mu m$ zircon sand

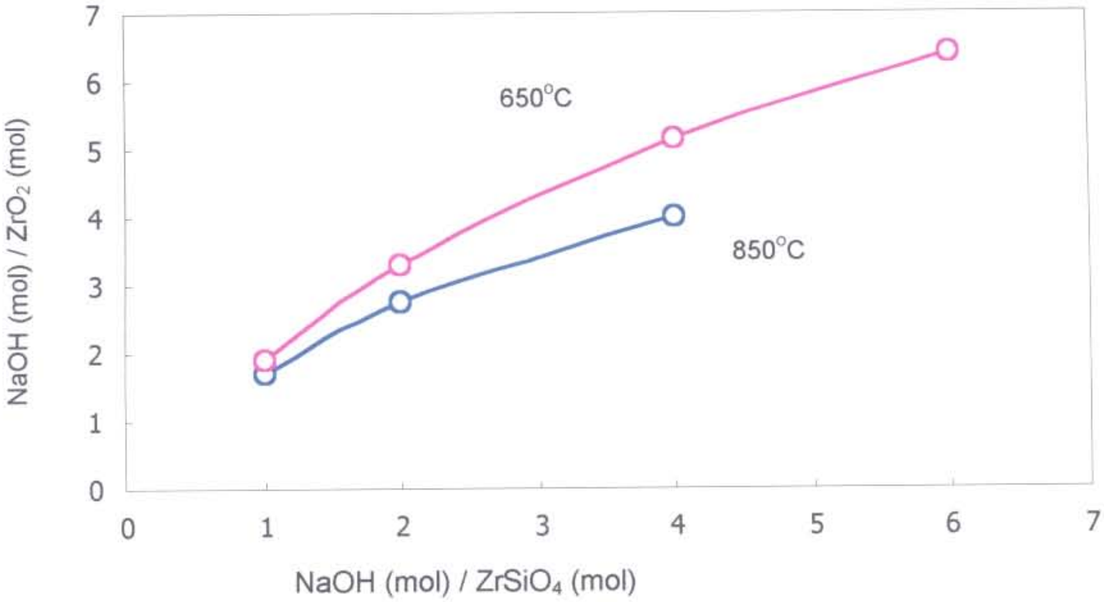

FIGURE 9.7: The influence of sodium hydroxide to zircon mole ratio on the efficiency of zirconia yield. Fusion time was 336 hours for the $d_{50} \approx 9$ μm zircon sand

9.3 RESULTS AND DISCUSSIONS

9.3.1 FUSION FOR TWO HOURS

Figure 9.2 shows the effect that the fusion temperature had on yield of zirconia. For the sub-stoichiometric fusion the yield of zirconia increases from approximately 45% at 650°C to about 58% at 850°C.With increase is sodium hydroxide the yield was observed to increase as the moles of sodium hydroxide and temperature increased (Figure 9.2). The results confirm that the yield of zirconia increases from a minimum of approximately 45% at 650°C when fusing with $NaOH/ZrSiO_4 = 2$, to near complete decomposition at 850°C when fusing with $NaOH/ZrSiO_4 = 6$

To determine the most efficient reaction, the fraction NaOH (mol)/ ZrO_2 (mol) was defined. The fraction indicates the number of moles of sodium hydroxide required to liberate a mole of zirconia from the zircon lattice. The theoretical limit, determined from reaction 9.1A (Scheme 9.1), is where the fraction has a magnitude of 1.33. The reaction at 850°C fusion with two moles of sodium hydroxide has the closest value to the theoretical limit (Figure 9.2). Thus this reaction condition is the most efficient.

Figure 9.3 shows the effect that sodium hydroxide had on the yield of silica. The yield was observed to increase as the moles of sodium hydroxide increased. The results confirm that the yield of silica increases from a minimum of approximately 35% when at 650°C with $NaOH/ZrSiO_4 = 2$, to about 90% at 850°C for $NaOH/ZrSiO_4 = 6$. In comparison to the zirconia yields the silica yields were observed to be lower, at times about 10% lower. This could be attributed to the insolubility of many complex alkali zirconium silicates [14]. This effect is further supported by the high silica composition of the residue collected after the removal of zirconium sulphate tetrahydrate, as seen in the XRF and ICP elemental analysis in Table 9.1. Never the less the silica yields remain a *rough* indicator of the extent of decomposition. Figure 9.3 have similar suggestion about efficiency and yield as the zirconia plots of such variables.

Figure 9.5 shows the effect that sodium hydroxide and temperature had on the amount of undecomposed zircon. The unreacted zircon was observed to decrease as the amount of sodium hydroxide and temperature were increased.

The reaction condition at 850°C NaOH/$ZrSiO_4$ = 6 for was observed as the point with the minimum amount of solids. The majority of the solids were actually silica. This further emphasised the extent of zircon decomposition. The reaction condition at 650°C and two moles of sodium hydroxide for the same particle size was observed as the point with the highest amount of solids. The elemental analysis (XRF and ICP) suggests that the solids constitute zircon in majority and free silica in minority.

9.3.2 FUSION FOR 336 HOURS

Figure 9.6 shows the improved decomposition obtained from decomposing the zircon sand over a period of two weeks with periodic milling. The reaction at 850°C when fusing with NaOH/$ZrSiO_4$ = 4 showed near complete decomposition. This is a point that was suggested by the characterisation with XRD, Raman and infra red spectroscopy. The reaction at 850°C fusion with one mole of NaOH per mole of zircon almost showed a 60% zirconia yield. This amount is comparable to that attained at the same temperature but at twice the amount of caustic soda without the intermediate milling step.

Figure 9.7 shows the plot of the fraction NaOH (mol) /ZrO_2 (mol) that was defined to determine the most efficient reaction condition. When fusing with NaOH (mol) /ZrO_2 (mol) =1 were observed to have the most efficient caustic soda consumption.

The increased efficiency at 650°C can be attributed to the polymerisation of the Na_4SiO_4 monomers (high in sodium content) to the metasilicate Na_2SiO_3 (low in sodium) chains. The more increased efficiency at 850°C when fusing with NaOH/$ZrSiO_4$ < 2 can be attributed to the formation of the phases Na_2ZrSiO_5, $Na_4Zr_2Si_3O_{12}$ and ZrO_2. The phases liberate high amounts of zirconium while consuming low amounts of sodium.

9.4 CONCLUSIONS

9.4.1 FUSION FOR TWO HOURS

Increments of sodium hydroxide and temperature are desirable for complete zircon decomposition.

Near complete decomposition at 850°C was observed when fusing with $NaOH/ZrSiO_4 = 6$. The other advantage associated with this is the minimal amounts of solids that constitute silica in majority. In the case of re-circulation the silica in the solids poses a problem (if it is not separated) in the consumption of raw materials, thus complicating reactor design, since the decomposition would be affected. The free silica can be separated by physical means from the undecomposed zircon due to the large density difference between the two. Centrifugation (5 000 r.p.m.) was also observed to separate zircon from the free hydrated silica.

The most efficient reaction condition was observed at 850°C when fusing a mole of zircon with two moles of sodium hydroxide. This was the reaction condition that had the closest value to the theoretical limit.

9.4.2 FUSION FOR 336 HOURS WITH INTERMEDIATE MILLING

The reaction at 850°C fusion with four moles of caustic showed near complete decomposition. This is a point that was first suggested by the characterisation with XRD, Raman and IR spectroscopy. The reaction at 850°C fusion with one mole of NaOH per mole of zircon almost showed a 60% zirconia yield. This amount is comparable to that attained at the same temperature but at twice the amount of caustic soda without the intermediate milling step.

Figure 9.7 shows the influence of the moles of sodium hydroxide on the efficiency. The reactions at sub-stoichiometric fusion were observed to have the most efficient caustic soda consumption. The increased efficiency at 650°C can be attributed to the polymerisation of the Na_4SiO_4 monomers to the metasilicate Na_2SiO_3 chains (low in sodium). The more increased efficiency at 850°C $NaOH/ZrSiO_4 < 2$ can be attributed to the synthesis of reactive phases Na_2ZrSiO_5, $Na_4Zr_2Si_3O_{12}$ and ZrO_2. The phases liberate high amounts of zirconium while consuming low amounts of sodium.

TABLE 9.1: ELEMENTAL ANALYSIS OF THE CALCINED PRODUCTS (concentration in mass percent)

Product	ZrO_2+ HfO_2	SiO_2	Na_2O	Trace
Zirconia 1 : 6 @ 850	98. 4 %	470 ppm	570 ppm	1. 49 %
Zirconia 1 : 4 @ 850	98. 5 %	480 ppm	560 ppm	1. 39 %
Zirconia 1 : 2 @ 850	98. 4 %	320 ppm	450 ppm	1. 46 %
Silica 1 : 6 @ 850	1. 03 %	98. 80 %	430 ppm	0. 17 %
Silica 1 : 4 @ 850	0. 09 %	99. 10 %	690 ppm	0. 80 %
Silica 1 : 2 @ 850	0. 40 %	99. 20 %	560 ppm	0. 42 %
Residue 1 : 6 @ 850	22. 9 %	76. 18 %	480 ppm	0. 93 %
Residue 1 : 4 @ 850	52. 4 %	46. 54 %	320 ppm	1. 05 %
Residue 1 : 2 @ 850	56. 2 %	41. 21 %	540 ppm	1. 30 %
Zirconia 1 : 6 @ 750	98. 3 %	460 ppm	540 ppm	1. 46 %
Zirconia 1 : 4 @ 750	98. 4 %	470 ppm	560 ppm	1. 52 %
Zirconia 1 : 2 @ 750	98. 2 %	420 ppm	350 ppm	1. 38 %
Silica 1 : 6 @ 750	1. 02 %	97. 80 %	830 ppm	0. 27 %
Silica 1 : 4 @ 750	0. 62 %	98. 20 %	490 ppm	1. 30 %
Silica 1 : 2 @ 750	0. 53 %	98. 30 %	260 ppm	1. 43 %
Residue 1 : 6 @ 750	22. 7 %	73. 18 %	780 ppm	1. 94 %
Residue 1 : 4 @ 750	50. 3 %	47. 74 %	420 ppm	1. 52 %
Residue 1 : 2 @ 750	54. 2 %	44. 09 %	520 ppm	1. 80 %
Zirconia 1 : 6 @ 750	98. 1 %	370 ppm	560 ppm	1. 51 %
Zirconia 1 : 4 @ 650	98. 2 %	580 ppm	570 ppm	1. 29 %
Zirconia 1 : 2 @ 650	98. 3 %	350 ppm	540 ppm	1. 62 %
Silica 1 : 6 @ 650	1. 05 %	98. 60 %	340 ppm	1. 18 %
Silica 1 : 4 @ 650	0. 07 %	98. 20 %	690 ppm	1. 90 %
Silica 1 : 2 @ 650	0. 60 %	98. 50 %	460 ppm	1. 52 %
Residue 1 : 6 @ 650	27. 9 %	70. 80 %	580 ppm	1. 20 %
Residue 1 : 4 @ 650	50. 4 %	48. 74 %	620 ppm	1. 05 %
Residue 1 : 2 @ 650	48. 7 %	37. 69 %	340 ppm	2. 30 %

KEY: The name of the product is given first, then the reaction conditions. For an example the sample "Silica 1:6 @ 850" stands for the silica product at six moles sodium hydroxide and 850°C fusion temperature.

9.5 REFERENCES

1. Farnworth, E. Jones, S. L. and McAlpine, I. (1980) The Production, Properties and uses of zirconium chemicals, Magnesium Elektron Ltd, Twickenham U.K.
2. Skidmore, C. (1998) Zirconium Oxides and Chemicals: A Review of Raw Materials, Markets and Future Prospects, Industrial minerals.
3. Mitchell, V. (1995) Zirconia Overview: 1 980–2 000, ZIRCON 95; Industrial minerals.
4. Nielsen, R. Chang, T. W. (1996) Ullman's Encyclopaedia of Industrial Chemistry, A (28) 543-567.
5. Hedrick, J. B. (1997) Zirconium, U. S. Geological Survey-Minerals information.
6. Stevens, R. (1986) Zirconia and Zirconia ceramics, Magnesium Elektron Ltd., Twickenham, U.K.
7. Nyman, H. Hyde, B. G. and Andersson, S. (1984) Acta Cryst. B (40) 441
8. Hyde, B. G. Andersson, S. (1989) Inorganic crystal structures, A Wiley-Interscience publication, New York.
9. Hancock, J. D. (1977) A review of conventional and novel processes for the extraction of zirconia from zircon. Mineral Science and Engineering, 1 (9) 25-31.
10. Chra'ska, P. Neufuss, K. and Herman, H. (1997) Plasma spraying of zircon, J. Thermal Spray technology 6 (4) 445-448.
11. Ault, N. N. (1957) Characteristics of refractory oxide coatings produced by flame spraying, J. Am. Ceram. Soc., 3 (40) 69-74.
12. Evans, A. M. and Williamson, J. P. H. (1977) J. Mater. Sci. 4 (12) 779-790.
13. Suzuki, M. Sodeoka, S. Inoue, T. and Ueno, K. (1998) Effect of heat treatment of Plasma-sprayed zircon. Materials and manufacturing processes 4 (13) 575-580.
14. Murty B. N., Yadav R. B. and Syamsundar, S. (1994) .Preparation of high-purity zirconia from zircon: an anion-exchange purification process, Separation Science and Technology, 2 (29) 249-259.

Chapter 10

THE *in-situ* ZBS PURIFICATION STEP

10.1 INTRODUCTION

The De Wet process provides a rapid purification method when compared with other wet-chemical zirconium processes. This is due to the use of a mineral acid washing step, which is much more rapid than precipitation methods [1-3]. This step is capable of removing the concentration of Uranium and Thorium compounds to concentrations below parts per million. The key is the synthesis of a stable and insoluble zirconium basic sulphate of the formula $Zr_5O_7(SO_4)_3nH_2O$. The basic sulphate remains insoluble to mineral acid washes e.g. HCl and the radioactive compounds form soluble products thus are easily washed out.

Since this step proves to be the most crucial, the stability of this basic sulphate, with respect to zirconia losses per HCl washing step, was investigated.

10.2 RESULTS

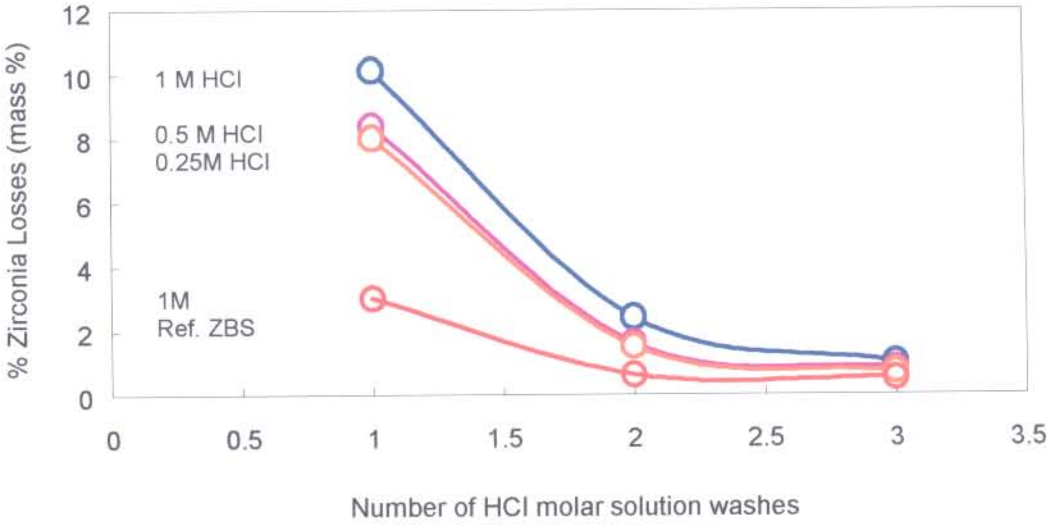

FIGURE 10.1: The influence of the number of washes on the *in-situ* ZBS solubility. In the first wash the ZBS was digested with hot (90°C) HCl molar solutions. Reference ZBS (Ref. ZBS) was washed with one molar HCl solution.

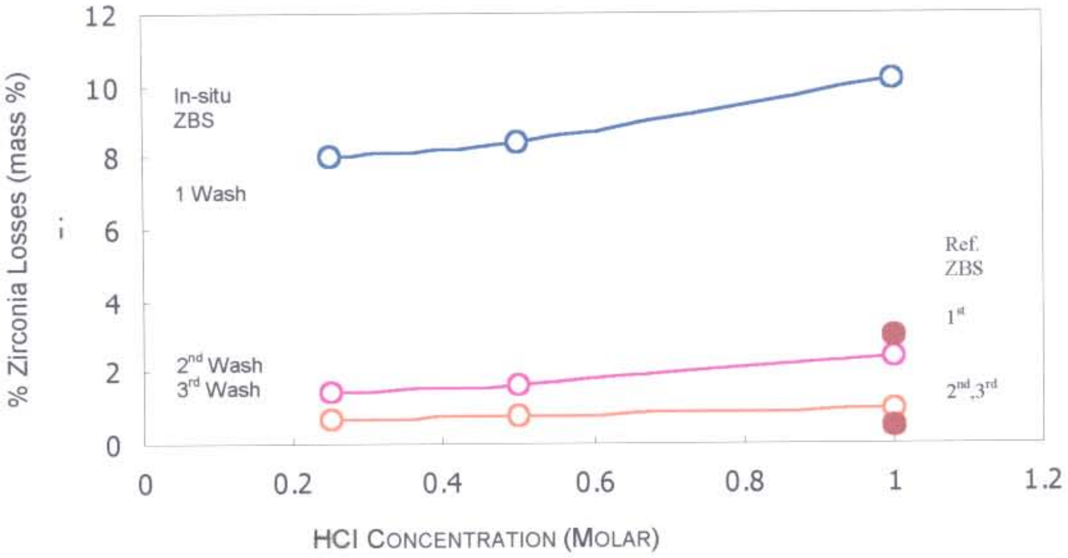

FIGURE 10.2: The influence of increasing HCl molarity on the solubility of *in-situ* and Ref. ZBS products. In the first wash, the ZBS wash digested with hot (90°C) HCl molar solutions.

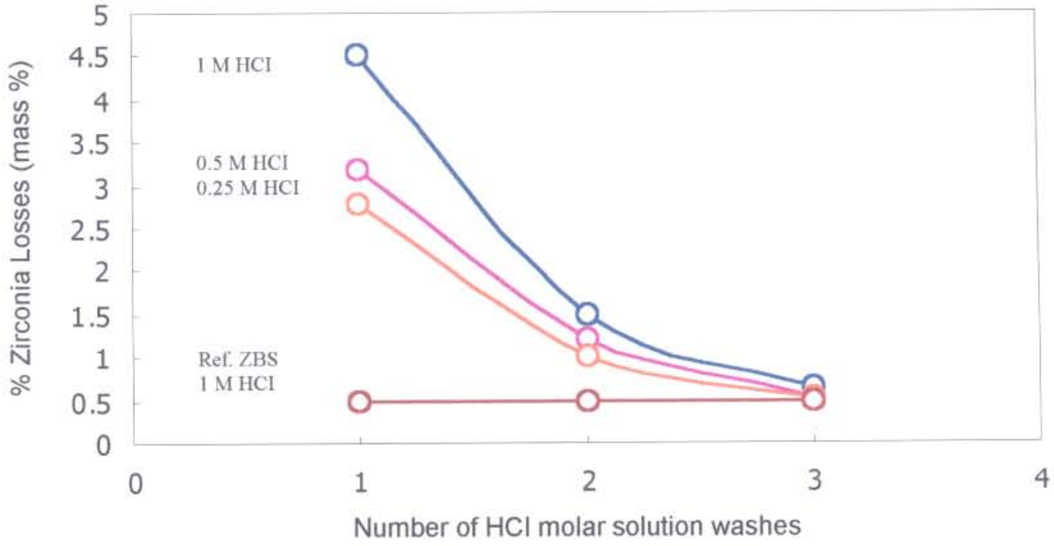

FIGURE 10.3: The influence of the number of washes on the *in-situ* and Ref. ZBS solubility. The ZBS was washed with HCl molar solutions at room temperature.

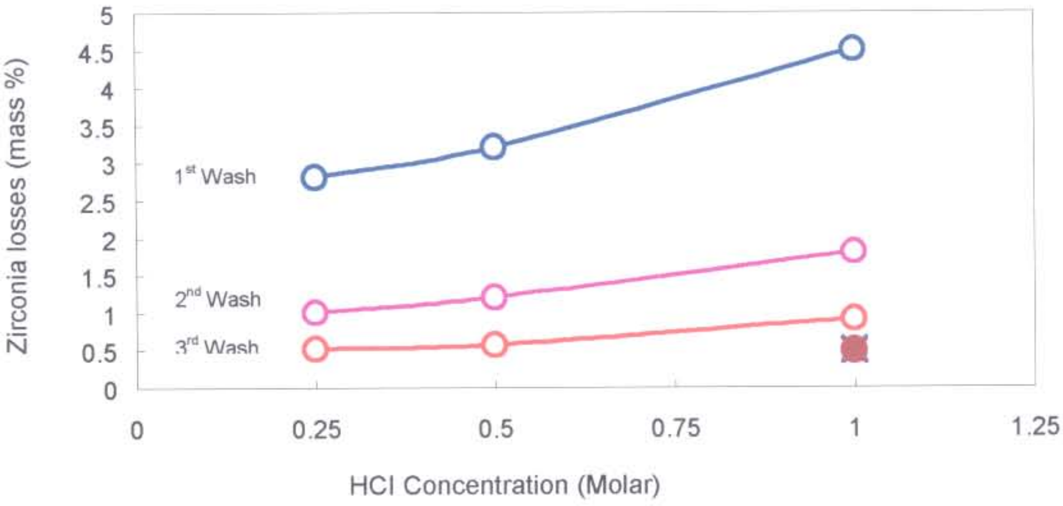

FIGURE 10.4: The influence of increasing HCl molarity on the solubility of *in-situ* and Ref. ZBS products. The ZBS was washed with HCl molar solutions at room temperature.

10.3 DISCUSSIONS

Figure 10.1 shows plots of the zirconia losses with the number of washes. Both in-situ and Ref. ZBS were digested with HCl solutions at 90°C. The curves are seen to be exponential. The initial washing step was seen to have the highest zirconia losses, the last with the least zirconia losses. This shows the increasing stability or insolubility of the ZBS paste to the HCl solutions.

Figure 10.2 shows the zirconia losses with increments in the HCl molarity. The zirconia loses were observed to increase with increasing molarity of HCl. The reference ZBS showed loses up to 3% m/m of ZrO_2 in the first wash when digested with a one molar HCl solution. While the in-situ ZBS showed losses up to 10% m/m of ZrO_2 for digestion at the similar molarity. The first wash, for all three molar concentrations, for both in-situ and reference ZBS, was observed to cause the highest zirconia losses. Two possibilities could be responsible for these high losses. Firstly the incomplete conversion of the hydrous zirconia to ZBS. Secondly the instability of the ZBS to hot 90°C HCl solutions.

To verify each possibility both types of ZBS were washed with HCl solutions at room temperature. Figures 10.3 and 10.4 show the influence that washing at room temperature had on the zirconia losses. The reference ZBS showed minimal to negligible losses ($< 0.5\%$ m/m of ZrO_2), while the in-situ ZBS showed losses less than 5% m/m of ZrO_2. This indicates the incomplete conversion of the hydrous zirconia to in-situ ZBS.

Table 10.1 shows the elemental analysis of the zirconia that was lost and the in-situ ZBS that was collected after each washing step. The ZBS was converted to the AZST to separate it from the residue. For the one molar HCl first wash, the AZST had a Uranium and Thorium concentration that was below three parts per million. A similar observation was made for the half a molar HCl solution. The quarter molar solution was observed to have a similar effect after the third wash.

10.4 CONCLUSIONS

The zirconia losses for the in-situ ZBS are due to both incomplete conversion and increased molarity of the mineral acid, e.g. HCl.

The in-situ ZBS showed losses up to 10% m/m of ZrO_2 when washed with HCl solution with molarity greater than 0.5M. For solution with molarity greater than 0.5M, digestion in the first wash is necessary to remove the Uranium and Thorium to levels below three parts per million. To minimise the zirconia losses for the in-situ ZBS route, the ZBS can be washed with water to dissolve AZST. The AZST can then be re-circulated to the sodium removal step or precipitated with ammonia to hydrous zirconia. The Ref. ZBS route has minimal loses but is process time and energy consuming. This is because the Ref. ZBS is prepared by precipitation from hot solutions while stirring.

TABLE 10.1: ELEMENTAL ANALYSIS OF THE LOST SOLIDS AND THE *in-situ* ZBS

Sample	U_3O_8	ThO_2	ZrO_2	SO_3	Al_2O_3	Fe_2O_3
ZrO_2 1M@1W	0.204 %	0.165 %	97.2 %	0.237 %	0.01 %	0.17 %
ZrO_2 1M@2W	< 3 ppm	< 3 ppm	98.1 %	0.136 %	0. 11 %	0.42 %
ZrO_2 1M@3W	< 3 ppm	< 3 ppm	97.6 %	0.242 %	0.02 %	0.23 %
AZST1M@1W	< 3 ppm	< 3 ppm	62.6 %	34.8 %	1.19 %	890 ppm
AZST1M@2W	< 3 ppm	< 3 ppm	69.7 %	23.0 %	1.16 %	730 ppm
AZST1M@3W	< 3 ppm	< 3 ppm	65.6 %	29.1 %	1.12 %	800 ppm
ZrO_2 0.5M@1W	0.46 %	0.146 %	96.7 %	0.213 %	0.05 %	0.43 %
ZrO_2 0.5M@2W	0.25 %	0.082 %	94.3 %	0.260 %	0.123 %	0.54 %
ZrO_2 0.5M@3W	< 3 ppm	< 3 ppm	97.2 %	0.134 %	0.08 %	0.91 %
AZST0.5M@1W	480 ppm	690 ppm	64.7 %	32.8 %	1. 23 %	790 ppm
AZST0.5M@2W	< 3 ppm	< 3 ppm	68. 1 %	30.7 %	0.89 %	980 ppm
AZST0.5M@3W	< 3 ppm	< 3 ppm	66.3 %	31.7 %	0.78 %	450 ppm
ZrO_2 0.25M@1W	0.173 %	0.096 %	96.6 %	0.320 %	0.23 %	0.12 %
ZrO_2 0.25M@2W	0.123 %	0.070 %	98.4 %	0.434 %	0.12 %	0.16 %
ZrO_2 0.25M@3W	0.023 %	0.033 %	98.2 %	0.323 %	0.04 %	0.17 %
AZST0.25M@1W	360 ppm	720 ppm	66.7 %	30.12 %	1.09 %	745 ppm
AZST0.25M@2W	100 ppm	320 ppm	64.4 %	33.9 %	0.98 %	950 ppm
AZST0.25M@3W	< 3 ppm	< 3 ppm	68.9 %	29.7 %	0.74 %	420 ppm

KEY: The Sample names are given first, then the concentration of the HCl solution and then number of the wash. For example, ZrO_2 0.25M@3W is the zirconia sample from the 0.25M HCl solution after the third wash.

10.5 REFERENCES

1. Nielsen, R. Chang, T. W. (1996) Ullman's Encyclopaedia of Industrial Chemistry, A (28) 543-567.
2. Hancock, J. D. (1977) A review of conventional and novel processes for the extraction of zirconia from zircon. Mineral Science and Engineering, 1 (9) 25-31.
3. Houchin, M. R. Jenkins, B.E. Sinha, H.N. (1990) Production of high quality zirconia for ceramics, Mineral, Materials and Industry 14th congress of the council of mining and metallurgy Institute, organised by IMM.
4. Clearfield, A. (1964) Structural aspects of Zirconium Chemistry. Rev. Pure and Appl. Chem. (14) 9

CHAPTER 11

CONCLUSIONS AND RECOMMENDATIONS

11.1 INTRODUCTION

There are two industrial sources of zirconia: zircon and baddeleyite [1-5]. The baddeleyite reserves in Phalaborwa (the world's major baddeleyite source) are expected to be depleted by the year 2 005 [1-3]. This leaves the Russian Baddeleyite (Kola Peninsula) and zircon as the only industrial sources of zirconia.

The major drawback to zircon use is the large amounts of impurities it is found concentrated with, especially radioactive impurities (Uranium and Thorium) [2-3]. Acid leaching of zircon does not remove these impurities [4-5]. The impurities are usually included in the zircon lattice. The tetragonal structure of zircon with the high coordinated bisdisphenoids ZrO_8 and low coordinated tetrahedra SiO_4 create a safe (inaccessible and stable) habitat for these impurities [7].

Processes for the recovery of zirconia and zirconium chemicals rely heavily on precipitation or crystallisation techniques for purification [8-16]. Precipitation techniques need to be repeated to obtain the required purity. The purity of products from such methods is still suspect, as there still remains a high radioactivity content after purification [2]. The long process time is another disadvantage of these precipitation processes. These factors together are the reason for the high cost of zirconia and zirconium chemicals.

Zirconium and its compounds are regarded to be of low toxicity [1-6]. This implies that they have a great potential of replacing numerous high toxic chemicals. Prominent examples are seen in leather tanning and paints. In leather tanning chromium chemicals can be replaced. In paints lead driers and chromium chemicals for corrosion resistance can be replaced.

The objective of this study was to characterise and optimise the De Wet's alkali fusion processes for the beneficiation of zircon sand into high purity zirconia and zirconium chemicals. However, at each process step some factors were varied e.g. fusion temperature, reactant ratios and composition of leach solutions. Attention was also paid to reducing the total number of process steps. The products produced at each step were analysed. Particular attention was given to the fate of the radioactive impurities.

11.2 ZIRCON DECOMPOSITION

The decomposition of zircon was carried out in open reaction vessels. A mole of zircon was decomposed using from one to six moles of sodium hydroxide and fusion temperatures of 650, 750 and 850°C. When the fusion time is limited to two hours non-equilibrium phases form and the products formed depend on reaction kinetics. For prolonged fusion times (e.g. 336 hours) the reaction products tend towards the expected equilibrium phases. These are the two factors that determine phase formation.

The tetragonal structure of zircon is stabilised by the bisdisphenoids linkages. The silicate phases that are formed can be polymerised to silicates low in sodium (e.g. Na_2SiO_3 or $Na_2Si_2O_5$). This allows the sodium to be released for further decomposition reactions. At 850°C and long fusion times the phases observed are thermodynamically stable one to those reported for higher temperatures by D'Ans and Loeffler (1930) [24, 25]. However, the phase diagram observed at 650°C differs from that obtained by them: The phases Na_2ZrSiO_5 and $Na_4Zr_2Si_3O_{12}$ were not observed.

11.2.1 DECOMPOSITION AT 650°C

Prolonged fusion at 650°C with $NaOH/ZrSiO_4 \leq 2$ mole ratio leads to the formation of sodium metasilicate and zirconia (Scheme 8.2). The XRD reveals the presence of metasilicate and zirconia in trace- or in minor amounts. The low level of detection of these compounds could be due to an amorphous state of the samples (Figure 8.24). The IR bands at 710 and 600 cm^{-1} support the presence of polymerised silicates (e.g. the sodium metasilicate).

Prolonged fusion (336 hours) at 650°C with $4 \leq$ NaOH moles ≤ 6 leads to the formation of sodium silicates high in sodium and the polymerisation (Scheme 8.1) of the orthosilicate monomers to metasilicate chains. The IR supports this conclusion showing the presence of the δ(Si-O-Si) band at 686 cm^{-1} (for the fusion done in two hours). The split in the band at 686 to ones at 710 and 600 cm^{-1} is indicative of the presence of highly polymerised silicates. The band at 600 cm^{-1}indicates the presents of silicates with rings with more than six members [19-23].

When fusing for two hours, increasing the amount of sodium hydroxide leads to the formation of silicates high in sodium (e.g. Na_4SiO_4) and zirconia. Zirconia, in its reduced state, is formed rather than sodium zirconate. This is a consequence of the stability of the ZrO_8 bisdisphenoids and the instability of the SiO_4 tetrahedra linkages at this temperature.

For prolonged fusion with $NaOH/ZrSiO_4 \leq 2$ mole ratio, most of the sodium followed the silicates. This suggests that the zirconium compound in the AFDZ was low in sodium or hydrolysed easily [17].

11.2.2 DECOMPOSITION AT 850°C

When zircon is decomposed with sodium hydroxide at higher temperatures e.g. 850°C, the formation of sodium silicates and sodium zirconates is observed. This is an indication that at this temperature the ZrO_8 bisphenoid linkages are not resistant to Na_2O attack.

Prolonged fusion (e.g. 336 hours) at 850°C with $NaOH/ZrSiO_4 < 2$ mole ratio leads to the formation of the phase $Na_4Zr_2Si_3O_{12}$ and ZrO_2 (Scheme 8.4).

Prolonged fusion at 850°C with $NaOH/ZrSiO_4$ = 2 mole ratio leads to the formation of the phase Na_2ZrSiO_5 (Scheme 8.4). The formation of these phases ($Na_4Zr_2Si_3O_{12}$ and Na_2ZrSiO_5) was not detected at 650°C.

11.3.1 THE IN-SITU ZBS PURIFICATION STEP

The impurities are removed from ZBS with mineral acid washes at 90°C; the concentration was varied from 0.25M to 1M HCl. The mineral acid leads to zirconia losses; these are due to both incomplete conversion and increased molarity of acid. The in-situ ZBS showed losses up to 10% m/m of zirconia for HCl of one molar. Washing ZBS with solutions of molarity greater than 0.5M HCl removes Uranium and Thorium to levels below parts per million.

A way to minimise the zirconia losses for the in-situ ZBS route is to wash it with water to dissolve AZST. The AZST can then be re-circulated to the sodium removal step or precipitated with ammonia to hydrous zirconia.

The hydrous zirconia can be reacted with stoichiometric amounts of sulphuric acid to form ZBS. The ZBS can then be washed with mineral acid to remove impurities.

11.3.2 THE REF. ZBS PURIFICATION ROUTE

The Ref. ZBS route has minimal zirconia losses but a longer process time; ZBS precipitates out of solution after long periods. For example when heating a 20.0 g of zirconyl chloride solution between 90 and 100°C, with stoichiometric amounts of sulphuric acid, a fine grain ZBS precipitated (about 9.0g ZrO_2) after 30 minutes.

This ZBS is much more stable than the in-situ ZBS (prepared from hydrous zirconia at approximately 120°C with stoichiometric amounts of sulphuric acid), this stability is attributed to a series of olation reactions and the formation of sulphate bridges through a slow ordered precipitation reaction. This route could be have been adopted by De Wet; it has minimal zirconia losses (about 2% m/m when washed with 1M HCl at 90°C).

11.4 THE ALKALI SILICATE BY-PRODUCT

The by-product contains sodium metasilicate as well as sodium carbonate. The presence of the latter is attributed to the reaction of atmospheric carbon dioxide with excess sodium during crystallisation. The observed Na_2O/SiO_2 mol ratio, in the sodium silicate stream, exceeded three for all reagent ratios for a 2 hour fusion time.

11.5 THE AZST PRODUCT

The zirconium sulphate tetrahydrate (AZST) prepared in this study consists of many phases owing to the nature of the crystallisation process. Similar observations were made by Bear and Mumme (1971) [19]. Appendix K confirms that a product of very high purity can be obtained.

11.6 THE ZIRCONIA PRODUCT

The zirconia prepared in this study is predominantly monoclinic. It consisted of oblong, spherical particles with a dimension of about 90 nm. The zirconia obtained was also of high purity as shown in Appendix K.

11.7 THE RESIDUE AND RE-CIRCULATION

The residue (the solids remaining after the removal of AZST) constitutes free silica and unreacted zircon. The silica can be separated from the zircon by physical means. This is due the large density difference between silica and zircon. For example when using a centrifuge (5 000 r.p.m) it was possible to separate the two. The unreacted zircon can then be re-circulated for further decomposition.

11.8 THE DE WET PROCESS

Finally, the De Wet's zirconium extraction process is rapid when compared to precipitation processes. The in-situ ZBS is very stable and can be washed with mineral acids to remove impurities. The in-situ ZBS is not as stable as Ref. ZBS prepared from a single precipitation route.

The products and by-product synthesised by the De Wet process are of very high purity, better than any commercial products; washing Ref. ZBS with mineral acids can attain similar purity.

The only disadvantage of this process is how it synthesises ZBS. To synthesise ZBS from hydrous zirconia with stoichiometric amounts of sulphuric acid, is difficult. Any excess or insufficient acid can lead to zirconia loses as AZST or ZOC respectively. Maintaining the ZBS as a paste during the synthesis at approximately 150°C is another complication since crosslinking of the hydroxyl groups is possible if the paste is dried. The ZBS may crosslink at the terminal hydroxyl groups including the impurities within the polymer matrix; removal of impurities from the crosslinked ZBS remains a scope for further research.

11.9 REFERENCES

1. Hedrik, J. B. (1997) Zirconium, U.S. Geological Survey-Minerals Information.
2. Skidmore, Charles (1998) Zr oxides and chemicals, Sources, markets and Outlook, Industrial Minerals.
3. Reeves, R. G. (2 000) Zircon out West, Progress on the escalante Utah zircon trend, Industrial Minerals.
4. Blumenthal, W.B. (1958) The Chemical Behaviour of Zirconium, Van Nostrand, N.J., U.S.A. New York.
5. Anil K. Mukherji, (1970) Analytical Chemistry of Zirconium and Hafnium, Pergamon press.
6. Ralph Nielsen, Teledyne Wah Chang, (1996) Ullman's Encyclopaedia of Industrial Chemistry, A (28) 543-567.
7. Hyde, B. G. Andersson, S. (1989) Inorganic crystal structures, A Wiley-Interscience publication, New York.
8. Jenkins, D. H. (1986) Process for the production of high purity zirconia powder. International patent WO 86/04614. World intellectual property organisation.
9. Hancock, J.D. (1977) A review of conventional and novel processes for the extraction of zirconia from zircon. Mineral Science and Engineering, 1 (9) 25-31.
10. Olby, J. K. (1963) Manufacture of zirconium oxide from zircon, U.S. Patent 3,109,704.
11. Recasens, J. Urffer, D. Ferlanda, P. (1992) Reactive zirconium oxide and its preparation, U.S. Patent 5149510.
12. Farnoworth, F. Jones, S. L. and McAlpine, I. (1980) The Production, Properties and uses of zirconium chemicals, Magnesium Elektron Ltd. Twickenham, U. K.

13. Houchin, M. R. Jenkins, B.E. Sinha, (1990) H.N Production of high quality zirconia for ceramics, Mineral, Materials and Industry 14th congress of the council of mining and metallurgy Institute.
14. Schoenlaub, R. A. (1955) Production of calcium zirconate, U. S. Patent 2,721,117
15. Schoenlaub, R. A. (1974) Method of Manufacturing zirconium oxide and salts, U. S. Patent 3,832,441.
16. Herzfield, H. (1914) German patent 290, 878 followed by (1916) J. Soc. Chem. Ind., (35) 634.
17. Clearfield, A. (1964) Structural aspects of Zirconium Chemistry. Rev. Pure and Appl. Chem. (14) 9
18. Bear, I. J. and. Mumme, W. G. (1971) Normal Sulphates of Zirconium and Hafnium, Rev. Pure and Appl. Chem., (21) 189.
19. Nakamoto, K. (1986) The infrared and Raman spectroscopy of inorganic and coordination compounds, 4th edition. A John Wiley and Sons publication, New York.
20. Sitarz, M. Mozgawa, W. Handke, M. (1999) Rings in the structure of silicate glasses, Journal of Molecular Structure, (511-512) 281-285.
21. Mysen, B. O. Virgo, D. Seifert, F. A. (1982) Am. Min. (67) 686-695.
22. Sitarz, M. Mozgawa, W. Handke, M. (1997) Vibrational spectra of complex ring silicate anions-method of recognition, Journal of Molecular structure, (404), 193-197.
23. Huang, Y. Zhimei, J. and Schwieger, W. (1999) Vibrational spectroscopic studies of layered silicates, Chem. Mater. (11), 1210-1217.
24. D' Ans, J. and Loeffler, J. (1930) Z. Anorg. Allg. Chem., (191) [1-2], 22.
25. Sircar, A. and Brett, N. H. (1970) Trans. Brit. Ceram. Soc., (69) [3], 133.

APPENDIX A

A TABULATION OF THE VALUES USED IN THE OPTIMISATION OF THE DECOMPOSITION OF ZIRCON WITH SODIUM HYDROXIDE AFTER TWO HOURS OF FUSION WITH OUT INTERMEDIATE MILLING

Fusion ratio: a moles $ZrSiO_4$ to moles of NaOH	ZrO_2 in grams	Yield of ZrO_2 % (m/m)	ZrO_2 in moles	ZrO_2 g / $ZrSiO_4$ g × 100 %	Efficiency Fraction NaOH (mol) / ZrO_2 (mol)	SiO_2 in grams	Yield of SiO_2 %	SiO_2 g / $ZrSiO_4$ g × 100 %	Residue in grams (Unreacted $ZrSiO_4$ and SiO_2)	Residue g / Used $ZrSiO_4$ g × 100 %	Mass of AFDZ used in grams	Volume of HCl (ml) used to neutralise zirconates solids	Volume of HCl (ml) used to neutralise silicate (liquids)	Na_2O % m/m in solids	Na_2O % m/m in liquids
For the 850°C temperature region															
1: 2	6.800	58.0	0.0577	38.850	3.470	2.700	45.0	14.75	5.500	30.05	23.80	4.00	15.0	21.0	79.0
1: 4	9.640	82.0	0.0818	55.110	4889	4.32	72.0	23.11	4.800	23.60	29.90	8.50	29.50	22.0	78.0
1: 6	11.530	98.0	0.0979	65.890	6.129	5.20	87.0	28.4	0.96	28.50	35.80	18.0	96.0	16.0	84.0
For the 750°C Temperature region															
1: 2	6.230	53.0	0.0528	35.600	3.788	2.28	38.0	12.45	9.110	12.46	23.90	4.50	15.0	21.0	79.0
1: 4	8.940	76.0	0.0759	51.090	5.270	3.960	66.0	21.66	4.820	21.48	29.90	8.00	29.0	22.0	78.0
1:6	10.950	93.0	0.0928	62.500	6.470	4.98	83.0	27.10	1.80	27.20	35.70	17.5	96.0	16.0	84.0
For the 650°C Temperature region															
1: 2	5.290	45.0	0.0448	30.240	4.460	2.05	34.0	11.20	10.260	11.12	23.90	4.50	15.0	21.0	79.0
1: 4	8.230	70.0	0.0698	47.029	5.730	3.6	60.0	19.67	5.830	19.70	29.90	8.50	29.5	22.0	78.0
1: 6	10.12	86.0	0.086	57.800	6.970	4.68	78.0	25.57	2.900	25.60	35.80	17.0	96.0	16.0	84.0

APPENDIX B

A TABULATION OF THE MASS BALANCE USED IN THE OPTIMISATION OF THE DECOMPOSITION OF ZIRCON AT 650°C WITH SODIUM HYDROXIDE AFTER TWO HOURS OF FUSION WITH OUT INTERMEDIATE MILLING

ASSUMPTIONS

1. Free sodium = HCl used to neutralise the sodium silicate solution
2. Ignored losses during purification
3. Ignored losses during water wash

EXPERIMENTAL Temperature (°C)	AFDZ Theoretical	AFDZ found	AFDZ yield	NaOH (g)	Sodium silicate 32% HCl (ml)	Solid 32% HCl (ml)	ZrO_2 (g)	Residue: Silica&zircon (g)	Silica in SS (g)
650	49.00	23.90	0.49	16	15	4.5	5.29	10.26	4.1
	61.39	29.90	0.49	32	29.5	8.5	8.23	5.83	7.2
	73.79	35.80	0.49	48	48	8.5	10.12	2.9	9.36

CALCULATIONS

Basis: 100 kg zircon feed

NaOH/Zircon mol ratio	NaOH kg	Zirconia yield kg	Zircon recycle 2 kg	NaOH in SS kg	SiO_2 in SS kg	SiO_2/Na_2O	NaOH in Solid kg	Error in NaOH %	Silica waste kg	Silica waste kg
2	43.72	29.63	55.92	34.22	11.20	0.42	10.27	-1.78	3.24	1.55
4	87.43	46.17	31.32	67.41	19.67	0.38	19.42	0.68	2.84	1.39
6	131.15	56.99	15.22	110.11	25.57	0.30	19.50	1.17	2.21	1.11
Theoretical:	ZrO_2	67.22								
	SiO_2	32.78								

APPENDIX C

A TABULATION OF THE MASS BALANCE USED IN THE OPTIMISATION OF THE DECOMPOSITION OF ZIRCON AT 750°C WITH SODIUM HYDROXIDE AFTER TWO HOURS OF FUSION WITH OUT INTERMEDIATE MILLING

ASSUMPTIONS

Corrected for losses during fusion

1 Free sodium = HCl used to neutralise the sodium silicate solution

2 Ignored losses during purification

3 Ignored losses during water wash

EXPERIMENTAL

Temperature (°C)	AFDZ Theoretical	AFDZ found	AFDZ yield	NaOH (g)	Sodium silicate 32% HCl (ml)	Solid 32% HCl (ml)	ZrO2 (g)	Residue: Silica &zircon (g)	Silica in SS (g)
	49.00	23.90	0.49	16	15	4.5	6.23	9.11	4.56
	61.39	29.90	0.49	32	29	8	8.94	4.82	7.92
750	73.79	35.70	0.48	48	48	8.75	10.95	1.8	9.96

CALCULATIONS

Basis: 100 kg zircon feed NaOH/Zircon		NaOH kg	Zirconia yield kg	Zircon recycle2 kg	NaOH in SS kg	SiO_2 in SS kg	$SiO2/Na_2O$	NaOH in Solid kg	Error in NaOH %	Silica waste kg (SiO_2)	Silica wast kg (zirconium
mol ratio	2	43.72	34.90	48.09	34.22	12.46	0.47	10.27	-1.78	4.55	2.94
	4	87.43	50.15	25.39	66.27	21.64	0.42	18.28	3.29	2.81	1.65
	6	131.15	61.84	8.01	110.42	27.21	0.32	20.13	0.46	2.94	2.15
Theoretical:		ZrO_2	67.22								
		SiO_2	32.78								

APPENDIX D

A TABULATION OF THE MASS BALANCE USED IN THE OPTIMISATION OF THE DECOMPOSITION OF ZIRCON AT 850°C WITH SODIUM HYDROXIDE AFTER TWO HOURS OF FUSION WITH OUT INTERMEDIATE MILLING

ASSUMPTIONS

Corrected for losses during fusion

1 Free sodium = HCl used to neutralise the sodium silicate solution

2 Ignored losses during purification

3 Ignored losses during water wash

EXPERIMENTAL

Temperature (°C)	AFDZ Theoretical	AFDZ found	AFDZ yield	NaOH (g)	Sodium silicate 32% HCl (ml)	Solid 32% HCl (ml)	ZrO2 (g)	Residue: Silica &zircon (g)	Silica in SS (g)
850	49.00	24.62	0.50	16	20	5	7.78	7.05	2.53
	61.39	32.00	0.52	32	41	7.9	9.51	0.772	3.29
	73.79	35.80	0.49	48	48	9	11.53	1.15	10.4

CALCULATIONS

Basis: 100 kg zircon feed

NaOH/Zircon Mol ratio	NaOH kg	Zirconia yield kg	Zircon recycle 2 kg	NaOH in SS kg	SiO_2 in SS kg	SiO_2/Na_2O	NaOH in Solid kg	Error in NaOH %	Silica waste kg (SiO_2)	Silica waste kg (zirconium)
										1.26
										-21.80
2	43.72	42.30	37.07	44.30	6.91	0.20	11.07	-26.67	13.71	3.07
4	87.43	49.85	25.84	87.55	8.99	0.13	16.87	-19.42	15.32	
6	131.15	64.93	3.41	110.11	28.42	0.33	20.65	0.30	3.24	
Theoretical:	ZrO_2	67.22								
	SiO_2	32.78								

APPENDIX E

A TABULATION OF THE MASS BALANCE USED IN THE OPTIMISATION OF THE DECOMPOSITION OF ZIRCON WITH SODIUM HYDROXIDE AT 750°C AFTER 336 HOURS OF FUSION WITH OUT INTERMEDIATE MILLING

Fixed

ASSUMPTIONS

Corrected for losses during fusion

1 Free sodium = HCl used to neutralise the sodium silicate solution

2 Ignored losses during purification

3 Ignored losses during water wash

EXPERIMENTAL Values

Temperature (°C)	AFDZ Theoretical	AFDZ found	AFDZ yield	NaOH (g)	Sodium silicate 32% HCl (ml)	Solid 32% HCl (ml)	ZrO_2 (g)	Residue: Silica &zircon (g)	Silica in SS (g)
	21.86	40.74	1.86	8	2	22	17.49		
750	49.00	49.58	1.01	16			21.81		
	61.39		0.00	32					
	73.79		0.00	48					

CALCULATIONS

Basis: 100 kg zircon feed

NaOH/Zircon mol ratio	NaOH Kg	Zirconia yield kg	Zircon recycle2 kg	NaOH in SS kg	SiO2 in SS kg	SiO2/Na2O	NaOH in Solid kg	Error in NaOH %	Silica waste kg (SiO2)	Silica waste kg (zirconium)
1	21.86	25.64	61.86	1.19	0.00	0.00	13.14	34.43	12.50	-61.86
2	43.72	58.89	12.40	0.00	0.00	#DIV/0!	0.00	100.00	28.71	-12.40
4	87.43	#DIV/0!	#DIV/0!	#DIV/0!	0.00	#DIV/0!	#DIV/0!	#DIV/0!	#DIV/0!	#DIV/0!
6	131.15	#DIV/0!	#DIV/0!	#DIV/0!	0.00	#DIV/0!	#DIV/0!	#DIV/0!	#DIV/0!	#DIV/0!
Theoretical:	ZrO_2	67.22								

APPENDIX F

A TABULATION OF THE MASS BALANCE USED IN THE OPTIMISATION OF THE DECOMPOSITION OF ZIRCON AT 650°C WITH SODIUM HYDROXIDE AFTER 336 HOURS OF FUSION WITH OUT INTERMEDIATE MILLING

ASSUMPTIONS

Corrected for losses during fusion

1 Free sodium = HCl used to neutralise the sodium silicate solution

2 Ignored losses during purification

3 Ignored losses during water wash

EXPERIMENTAL

Temperature (°C)	AFDZ Theoretical	AFDZ found	AFDZ yield	NaOH (g)	Sodium silicate 32% HCl (ml)	Solid 32% HCl (ml)	ZrO_2 (g)
	21.86	39.99	1.83	8	17.5	1	12.29
650	49.00	40.74	0.83	16	34	4	14.74
	61.39	57.70	0.94	32	51	24	19.19
	73.79	72.38	0.98	48	75	40	23.13

CALCULATIONS

Basis: 100 kg zircon feed

NaOH/Zircon mol ratio	NaOH kg	Zirconia yield kg	Zircon recycle2 kg	NaOH in SS kg	SiO_2 in SS kg	SiO_2/Na_2O	NaOH in Solid kg	Error in NaOH %	Silica waste kg (SiO2)	**Silica waste kg (zirconium)**
1	21.86	18.36	72.69	10.65	0.00	0.00	0.61	48.51		
2	43.72	48.44	27.94	45.51	0.00	0.00	5.35	-16.36	23.62	**-27.94**
4	87.43	55.79	17.01	60.40	0.00	0.00	28.42	-1.58	27.20	**-17.01**
6	131.15	64.43	4.16	85.10	0.00	0.00	45.39	0.50	31.41	**-4.16**
Theoretical:	ZrO_2	67.22								
	SiO_2	32.78								

APPENDIX G

A TABULATION OF THE VALUES USED IN THE OPTIMISATION OF THE DECOMPOSITION OF ZIRCON WITH SODIUM HYDROXIDE AFTER 336 HOURS OF FUSION WITH INTERMEDIATE MILLING

Fusion ratio: $ZrSiO_4$ (mol) : NaOH (mol)	ZrO_2 (g)	Yield of ZrO_2 % (m/m)	ZrO_2 (mol)	ZrO_2 g / $ZrSiO_4$ g × 100 %	Efficiency Fraction NaOH (mol) / ZrO_2 (mol)	NaOH (g) / 18.3 (g) of $ZrSiO_4$	NaOH (mol)	Mass of Silica	Percentage Yield of SiO_2 (m / m)	Mass of AFDZ (g)	Volume of HCl (ml) used to neutralise zirconates solids	Volume of HCl (ml) used to neutralise silicate (liquids)	Na_2O % m/m in solids	Na_2O % m/m in liquids
For the 850°C temperature region														
1: 1	7.130	58.0	0.0578	38.960	1.730	4.0	0.100			23.90	16.0	2.0	90.0	10.0
1: 2	8.970	73.0	0.0728	49.016	2.747	8.0	0.200			29.90	32.0	4.0	90.0	10.0
1: 4	12.060	98.0	0.0979	68.850	4.086	16.0	0.400			35.80	27.0	48.0	36.0	64.0
For the 650°C temperature region														
1: 1	6.150	50.0	0.0499	33.60	2.004	4.0	0.100			21.20	1.0	16.0	6.0	94.0
1: 2	7.380	60.0	0.0598	40.33	3.344	8.0	0.200			23.90	4.0	32.0	11.0	89.0
1: 4	9.590	78.0	0.0778	52.40	5.141	16.0	0.400			29.90	48.0	27.0	64.0	36.0
1: 6	11.56	94.0	0.0938	63.17	6.397	24.0	0.600			35.80	38.0	76.0	66.0	34.0

APPENDIX H

CALCULATED ZIRCONIA AND SILICA YIELDS IF THE PREDOMINANT PHASES ARE THOSE SUGGESTED BY THE REACTIONS IN CHAPTER 8

The mole ratio of zircon and NaOH	Expected Zirconia yield if Na_2SiO_3 and ZrO_2 are the predominant phases formed (% m/m)	Expected ZrO_2 yield if Na_4SiO_4 and Na_2ZrO_3 are the predominant phases	Expected zirconia yields if $Na_4Zr_2Si_3O_{12}$ and ZrO_2 are the predominant phase	Expected Zirconia yields if Na_2ZrSiO_5 is the predominant phases	Expected Silica yields if Na_2SiO_3 and ZrO_2 are the predominant phases formed	Expected Silica yields if Na_4SiO_4 and Na_2ZrO_3 are the predominant phases	Expected Silica yields if $Na_4Zr_2Si_3O_{12}$ and ZrO_2 are the predominant phase	Expected Silica yields if Na_2ZrSiO_5 are the predominant phases
For the 650°C temperature region								
1: 1	50	16.697			50	16.67		
1: 2	100	33.394			100	33.33		
1: 4	100	66.788			100	66.67		
1: 6	100	100			100	100		
For the 750°C or 850°C Temperature region								
1: 1			75.137	50			0.0	0.0
1: 2			100	100			0.0	0.0
1: 4			100	100			0.0	0.0
1: 6			100	100			0.0	0.0

The Yields of silica are those expected for soluble silica [silica that removed after the dissolution of AFDZ after fusion (Procedure 7.4.3)].

APPENDIX I

CALCULATED AMOUNTS OF SODIUM(Na_2O m/m) IN THE IN SITU ZIRCONATES OR SODIUM ZIRCONIUM SILICATES, IF THE PREDOMINANT PHASES ARE THOSE SUGGESTED IN CHAPTER 8

The mole ratio of zircon and NaOH	Expected Na_2O % (m/m) in insoluble solids if Na_2SiO_3 and ZrO_2 are the predominant phases formed	Expected Na_2O % (m/m) in insoluble solids if Na_4SiO_4 and Na_2ZrO_3 are the predominant phases	Expected Na_2O % (m/m) in insoluble solids if $Na_4Zr_2Si_3O_{12}$ and ZrO_2 are the predominant phase	Expected Na_2O % (m/m) in solids if Na_2ZrSiO_5 is the predominant phases	Expected Na_2O % (m/m) in insoluble solids if Na_2ZrO_3 and Na_2SiO_3 are the predominant phases	Expected Na_2O % (m/m) soluble Silicates if Na_2SiO_3 and ZrO_2 are the predominant phases formed	Expected Na_2O % (m/m) in soluble Silicates if Na_4SiO_4 and Na_2ZrO_3 are the predominant phases	Expected Na_2O % (m/m) in soluble silicates if $Na_4Zr_2Si_3O_{12}$ and ZrO_2 are the predominant phase	Expected Na_2O % (m/m) in soluble silicates if Na_2ZrSiO_5 is the predominant phases	Expected Na_2O % (m/m) in soluble silicates if Na_2ZrO_3 and Na_2SiO_3 are the predominant phase
For the 650°C temperature region										
1: 1	0.0	33.33			50	100	66.67			50
1: 2	0.0	33.33			50	100	66.67			50
1: 4	0.0	33.33			50	100	66.67			50
1: 6	0.0	33.33			50	100	66.67			50
For the 750°C or 850°C Temperature region										
1: 1			100	100	50			0.0	0.0	50
1: 2			100	100	50			0.0	0.0	50
1: 4			100	100	50			0.0	0.0	50
1: 6			100	100	50			0.0	0.0	50

The above calculations do not only assume complete conversion to the phases in the table, but that the zirconates are not hydrolysed to NaOH and hydrated zirconia.

APPENDIX J

A TABULATION OF THE VALUES USED IN THE OPTIMISATION OF THE DECOMPOSITION OF ZIRCON WITH SODIUM HYDROXIDE AFTER 336 HOURS OF FUSION WITH INTERMEDIATE MILLING

ASSUMPTIONS

Corrected for losses during fusion

1 Free sodium = HCl used to neutralise the sodium silicate solution
2 Ignored losses during purification
3 Ignored losses during water wash

EXPERIMENTAL

Temperature (°C)	AFDZ Theoretical	AFDZ found	AFDZ yield	NaOH (g)	Sodium silicate 32% HCl (ml)	Solid 32% HCl (ml)	ZrO_2 (g)
850	21.86	39.64	1.81	8	2	16	14.26
	49.00	46.87	0.96	16	4	32	17.96
	61.39	57.38	0.93	32	48	27	22.99

CALCULATIONS

Basis: 100 kg zircon feed

NaOH/Zircon mol ratio	NaOH kg	Zirconia yield kg	Zircon recycle2 kg	NaOH in SS kg	SiO_2 in SS kg	SiO_2/Na_2O	NaOH in Solid kg	Error in NaOH %	Silica waste kg (SiO2)	Silica waste kg (zirconium)
1	21.86	21.48	68.05	1.23	0.00	0.00	9.82	49.46		
2	43.72	51.30	23.69	4.65	0.00	0.00	37.23	4.19	25.01	-23.69
4	87.43	67.20	0.03	57.16	0.00	0.00	32.15	-2.15	32.77	-0.03

APPENDIX K: THE ELEMENTAL ANALYSIS OF THE ALKALI FUSION PROCESS (All percentages are given as mass percent)

Sample	ZrO_2	HfO_2	SiO_2	Na_2O	CaO	Y_2O_3	Al_2O_3	TiO_2	MgO	SO_3	Fe_2O_3	Cl	P_2O_5	U_3O_8	ThO_2	V_2O_5
$ZrSiO_4$	66.5	1.64	28.6	0.220	0.205	0.180	1.23	0.382	0.165		0.216		0.151	470ppm	870ppm	79ppm
Na_2ZrO_3	59.0	1.28	15.6	22.0	0.16	0.361	1.03	660ppm			520ppm			480ppm	880ppm	86ppm
Na_2ZrO_3	56.0	1.08	24.6	32.0	0.20	0.45	1.35	0.1			660ppm			760ppm	340ppm	87ppm
Na_2ZrO_3	46.0	1.34	25.9	28.0	0.14	0.145	1.24	0.185			870ppm			340ppm	450ppm	45ppm
$ZrO_2.nH_2O$	62.0	1.08	12.6	680ppm	0.12	0.231	1.03	0.16						460ppm	780ppm	
$ZrO_2.nH_2O$	58.0	1.18	23.4	48ppm	0.10	0.782	1.35	0.15						320ppm	600ppm	
$ZrO_2.nH_2O$	28.0	1.32	27.2	220ppm	0.24	0.122	1.24	0.185						540ppm	800ppm	
Na_2SiO_3	1.01		7.09	85.9	120ppm		0.107	66ppm	370ppm		200pm		390ppm			
Na_2SiO_3	0.144		8.45	86.7	130ppm		0.230	54ppm	258ppm		180ppm		380ppm			
Na_2SiO_3	0.323		9.32	88.2	126ppm		0.142	87ppm	430ppm		320ppm		420ppm			
NaCI	0.440		1.04	54.9	0.145		380ppm			0.980	99ppm					
NaCI	0.132		1.02	52.7	0.133		240ppm			0.860	120ppm	42.5				
NaCI	0344		1.84	62.0	0.124		320ppm			0.670	86ppm	43.8				
AZST	50.4	1.09	0.420	0.690ppm	360ppm	0.115	0.112	930ppm		47.4	600ppm	44.6				
AZST	50.7	1.07	0.260	0.797ppm	320ppm	750ppm	0.123	690ppm	500ppm	47.4	490ppm					
AZST	62.6	1.08	0.134	0.633ppm	0.259	0.201	0.106	0.105	670ppm	34.8	812ppm					
ZrO_2	98.54	1.09	0.124	240ppm	320ppm	24ppm	0.101	630	500ppm	0.130	260ppm					
ZrO_2	98.62	1.04	0.234	234ppm	450ppm	750ppm	0.120	690ppm	670ppm	0.05	490ppm					
ZrO_2	98.42	1.12	0.101	560ppm	0.359ppm	20ppm	0.134	220ppm	220ppm	0.12						
R-AZST	69.7	1.53	0.134	0.227	0.384	0.377	0.134	0.127		23.0	940ppm	3.50	0.214	0.204	0.143	
R-AZST	72.3	1.62	0.142	0.234	0.352	0.420	0.147	0.110		19.2	960ppm	2.58	0.310	0.101	0.098	

KEY: - $ZrSiO_4$ is zircon. - Na_2ZrO_3 are the zirconates or zirconium silicates before HCl titration. - $ZrO_2.nH_2O$ is the hydrous zirconia after the removal of sodium. - Na_2SiO_3 is the silicate by-product. - NaCl is the sodium chloride effluent. - AZST is the zirconium sulphate used as a central chemical in the synthesis of zirconium chemicals. - ZrO_2 is the zirconia product obtained from the calcinations of AZST. R-AZST is the AZST effluent obtained from the purification of ZBS (note the high uranium and thorium content)